AD_____

Award Number: W 81X WH-06-1-0280

TITLE:

Receptor Tyrosine Kinases as Targets for Treatment of Peripheral Nerve Sheath Tumors in NF 1 Patients

PRINCIPAL INVESTIGATOR:

Dr. Victor-Felix Mautner

CONTRACTING ORGANIZATION:

University Aet Sklinikum Hamburg-Eppendorf
20246 Hamburg, Germany

REPORT DATE: March 2010

TYPE OF REPORT: Final

PREPARED FOR: U.S. Army Medical Research and Materiel Command Fort Detrick, Maryland 21702-5012

REPORT DOCUMENTATION PAGE

Form Approved
OMB No. 0704-0188

1. REPORT DATE *(DD-MM-YYYY)*	2. REPORT TYPE	3. DATES COVERED *(From - To)*
01-03-2010	Final	1 MAR 2006 - 28 FEB 2010

4. TITLE AND SUBTITLE
Receptor Tyrosine Kinases as Targets for Treatment of Peripheral Nerve Sheath Tumors in NF 1 Patients

5a. CONTRACT NUMBER

5b. GRANT NUMBER
W81XWH-06-1-0280

5c. PROGRAM ELEMENT NUMBER

6. AUTHOR(S)
Dr. Victor-Felix Mautner kluwe@uke.de

5d. PROJECT NUMBER

5e. TASK NUMBER

5f. WORK UNIT NUMBER

7. PERFORMING ORGANIZATION NAME(S) AND ADDRESS(ES)
University Aet Sklinikum Hamburg-Eppendorf
20246 Hamburg, Germany

8. PERFORMING ORGANIZATION REPORT NUMBER

9. SPONSORING / MONITORING AGENCY NAME(S) AND ADDRESS(ES)
U.S. Army Medical Research and Materiel Command
Fort Detrick, Maryland 21702-5012

10. SPONSOR/MONITOR'S ACRONYM(S)

11. SPONSOR/MONITOR'S REPORT NUMBER(S)

12. DISTRIBUTION / AVAILABILITY STATEMENT
Approved for public release; distribution unlimited

13. SUPPLEMENTARY NOTES

14. ABSTRACT

Nine MPNST and 28 PNF were recruited, from which one new MPNST cell culture (1507) was established and two additional MPNST cultures in early passages are promising. We found frequent copy number changes for EGFR and ERBB2, as well as for PTEN CDKN2A and TP53 in MPNST. CDKN2A loss was associated with metastasis. In vitro and in vivo models for MPNST and PNF were established and used to test several available tyrosine kinase inhibitors. AMN107 (Nilotinib) inhibited MPNST cell proliferation in vitro while Imatinib and Gefinitib did not. Glivec and AMN107 did not exhibit any effect on xenografted MPNST in immunodeficient mice. Most interestingly, Imatinib treatment reduced vitalilty of primary cultured Schwann cells derived from PNF at an IC50 of 10 µM in vitro and led to significant size-reduction of xenografted PNF pieces in nude mice of more than 80%. A contract research from Novartis is in progress to test the efficacy of Nilotinib, the 2nd generation drug of Imatinib, on PNF using our xenografting model.

15. SUBJECT TERMS
NF1, MPNST, Xenograft, tyrosine kinase inhibitor, PDGFR-α, c-Kit, EGFR

16. SECURITY CLASSIFICATION OF:			17. LIMITATION OF ABSTRACT	18. NUMBER OF PAGES	19a. NAME OF RESPONSIBLE PERSON
a. REPORT	b. ABSTRACT	c. THIS PAGE			USAMRMC
U	U	U	UU	43	19b. TELEPHONE NUMBER *(include area code)*

Table of Contents

Page

INTRODUCTION

Plexiform neurofibromas (PNF) are a major manifestation of NF1 and develop in 30-50% of the patients. In contrast to cutaneous neurofibroma, which are the hallmark of NF1 but of mainly cosmetic significance, PNF cause various clinical deficits and have a high risk of malignant transformation into malignant peripheral nerve sheath tumours (MPNST) which is the main mortality factor for these patients. No effective medical therapy is available for either PNF or MPNST. This study is aimed to establish *in vitro* and *in vivo* models for the NF1-associated benign and malignant tumours and use them to test efficacy of tyrosine kinase receptor inhibitors.

BODY

Task 1 -to establish cell lines from MPNST from NF1 patients

A total of 9 MPNSTs and 28 PNFs were recruited. The 9 MPNSTs were used to culture tumor cells while two new MPNST cell cultures (1507 and 1844) have been genetically verified as containing tumour cells as the cells had the same somatic genetic alteration as the original tumour.

(1) newly established MPNST cell line 1507 has loss of heterozygosity (LOH) in the p53 region as the original tumor does. The 1st (constitutional) *NF1* mutation in this MPNST is a splicing mutation in intron 23-1 (-1G>A) which was found in the blood of the patient and in the cultured MPNST cells. The 2nd (somatic) *NF1* mutation in the MPNST cells is a 22-bp deletion in exon 10a. This line is now in the 28 passage.

(2) the 2nd newly established MPNST cell line 1844 has LOH of the NF1 region which is also the 2nd (somatic) alteration. This line is now in the 20 passage and cells grow rapidly.

Primary Schwann cells derived from PNF were used for treatment study.

Task 2 - to determine genetic alterations and expression of PDGFR-α, c-Kit, EGFR and Neu (ERBB2) in MPNST, pNF, and cultured MPNST cells

We studied expression and genetic alterations of EGFR and erbB2 in MPNST from 37 patients. No mutations were found within exons encoding the respective kinase domain. Gene dosage analysis was performed by multiplex ligation-dependent probe amplification for *EGFR* and *ERBB2,* and also for the tumor suppressor genes *PTEN CDKN2A* and *TP53*. MLPA revealed increased *EGFR* copy number in 28% of MPNST, which was confirmed by FISH. Loss of genetic material was detected for *ERBB2* (32%), *PTEN* (58%)*, CDKN2A* (58%), and *TP53* (39%). *CDKN2A* loss was associated with metastasis. Comparison of corresponding benign neurofibromas and MPNST suggested that genetic alterations occurred during progression from benign tumors to the malignat ones. On the protein level frequent expression of EGFR and erbB2 was detected in MPNST. Stronger EGFR expression was associated with increased *EGFR* gene copy numbers. In contrast, benign neurofibromas expressed EGFR, but rarely erbB2. The EGFR ligands *TGFA* and *EGF* were expressed stronger in MPNST than in neurofibromas.

Task 3 -to test single and multiple (combinations) tyrosine inhibitors *in vitro*

- in vitro efficacy study

For cultured MPNST cells 462, imatinib led to reduced cell number with a IC_{50} of <10 µM. Furthermore, imatinib prevented PDGF-AA induced phosphorylation in these cells with a pharmacologic IC50 of < 2 µM (Holtkamp et al. 2006). Also gefinitib reduced vitality of the MPNST cells (Fig. 1)

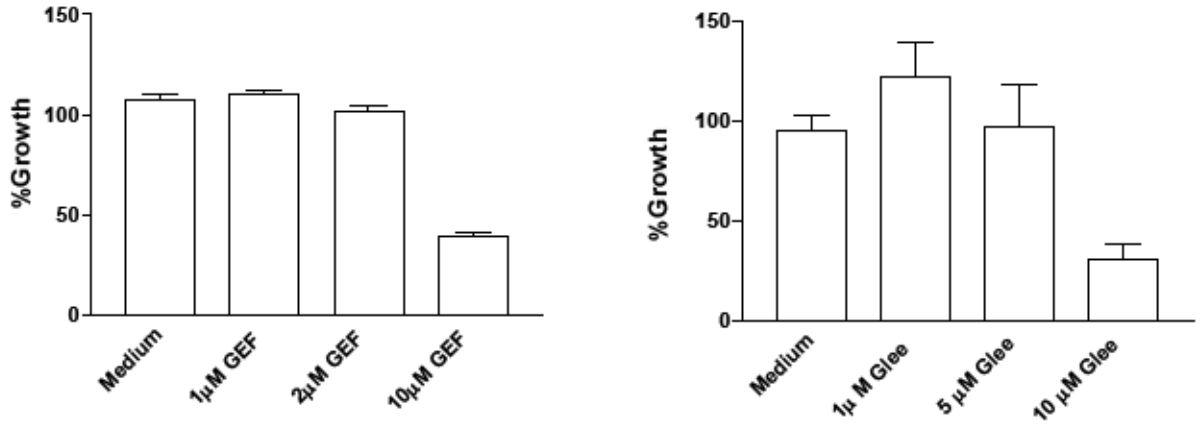

Figure 1. Effect of imatinib and gefinitib on proliferation of MPNST 462 cells measured by BrdU-incorporation.

We then examined effect of glivec (imatinib mesylate) on cultured primary Schwann cells derived from 5 human PNF. Schwann cells were identified as cells with elongated spindle shape and which are S100 positive. The proportion of Schwann cells in the cultures used for drug test was >85%. Treating the cells with imatinib mesylate for 28 days led to reduced viability of the cells with an IC_{50} of 10 µM (Fig. 2). When compared with the controls, the reduction of viability was significant for all drug concentration (P<0.001*** to P<0.05*). However, treatment for 7- and 14-days did not lead to significant reduction in cell viability when compared with the control.

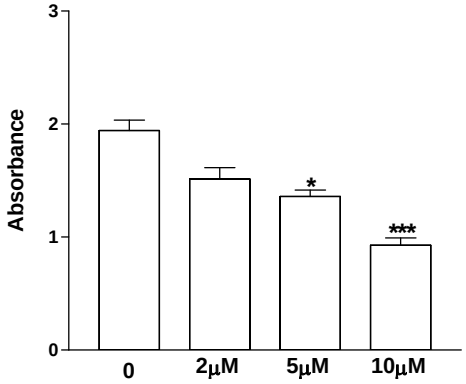

Figure 2. Viability of Schwann cells is decreased upon imatinib mesylate treatment *in vitro*. Schwann cell cultures were treated with imatinib mesylate for 28 days. Each column represents mean absorbance at each concentration with 12 replicates. (±SEM). non-parametric one way ANOVA, p<0.001 (***)post-hoc analysis Dunn's test: control versus 2 µM, p>0.05, control versus 5µM P<0.05 (*), control versus 10µM p<0.001 (***)

Task 4 - to inhibit receptor tyrosine kinases *in vivo*

In vivo model for MPNST

MPNST cell lines S462 and S805 were used to grow xenograft tumors in immunodeficient mice. Cell line S805 forms very slow growing tumors. Later, S805 genetic finger printing using microsatellite markers revealed that S805 cells were in fact S462 cells. Contamination of the faster growing 462 cells was the cause of the wrong origin. This illustrated the importance of regular genetic verification of the cultured cells. Also recovering of these MPNST cells from early passages failed as the cells did not grow well.

Thus, only MPNST cells 462 were used to generate tumor in nude mice by means of injecting the cultured cells into the flank of the mice. Tumors developed in 80% of the mice in 2- 3 weeks. Re-implant pieces of tumours grown in mice obtained new tumors in shorter period than in previous model using cultured cells.

In vivo model for PNFs

Freshly resected PNFs obtained from our department of maxillofacial surgery were cut into small pieces of approximately 1mm in diameter and grafted onto sciatic nerve of nude mice. These tumor-fragments persisted at least 60 day. Histologically, S100 positive spindle-shaped cells were found in the transplants at all time points. Staining with mouse-specific isolectin B4 revealed newly formed blood vessels at the tumour transplants. Angiogenesis in the tumour periphery was confirmed by FLK and VEGF expression in the same area.

We observed up to 10% enlargement of the implants around day 30 after the implantation (Fig. 3, left). However, detailed histological examinations suggested that proliferating cells are not of tumour origin but rather inflammatory cells of human or mouse origin (Fig. 3, right). Also CD68 positive mouse macrophages were mainly found in the periphery of the tumour but not within the tumour. These results suggest that the observed enlargement of tumour-transplants between days 7 and 35 is likely due to invasion of proliferating inflammatory cells rather than tumour cell proliferation.

Fig. 3 Size changes of PNF grafts in nude mice

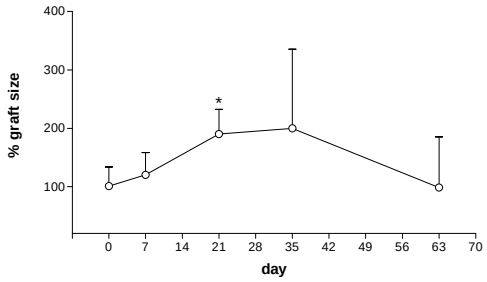

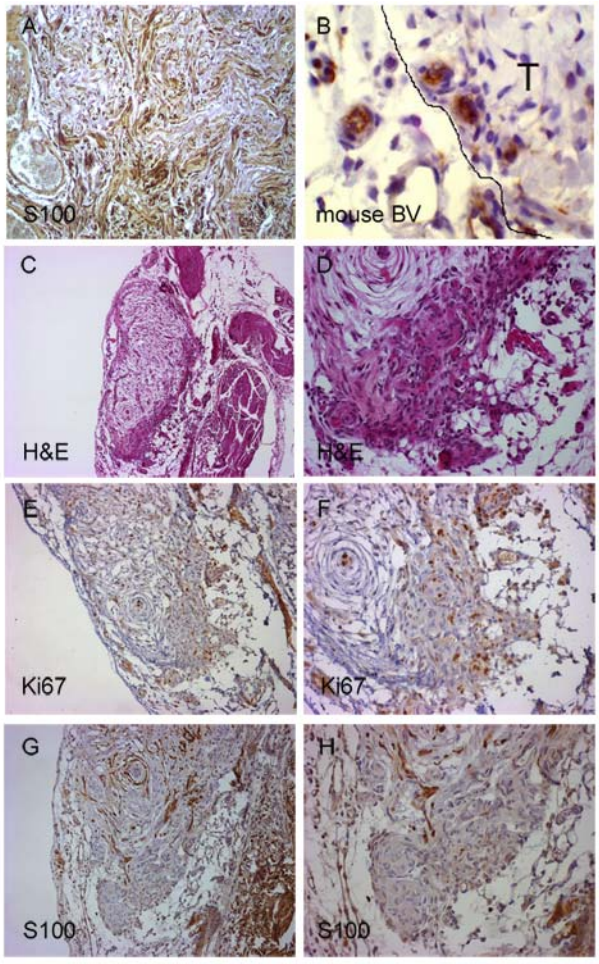

Fig. 4 Histology of PNF implants at 30 days post implantation. (**a**) S100+ Schwann cells in the implant (*x10)*. **(b)** Mouse endothelial cells labelled with BS-Lectin (specific for mouse endothelial cells). Mouse blood vessels invaded the grafts (tumour area, **T**) (*x40*). (**c, d**). granulose tissue in the area between the grafts and the mouse nerve (*x5, x20*). (**e, f**) Ki67 labels proliferative cells mostly in the inflammatory area (*x5, x20*). (**h, g**) S100+ cells mainly in the graft, but not in the inflammatory area (*x10, x20*).

This interpretation is in concordance with our recent clinical finding using magnetic resonance imaging which revealed indeed that PNFs do not grow in the majority of cases (Mautner et al. 2008). Furthermore, the few tumours that grew in the observation period grew at very slow rates. Thus, we do not expect a detectable growth of a PNF implant in mice in a period of 2 months. Such growth would not reflect the actual behaviour of this kind of benign tumour.

Later, we established an ultrasound-based measuring method for monitoring of the implanted tumours without killing the animals, making the *in vivo* model for PNF more easy to use for drug testing (Fig. 5).

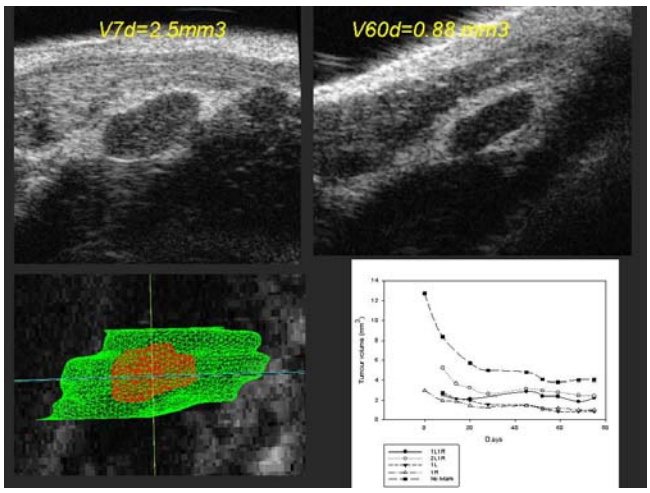

Fig. 5 Ultrasound measurement of a xenografted PNF tumour fragment at 7 (left) and 60 (upper right) days after implantation. Lower left: red represents the core tumour implant while green may correspond to the inflammatory areas around the implant. Lower right: tumour volume measured weekly. The calculation was carried out using five different definitions of the boundary.

Drug-treatment for MPNST in vivo

Mice with xenografted MPNST were treated with Glivec at 75mg/Kg/Day, Gefinitib at 50mg/Kg/day and nilotinib at 1mg/Kg/day.

Gefinintib suppressed tumor growth, however, the difference to the control groups did not reach statistical significance (Fig. 6). One reason could be the highly variable tumor growth and the small number of mice. An even smaller effect was observed in mice treated with Imatinib (Fig. 6), while nilotinib (data not shown) did not exhibit any effect.

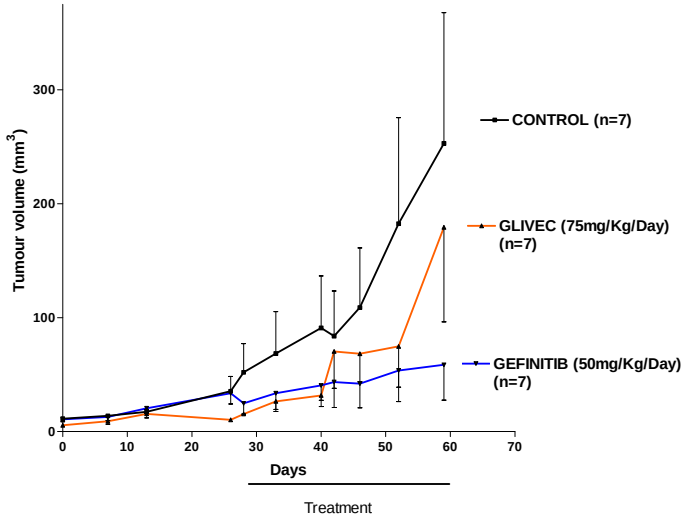

Fig. 6 Mice with xenografted MPNST were treated with imatinib and Gefinitib for 28 days. Reduction in tumour volume was observed in mice treated with gefinitib.

Imatinib-treatment for PNF *in vivo*

One week after transplantation, mice were treated with imatinib mesylate at a dose of 75mg/kg daily for 28 days. The grafts in the 8 treated group were reduced in size at an average of 80% (Fig. 7, right). In contrast, averaged size of the grafts in the 11 mice of the control group which were treated with saline did not change (Fig. 7, left). The size reduction of the grafts in the 8 treated mice was significantly different, from the original sizes within the group (P<0.001) and from sizes of the grafts in 11 untreated mice in the control group (P<0.001).

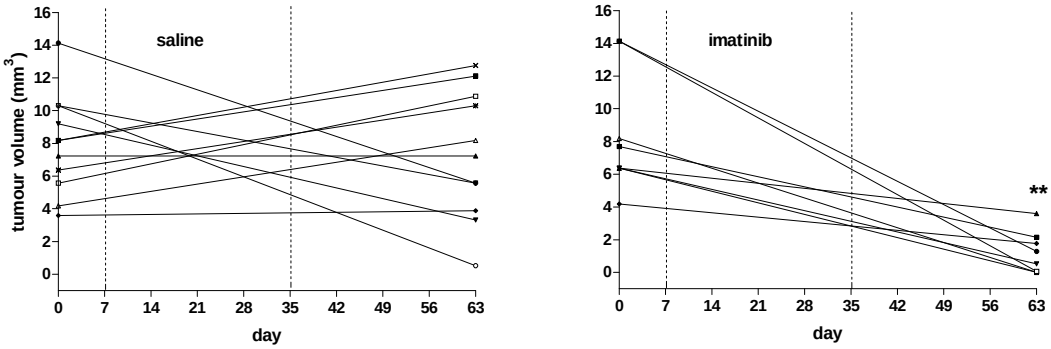

Fig. 7 Size changes of PNF grafts in nude mice. Dotted lines mark the 4-week treatment period

Our result is in concondance with the finding of Yang et al. (2008), and suggest potential therapeutic value of imatinib mesylate for PNF (Demestre et al. 2009). However, we cannot exclude the possibility that the effects of Glivec treatment were not due to direct interference with tumour cells in the graft but rather via immune reaction of the mice against the grafts. The mast cell density was assessed in both groups at 67 days post transplantation. However, no differences between the groups were observed (control group: 0.06412±0.0086/mm^2 (n=5), imatinib group (0.0641±0.0299/mm^2, n=3, non parametric Mann Whitney test, control group versus Imatinib group at day 67, p>0.5). To further exclude the influence of the mouse immune response on tumour growth, we repeated the experiment using severe combined immune-deficiency (SCID) mice. Enlargement of the implants was observed post implantation, however, due to increased morbidity and mortality of mice in all groups, no data could be obtained for evaluation.

Soon after publication of our in vivo model and the result of imatinib-treatment for PNF, Novartis contacted us, exploring the possibility of a contract research for the efficacy of a second generation drug of imatinib mesylate, nilotinib, for PNF. This project is now in progress.

KEY RESEARCH ACCOMPLISHMENTS

- completed recruitment of 9 MPNST and 28 PNF patients.

- established two new MPNST cell lines: 1507 and 1844.

- established an *in vivo* model for MPNST

- established an in vivo model for PNF where the size-reduction of the implants is regarded as the indicator of drug efficacy. Tumour size can be traced using an ultrasound device for small animals.

- Found that Glivec can reduce size of PNF-grafts in mice and in cultured Schwann cells from PNF.

REPORTABLE OUTCOMES

1 Holtkamp N, Okuducu AF, Mucha J, Afanasieva A, Hartmann C, Atallah I, stevez-Schwarz L, Mawrin C, Friedrich RE, Mautner VF, von Deimling A. Mutation nd expression of PDGFRA and KIT in malignant peripheral nerve sheath tumors, and its implications for imatinib sensitivity. Carcinogenesis. 2006 Mar;27(3):664-71.Epub 2005 Dec 15. PubMed PMID: 16357008.

2 Holtkamp N, Malzer E, Zietsch J, Okuducu AF, Mucha J, Mawrin C, Mautner VF, Schildhaus HU, von Deimling A. EGFR and erbB2 in malignant peripheral nerve sheath tumors and implications for targeted therapy. Neuro Oncol. 2008 Dec;10(6):946-57.

3 Demestre M, Messerli SM, Celli N, Shahhossini M, Kluwe L, Mautner V, Maruta H. 2009. CAPE (caffeic acid phenethyl ester)-based propolis extract (Bio 30) suppresses the growth of human neurofibromatosis (NF) tumor xenografts in mice. Phytother Res 23(2):226-30

4 Demestre M, Herzberg J, Holtkamp N, Hagel C, Reuss D, Friedrich RE, Kluwe L, Von Deimling A, Mautner VF, Kurtz A. Imatinib mesylate (Glivec) inhibits Schwann cell viability and reduces the size of human plexiform neurofibroma in a xenograft model. J Neurooncol. 2009 Nov 17. [Epub ahead of print]

CONCLUSION

We established two new MPNST cell lines with genetically verified authenticity, established in vivo models for MPNST and for PNF. These are valuable not only for studies in our group, but also for various studies in other research group. We found that imatinib mesylate reduced vitality of Schwann cells derived from PNF *in vitro* and reduced size of PNF implants in nude mice significantly, suggesting that this tyrosine kinase inhibitor may provide a therapeutic option for PNF in NF1 patients.

REFERENCES

Mautner VF, Hartmann M, Kluwe L, Friedrich RE, Funsterer C. MRI growth patterns of plexiform neurofibromas in patients with neurofibromatosis type 1. *Neuroradiology.* 2006, 48(3):160-165.

Yang FC, Ingram DA, Chen S, *et al*. Nf1-dependent tumors require a microenvironment containing Nf1+/-- and c-kit-dependent bone marrow. *Cell.* 2008, 135(3):437-448.

Appendices

J Neurooncol
DOI 10.1007/s11060-009-0049-4

LABORATORY INVESTIGATION - HUMAN/ANIMAL TISSUE

Imatinib mesylate (Glivec) inhibits Schwann cell viability and reduces the size of human plexiform neurofibroma in a xenograft model

Maria Demestre · Jan Herzberg · Nikola Holtkamp · Christian Hagel · David Reuss · Reinhard E. Friedrich · Lan Kluwe · Andreas Von Deimling · Victor-F. Mautner · Andreas Kurtz

Received: 28 April 2009 / Accepted: 26 October 2009

Abstract Plexiform neurofibromas (PNF), one of the major features of neurofibromatosis type 1 (NF1), are characterized by complex cellular composition and mostly slow but variable growth patterns. In this study, we examined the effect of imatinib mesylate, a receptor tyrosine kinase inhibitor, on PNF-derived Schwann cells and PNF tumour growth in vitro and in vivo. In vitro, PNF-derived primary Schwann cells express platelet-derived growth factors receptors (PDGFR) α and β, both targets of imatinib, and cell viability was reduced by imatinib mesylate, with 50% inhibition concentration (IC_{50}) of 10 μM. For in vivo studies, PNF tumour fragments xenografted onto the sciatic nerve of athymic nude mice were first characterized. The tumours persisted for at least 63 days and maintained typical characteristics of PNFs such as complex cellular composition, low proliferation rate and angiogenesis. A transient enlargement of the graft size was due to inflammation by host cells. Treatment with imatinib mesylate at a daily dose of 75 mg/kg for 4 weeks reduced the graft size by an average of 80% ($n = 8$), significantly different from the original sizes within the group and from sizes of the grafts in 11 untreated mice in the control group ($P < 0.001$). We demonstrated that grafting human PNF tumour fragments into nude mice provides an adequate in vivo model for drug testing. Our results provide in vivo and in vitro evidence for efficacy of imatinib mesylate for PNF.

Keywords Neurofibromatosis · Plexiform neurofibromas · Imatinib mesylate · Xenografts · Glivec

Abbreviations

GST	Glutathione transferase
PNF	Plexiform neurofibromas
NF1	Neurofibromatosis type 1
MPNSTs	Malignant peripheral nerve sheath tumours
PDGFR	Platelet-derived growth factor receptor
DMEM	Dulbecco's modified essential medium
PAS	Periodic acid-Schiff
VEGF	Vascular endothelial growth factor
DAPI	4′,6-Diamidino-2-phenylindole
SCID	Severe combined immunodeficiency

M. Demestre · J. Herzberg · R. E. Friedrich · L. Kluwe · V.-F. Mautner
Department of Maxillofacial Surgery, University Medical Centre Hamburg Eppendorf, Martinistrasse 52, 20246 Hamburg, Germany

C. Hagel
Institute of Neuropathology, University Medical Centre Hamburg Eppendorf, Martinistrasse 52, 20246 Hamburg, Germany

N. Holtkamp
Institute for Neuropathology, Charité Universitätsmedizin Berlin, Augustenburger Platz 1, 13353 Berlin, Germany

A. Kurtz (✉)
Berlin-Brandenburg Center for Regenerative Therapies, Charité Universitätsmedizin Berlin, Augustenburger Platz 1, 13353 Berlin, Germany
e-mail: andreas.kurtz@charite.de

D. Reuss · A. Von Deimling
Department of Neuropathology, Ruprecht-Karl-Universität and Clinical Cooperation Unit Neuropathology, German Cancer Research Centre, Im Neuenheimer Feld 280, 69120 Heidelberg, Germany

Published online: 17 November 2009

Background

Neurofibromatosis 1 (NF1) is an autosomal dominantly inherited disease characterized by multiple neurofibromas, melanogenic abnormalities, bone defects and cognitive deficits, among other characteristics. The genetic causes for NF1 are heterozygous inactivating mutations of the *NF1* tumour suppressor gene on chromosome 17.

Plexiform neurofibromas (PNF) are present in 30–50% of NF1 patients [1, 2]. Unlike cutaneous neurofibromas, the hallmark of NF1 in which tumours are mostly small and mainly of cosmetic relevance, PNF grow to various sizes, infiltrate the surrounding tissues and often have significant clinical consequences, including severe disfigurement, pain, organ compression and other functional impairments. PNF can become extremely large, and some of them affect the whole face, arm or leg. Occasionally, large lesions can erode adjacent bones and thus produce skeletal instability. Our recent study showed growth of PNF mostly in early childhood and adolescence [3]. PNF is the precursor of malignant peripheral nerve sheath tumours (MPNST), which develops in 6–13% of NF1 patients and is the leading cause of death due to this condition [4].

To date, treatment of PNF has been limited to surgical intervention. However, since the tumours often infiltrate adjacent tissues, complete resection is usually not possible without damaging nerves and healthy tissues. Currently, there is no established medical therapy available for PNF.

Imatinib mesylate (Glivec) is a receptor tyrosine kinase inhibitor that targets platelet-derived growth factor receptor (PDGFR)-α and -β, c-Kit, Bcr-Abl and Arg-kinase, and that exhibited efficacy for some cancers [5, 6]. We have previously shown that imatinib mesylate inhibits growth of MPNST cells in vitro [7], raising the hope that this drug may also be beneficial for benign PNF. A recent study showed that c-Kit inhibition by imatinib mesylate leads to reduced mast cell infiltration and neurofibroma growth inhibition in a transgenic mouse model of NF1 [8].

In the present study, we examined the effect of imatinib mesylate on the viability of primary PNF-derived Schwann cells in vitro and its impact on size and survival of PNF-derived tumour fragments in vivo.

Materials and methods

Patients and tumours

Plexiform neurofibromas were obtained from seven unrelated NF1 patients who underwent surgery at the University Hospital Hamburg Eppendorf (age range 12–57 years, mean 34 ± 7.208 years; five male, two female). Diagnosis of NF1 was conducted according to the modified National Institutes of Health (NIH) criteria [9]. All patients gave informed written consent, and the local ethics committee approved the study protocol. After saving sufficient material for histological examination, parts of each specimen were used to establish primary Schwann cell cultures and/or for xenografting into nude mice.

Schwann cell cultivation and treatment with imatinib mesylate

PNF from five patients (age range 16–57 years, mean 42 ± 7.2595 years; four male, one female) were cut into small pieces and placed overnight in Dulbecco's modified Eagle's medium (DMEM) containing 10% fetal bovine serum, 2 mM glutamine and 2 mM sodium pyruvate (Invitrogen, Karlsruhe, Germany). Cultivation and enrichment of Schwann cells was carried out as previously described [10]; heregulin was kindly provided by S. Carroll (Department of Neurobiology, University of Alabama at Birmingham). Proportion of Schwann cells was defined as the number of S100-positive Schwann cells divided by the number of nuclei stained with 4′,6-diamidino-2-phenylindole (DAPI, Vysis Inc., Downers Grove, USA).

For imatinib mesylate treatment, 10,000 cells were seeded in 100 µl medium into each well of a 96-well plate for viability assays or in chambers for immunocytochemistry. Imatinib mesylate (kindly provided by Novartis Pharma AG, Basel, Switzerland) was dissolved in water, and added at final concentrations of 2, 5 and 10 µM. Medium was changed every 5 days. Cell viability was evaluated on days 7, 14 and 28 of imatinib treatment using the XTT proliferation assay (Promega, Mannheim, Germany) by measurement of absorbance at 490 nm. Each drug concentration was tested in 12 replicates. Vitality and final number of cells was determined at the end of the experiment using Trypan Blue exclusion.

Xenograft implantation and imatinib mesylate treatment

Tumour tissue from freshly resected PNFs (12-year-old female and 16-year-old male) was placed in sterile DMEM and cut into 4–9 mm^3 pieces. These tumour pieces were soaked in Matrigel (R&D Systems, Wiesbaden, Germany) at 4°C and their sizes were determined using a calliper. Female athymic nu/nu Balb/c mice (Charles River, Sulzfeld, Germany) were anaesthetised with a mixture of xylasin and ketamin. A small incision was made into the skin to expose the sciatic nerve, and then an incision was made into the sciatic nerve, onto which one tumour piece was implanted. Muscle and skin layers were closed and sutured. To determine graft volume changes after transplantation,

mice were sacrificed at days 7 ($n = 4$), 21 ($n = 4$), 35 ($n = 3$) and 63 ($n = 3$) to determine size and for histological analysis.

For treatment with imatinib mesylate, Alzet mini-pumps containing either phosphate-buffered saline (control) or imatinib mesylate (treatment) were subcutaneously implanted into the back of mice [11]. Drug release was set to 75 mg/kg per day with pumping rate of 0.2 µl/h [12], giving an in vivo concentration in excess of the IC_{50} (10 µM) determined for inhibition of Schwann cell proliferation.

Imatinib mesylate treatment was started at day 7 and continued until day 35 post grafting. Mice were kept alive for further 28 days without treatment and sacrificed at day 63. Because of inflammation at the Alzet pump site, four mice of the treatment group had to be discontinued and were not included in the evaluation. Graft size was measured with a calliper and the volume was calculated as $(\pi/48)(\text{length} + \text{width})^3$. All animal experiments were approved by the local authority.

Histology

Tumours were fixed in 7% formalin and embedded in paraffin. Sections were stained with haematoxylin and eosin (H&E) or with Periodic acid-Schiff (PAS) stain to specifically detect mast cells. In addition, a series of immunohistochemical stainings were carried out using anti-human S100 (rabbit polyclonal, 1:800, Dako, Hamburg, Germany), anti-human Ki67 (rabbit monoclonal 1:50, Neomarkers, Asbach, Germany), anti-mouse macrophage surface marker CD68 (mouse monoclonal, 1:100, R&D Systems) and anti-human glutathione transferase (GST) (mouse monoclonal, 1:100, ABCAM, Cambridge, USA). Antibodies against human vascular endothelial growth factor (VEGF) (rabbit polyclonal 1:500) and FLK-1 (rabbit polyclonal, 1:100, Santa Cruz Biotechnology, Heidelberg, Germany) were used to detect blood vessels, while isolectin B4 (biotinylated, 20 µg/ml, Vector Laboratories, Peterborough, UK) was used to detect specifically mouse and non-human endothelial cells. For antibody detection, Envision Kit dual system peroxidase (Dako, Hamburg, Germany) was used. For isolectin detection, the ABC reagent (Vector Laboratories) was used. Colour reactions were developed with VectorRed (Vector Laboratories), and the nuclei were counterstained with haematoxylin.

Expression of receptor tyrosine kinases was examined by immunofluorescence staining on paraffin-embedded sections. Antigen retrieval was enhanced by heating in a microwave. Rabbit polyclonal antibodies against PDGFR-α (1:50) and PDGFR-β (1:50) were from Santa Cruz Biotechnology, while the antibody against c-Kit (1:100) was obtained from Dako. As secondary antibodies we utilized 1:100 dilutions of Cy3- (Dianova) and Alexa Fluor 488-conjugated (Invitrogen) anti-rabbit Ig. Nuclei were counterstained with DAPI. As positive controls we used skin and tonsil tissue. Negative control stainings without primary antibodies did not produce signals.

For immunocytochemistry, Schwann cells were grown on chamber slides, fixed with 4% paraformaldehyde and stained with antibodies against S100, PDGFR-α, and PDGFR-β. Alexa Fluor 488-conjugated antibody (1:1,000) from Invitrogen was used as the secondary antibody. Nuclei were counterstained with DAPI.

Mast cells stained with PAS were counted within the graft and in the adjacent inflammatory area at 40× magnification. The total area of the section was measured using morphometry software (Zeiss, Axiovision, V4.6), and the mast cell density was calculated as mast cells/mm^2 for each section. Five sections from the control and three from the imatinib mesylate-treated group were counted.

Data analysis

The effect of imatinib mesylate on viability of cultured PNF Schwann cells was tested using non-parametric analysis of variance (ANOVA) (Kruskal–Wallis test), and if significant, post hoc comparisons using Dunn's test was performed.

We used non-parametric one-way ANOVA to compare graft sizes at days 7, 21, 35 and 63 (untreated), which were normalized to the original size at grafting. If changes were significant, Dunn's post hoc test was applied for further analysis. A non-parametric test (Mann–Whitney test) was used to examine difference in graft sizes between the control and the treated groups before transplantation. The same test was used to assess possible differences in mast cell density between grafts from the control group and those from the treatment group. To analyse the effects of imatinib mesylate on graft sizes, non-parametric one-way ANOVA was applied for pairwise comparison of each graft before and after treatment, and when significant, post–hoc analysis (Dunn's test) was used to compare changes within the groups. Statistical significance levels were set to $P = 0.05$. Graphpad Prism software was used for all statistical analyses. Averaged values are expressed as mean ± standard deviation (SD).

Results

Expression of c-Kit and PDGFR in PNF and in PNF-derived Schwann cells

Immunostaining revealed expression of the tyrosine kinase receptors PDGFR-α and PDGFR-β in the PNFs used to

graft nude mice (Fig. 1a–d). Double staining for S100 showed that PDFGR-α was mainly expressed in S100-positive Schwann cells (Fig. 1c), and also co-expressed with PDGFR-β (Fig. 1d insert). Co-expression of the PDGFRs was also seen in blood vessels (Fig. 1e). c-Kit-positive cells within the PNF morphologically resembled mast cells (Fig. 1f).

Expression of PDFGR-α and PDGFR-β was also detected in primary Schwann cell cultures derived from human PNF (Fig. 1h, i).

Imatinib mesylate reduces PNF Schwann cell viability in vitro

Primary Schwann cell cultures were derived from five human PNF. More than 85% of the cells were S100 positive and exhibited an elongated, spindle-shaped morphology, which is typical for Schwann cells (Fig. 1g). Treatment with 5 and 10 μM imatinib mesylate for 28 days reduced cell viability significantly, with $P < 0.05$ and $P < 0.001$, respectively (Fig. 2). The total number and the proportion of vital cells were counted at the end of the experiment for non-treated and 10 μM treated groups. While the number of cells increased to 608% (±101) in the control group, cells treated with imatinib only increased to 308% (±137). No differences were observed in the proportion of vital cells (non-treated: 86.74 ± 4.083%; treated 85.053 ± 6.96%). In addition, the cells changed to a more compact morphology after treatment with 10 μM imatinib mesylate for 28 days (Fig. 1j, k).

No effect on cell viability was detected at days 7 or 14 of treatment using the XTT assay (data not shown).

Volume changes of PNF tumour grafts

To obtain a baseline tumour growth pattern for grafted PNFs, changes in the volume of the grafts over time were determined in untreated animals (Fig. 3a). Animals

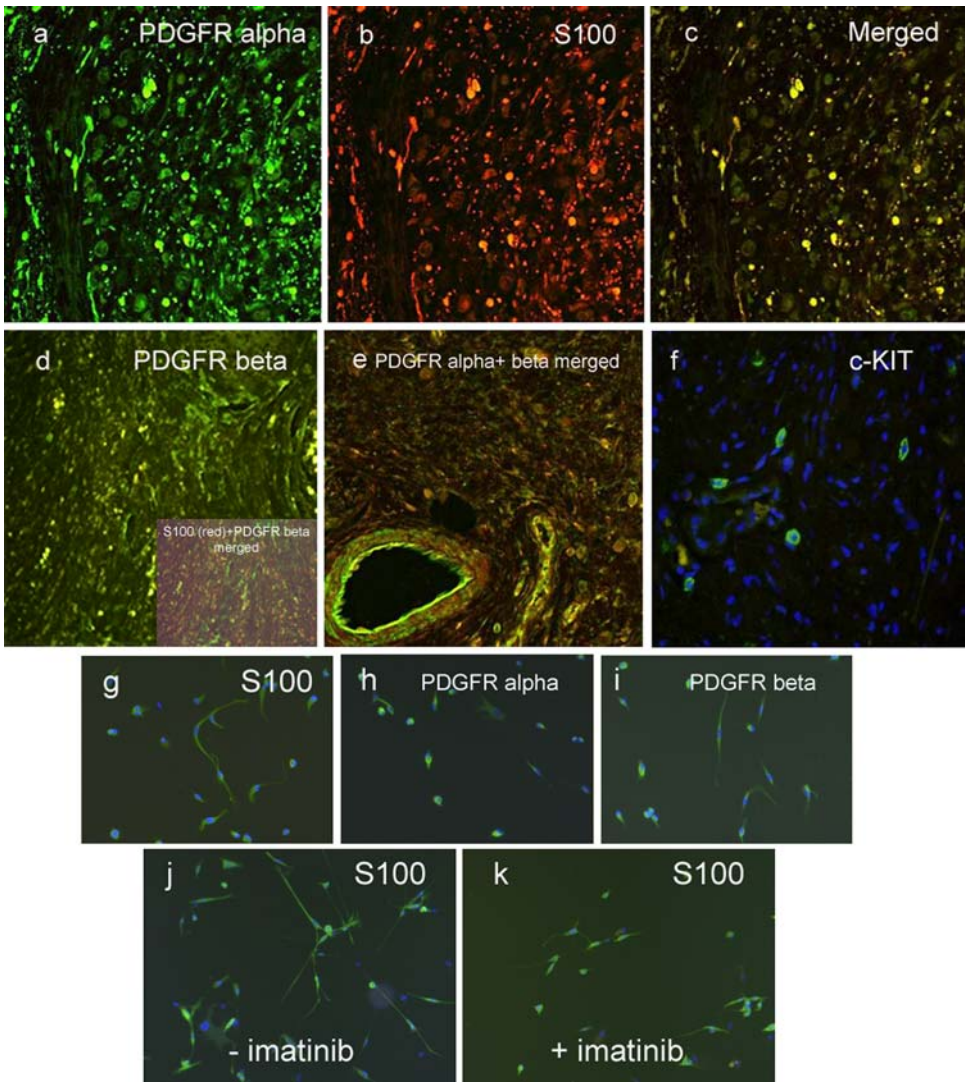

Fig. 1 Immunostaining of PNF (**a**–**f**) and cultured Schwann cells derived from PNF (**g**–**k**). **a** PDGFR-α expression (*green*) in PNF, **b** S100-positive Schwann cells (*red*) in PNF, **c** merged images of (**a**) and (**b**) showing expression of PDGFR-α in S100-positive Schwann cells. **d** PDGFR-β expression (*green*) in PNF. PDFGR-β was also co-localised with S100-positive cells (*insert*), **e** merged images of PDGFR-α (*green*) and PDGFR-β (*red*) indicating their co-expression in tumour cells and blood vessels, **f** c-Kit expression (*green*) in PNF, nuclei were counterstained with DAPI (*blue*), **g** S100-positive Schwann cells cultured from a PNF, **h**, **i** PDGFR-α and PDGFR-β expression in cultured PNF Schwann cells. **j**, **k** 28-day imatinib mesylate treatment (10 M) altered the morphology of S100-positive cells and the Schwann cell density. Original magnifications 20×, except for (**d**) 40×

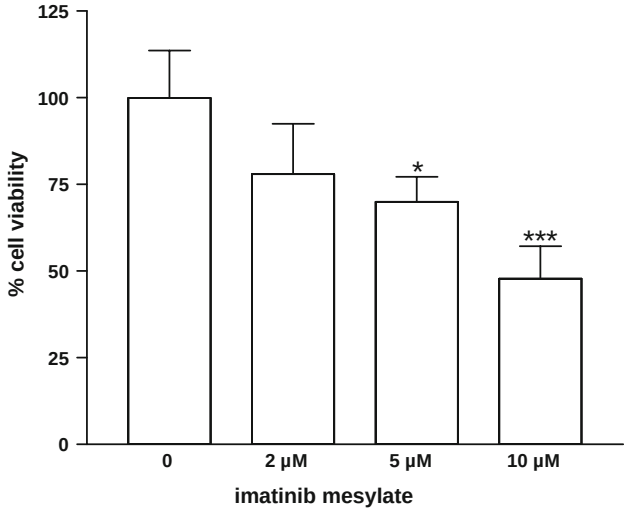

Fig. 2 Imatinib mesylate treatment reduced viability of PNF Schwann cells. Primary Schwann cell cultures derived from PNF were treated with imatinib mesylate at various concentrations for 28 days. Data was normalized from the absorbance values of untreated cells and data are expressed as percentage cell viability. Significant reduction in cell viability was detected for 5 and 10 µM imatinib mesylate treatment (*$P < 0.05$ and ***$P < 0.001$, respectively) when compared with untreated cells

($n = 14$) were sacrificed at different time points after transplantation [days 7 ($n = 4$), 21 ($n = 4$), 35 ($n = 3$) and 63 ($n = 3$)]. The average graft size increased until day 35. At day 63, graft size was comparable to the size of the original graft at day 0 (Fig. 3a). However, only grafts at day 21 post grafting were statistically significantly larger ($P < 0.05$) than those at grafting (day 0) and those at the end of experiment period of 63 days. At the other time points tumour volume variability was too large to reach statistical significance.

To investigate changes in tumour volume, PNF-derived tumour transplants were analyzed histologically at day 35 post grafting (Fig. 4). Tumour grafts, like the original tumours, consisted mostly of S100-positive cells (Fig. 4a). Staining with mouse-specific isolectin B4 antibody revealed newly formed blood vessels surrounding and invading the grafts (Fig. 4b). Angiogenesis at the graft periphery was confirmed by FLK and VEGF expression in the same area (not shown). Only a few cells in the S100-positive graft were Ki67 positive, suggesting that Schwann cell proliferation was slow. This is in concordance with the low proliferation rate of PNF tumours in humans. In contrast, proliferating Ki67-positive cells were mostly present in areas containing granulose tissue (Fig. 4 c, d) surrounding the grafts (Fig. 4 e, f), where S100-positive cells were only occasionally detected (Fig. 4g, h). In addition, CD68-positive mouse macrophages were mainly found in the granulose-containing periphery of the graft, but not within the tumour grafts themselves (not shown),

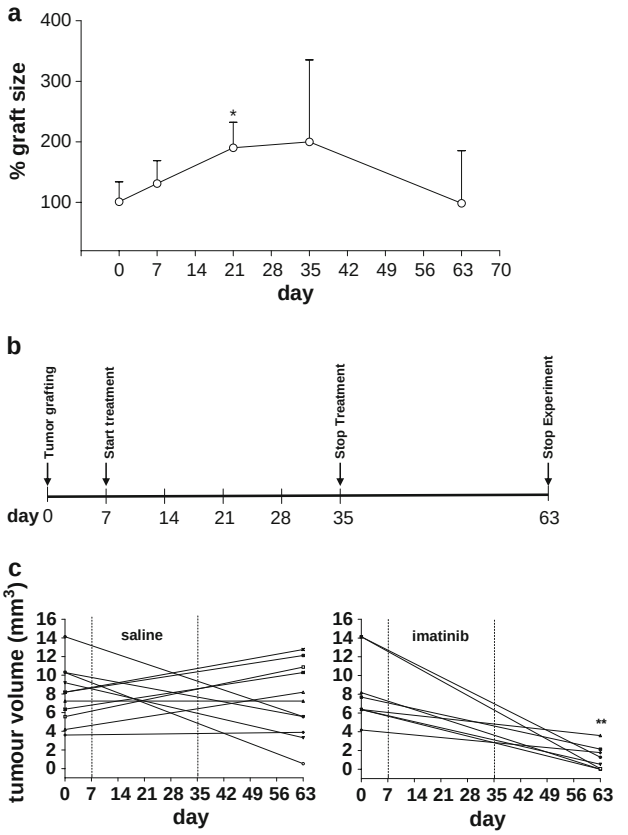

Fig. 3 Volume changes of PNF grafts in nude mice. **a** The growth pattern of non-treated grafted neurofibromas was assessed and the volume normalized at various time points post grafting. A significant increase in tumour volume compared with the time of grafting (day 0) was only seen on day 21 (*$P < 0.05$). **b** Time scale for imatinib mesylate treatment of grafted neurofibromas. **c** Changes in tumour volume are shown for grafts in untreated (saline, $n = 11$) and treated (imatinib mesylate, $n = 8$) mice, respectively. Only data at the beginning and at the end of the observation period are shown (group differences are significant at day 63, **$P < 0.01$). *Dotted lines* mark the 4-week treatment period

suggesting that the proliferating cells are not of human tumour origin but rather inflammatory cells. Human-specific GST antibody did not stain cells in the granulose tissue, supporting our interpretation that the inflammatory cells are of mouse origin (Fig. 4h, insert). These results suggest that the observed enlargement of the tumour grafts in the first 35 days post grafting is likely due to invasion of murine proliferating inflammatory cells rather than human tumour cell proliferation. The high variability of this increase in volume is most likely due to the variable dynamics of the physiological inflammatory process.

Imatinib mesylate reduces size of transplanted human PNFs

Treatment with imatinib mesylate started at day 7 post PNF grafting and continued for 28 days (Fig. 3b). This

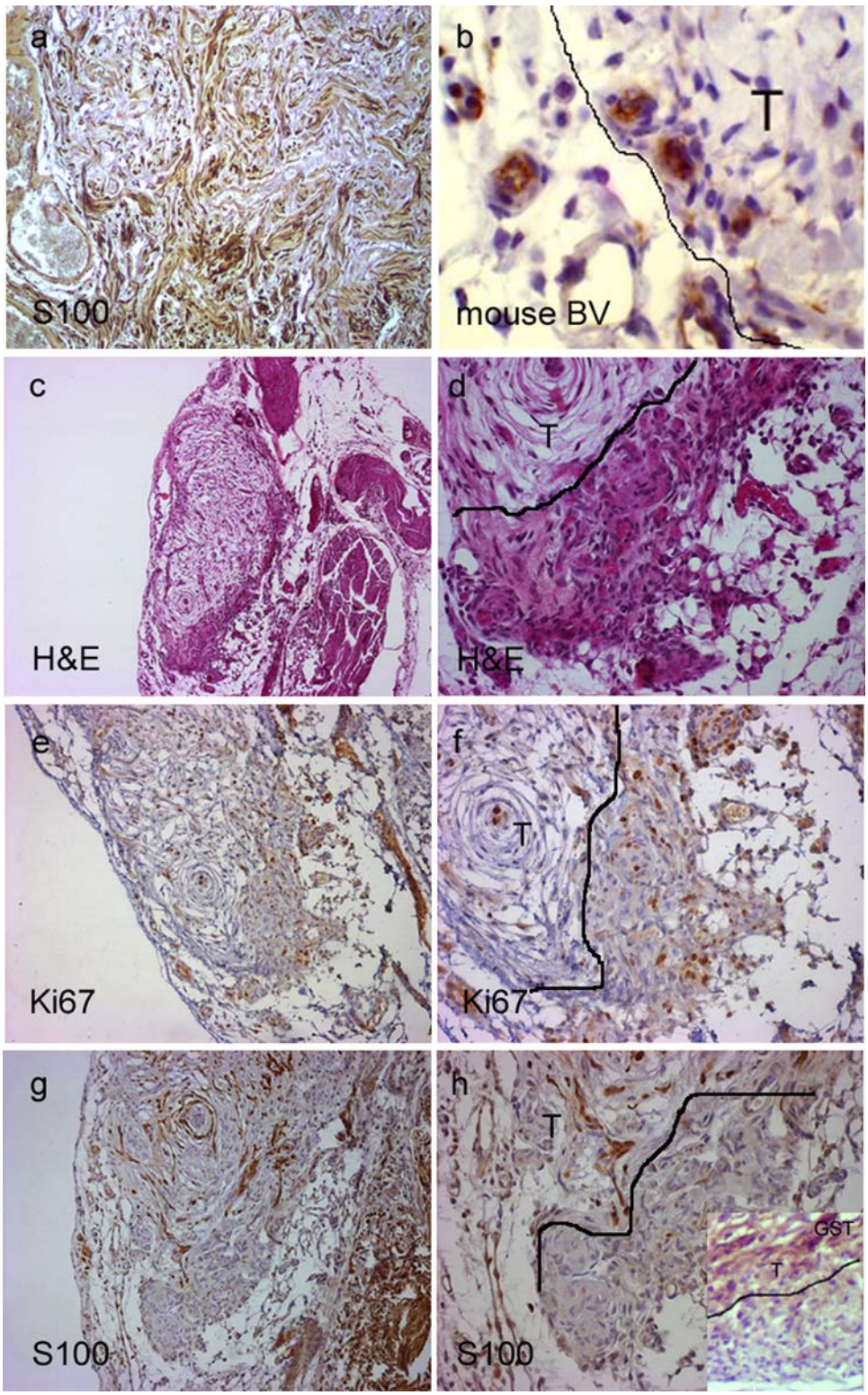

Fig. 4 Histology of PNF grafts at 35 days post grafting. Grafts areas (*lines*) are marked with **T** in **b**, **d**, **f** and **h**. **a** S100 staining indicates Schwann cells in the graft. **b** Mouse-specific isolectin B4 antibody stained mouse endothelial cells invading the tumour graft. **c**, **d** H&E staining revealed granulose tissue in area between the PNF graft and the mouse nerve. **e**, **f** Ki67-positive proliferative cells were mostly found in the inflammatory area surrounding the graft. **g**, **h** in contrast, S100-positive cells were mainly found within the graft but rarely in the inflammatory area. GST antibody labelled only human cells in the graft area but not the granulose tissue around (**h**, *insert*), suggesting non-human origin. *Original magnifications:* **c**, **e** >5×; **a**, **h** 10×; **d**, **f**, **g**, 20×; **b**, *insert in* **h**, 40×

schedule overlapped with the increase in tumour size due to inflammation. Mice were sacrificed at day 63 post transplantation, 28 days after treatment was discontinued, in order to observe whether tumours would recur post treatment (Fig. 3b). Initial sizes of grafts at grafting were similar in the control and the treatment group (7.93 ± 3.45 mm^3, $n = 11$ versus 8.428 ± 3.710 mm^3, $n = 8$) (non-parametric Mann–Whitney test, $P > 0.5$). At the end of the experiment at day 63, all eight PNF grafts in the treatment group decreased in size by an average of

82 ± 18.1% (Fig. 3c). This decrease is significant within the group (post hoc analysis using Dunn's test; $P < 0.001$). In contrast, only 4 out of 11 grafts in the control group decreased in size (by an average of 66%), while 5 increased in size and 2 remained unchanged (Fig. 3c). When all the tumours in the 11 control mice were averaged, there was no change in the graft size (0.4 ± 53%). At 63 days, graft sizes in the treatment and the control group were significantly different (non-parametric repeated-measures one-way ANOVA; $P < 0.001$).

Since insufficient nutritional supply may contribute to shrinkage of the grafts, especially in larger grafts (in both the control and treatment groups), we repeated the statistical analysis with only grafts that were smaller than 9 mm^3 at grafting (pieces of tumour larger than 9 mm^3 had all regressed in the control and treated groups), including six mice from the treatment and seven from the control group. The average reduction in graft size remained at 82 ± 8% in the treatment group, in comparison with a 45 ± 27% increase in the control group ($P < 0.001$, non-parametric repeated-measures one-way ANOVA). Post hoc analysis revealed that the size reduction within the treatment group itself was also significant ($P > 0.01$).

Histological analysis of grafts at day 63 showed healthy tumour tissue with mostly reduced inflammation in the control group (Fig. 5a). In the treatment group, a large inflammatory component was observed, which may be due to diminished viability of the tumour cells at this time point (Fig. 5b, c).

In order to assess whether imatinib mesylate influenced mast cell infiltration, mast cell density was assessed in grafts of both groups at the end of the experiment. No difference in mast cell density was observed between the control and the treatment groups: 34.64 ± 8.610/mm^2 versus 64.12 ± 0.2991/mm^2.

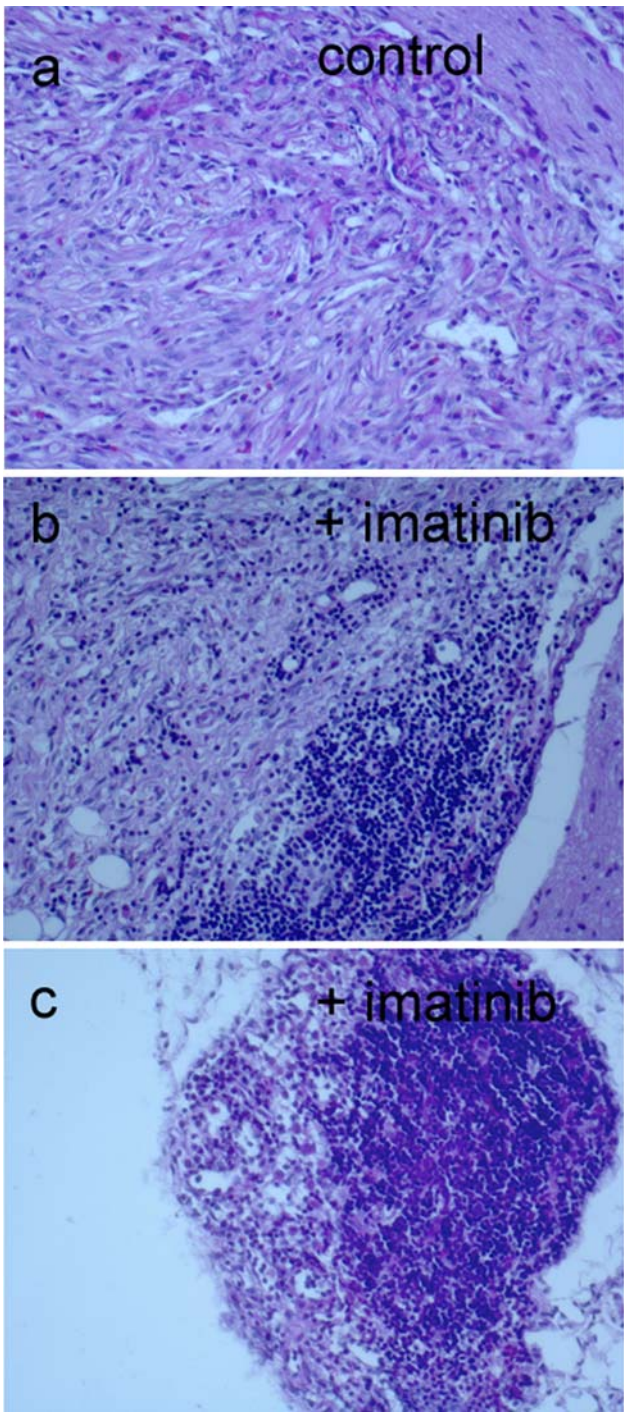

Fig. 5 Histology of PNF grafts at 63 days post grafting from control and treated mice. Sections were stained with Periodic acid-Schiff for mast cells, and counterstained with haematoxylin and eosin. **a** representative graft from a control mouse. **b**, **c** representative grafts from imatinib mesylate-treated mice. Inflammatory cells are abundant around but also within the remaining tumour tissue. Original magnifications 20×

Discussion

We grafted fragments of human PNF tumours semi-orthotopically into injured sciatic nerve of nude mice and found that the grafts persisted for at least 63 days without significant cell loss. The observed temporary increase in size at about 21 days post grafting appeared to be due to infiltration of Ki67-positive and S100-negative inflammatory cells of murine origin. After inflammation ceased, grafts reverted to their original size. According to our recent observation using magnetic resonance imaging, PNFs in patients do not grow, or grow only very slowly, in most cases [3]. Detectable growth of PNF grafts in mice within a period of 9 weeks clearly would not reflect the authentic growth pattern of this kind of tumour in patients. In contrast, lack of growth, as observed in this study, is the expected outcome in non-stressed, non-pregnant adult mice. For clinical trials for PNFs, it is becoming increasingly accepted that reduction in tumour size is the proper

measure of drug efficacy, but not growth inhibition. This is also applicable to in vivo models for PNF. Babovic-Vuksanovic et al. [13] used the persistence rate of PNF grafts as the measure of therapeutic outcome of anti-fibrotic pirfenidone treatment in a severe combined immunodeficiency (SCID) mouse xenograft model. PNF graft enlargement in nude mice within weeks has been interpreted as tumour growth in previous studies, which did not investigate inflammatory effects [14]. Another study reported growth of PNF-like tumours generated by xenografting cells of a tumour-derived Schwann cell line into nude mice [15]. This model using immortalized cells does not reflect the characteristic cellular heterogeneity and benign nature of PNFs.

The initial size of the grafts seems to affect their survival in vivo. In both, the control and treatment group, tumour grafts larger than 9 mm^3 decreased in size at the end of the 63-day experimental period. In contrast, smaller grafts remained unchanged or increased in size, if untreated. Size reduction of large grafts may be at least partially due to necrosis as a result of insufficient nutritional supply. The most drastic effect of imatinib mesylate treatment was observed for grafts >9 mm^3, possibly reflecting additive effect of the drug and intrinsic survival disadvantage due to large size.

Yang et al. [8] recently reported an effect of imatinib mesylate for neurofibromas in a transgenic mouse model and speculated that the observed tumour inhibition was via inhibition of *NF1*+/− mast cell infiltration. Here we show that PNF and PNF-derived Schwann cells express PDGFR-α and -β, both known targets of imatinib mesylate. The observation that imatinib mesylate indeed reduces viability of PNF-derived Schwann cells in vitro suggests a direct effect of the drug on the tumour cells. Furthermore, inhibition of neovascularization via the PDGF signalling pathway may have also played a role in the regression of these tumour grafts in mice. In recent studies, it has been shown that *NF1*+/− mice have increased neointima formation and vessel lumen occlusion in response to mechanical arterial injury; administration of imatinib mesylate to these mice prevented neointima formation, suggesting that neointima formation in NF1 is dependent on an imatinib mesylate-sensitive pathway [16]. It is unlikely that imatinib mesylate acts on mast cells via the c-Kit pathway in our model, as only very few infiltrating mast cells were found in both the control and the treated grafts. In addition, there was no difference in mast cell infiltration between imatinib mesylate treated and non-treated animals, and the inflammatory response follows similar patterns. Although we have not looked at systemic effects of the drug, it is unlikely that differences will be observed in immune-compromised nude mice.

Our findings support further exploitation of the established anti-cancer drug imatinib mesylate for treatment of PNF. Additional studies should be carried out to further clarify the mechanisms by which imatinib mesylate affects PNF survival.

Acknowledgments This study was sponsored by US Department of Defense (W81XWH-06-1-0280 and W81XWH-07-1-0359 to V. Mautner). We are very grateful to Novartis AG for the kind gift of imatinib mesylate.

References

1. Tonsgard JH, Kwak SM, Short MP, Dachman AH (1998) CT imaging in adults with neurofibromatosis-1: frequent asymptomatic plexiform lesions. Neurology 50(6):1755–1760
2. Mautner VF, Hartmann M, Kluwe L, Friedrich RE, Funsterer C (2006) MRI growth patterns of plexiform neurofibromas in patients with neurofibromatosis type 1. Neuroradiology 48(3):160–165. Epub 2006 Jan 24
3. Tucker T, Friedman JM, Friedrich RE, Wenzel R, Funsterer C, Mautner VF (2008) Longitudinal study of neurofibromatosis 1 associated plexiform neurofibromas. J Med Genet 17:17
4. Evans DG, Baser ME, McGaughran J, Sharif S, Howard E, Moran A (2002) Malignant peripheral nerve sheath tumours in neurofibromatosis 1. J Med Genet 39(5):311–314
5. Druker BJ, Guilhot F, O'Brien SG, Gathmann I, Kantarjian H, Gattermann N, Deininger MW, Silver RT, Goldman JM, Stone RM et al (2006) Five-year follow-up of patients receiving imatinib for chronic myeloid leukemia. N Engl J Med 355(23):2408–2417
6. Demetri GD, von Mehren M, Blanke CD et al (2002) Efficacy and safety of imatinib mesylate in advanced gastrointestinal stromal tumors. N Engl J Med 347(7):472–480
7. Holtkamp N, Okuducu AF, Mucha J et al (2006) Mutation and expression of PDGFRA and KIT in malignant peripheral nerve sheath tumors, and its implications for imatinib sensitivity. Carcinogenesis 27(3):664–671. Epub 2005 Dec 15
8. Yang FC, Ingram DA, Chen S et al (2008) Nf1-dependent tumors require a microenvironment containing Nf1+/−and c-kit-dependent bone marrow. Cell 135(3):437–448
9. Gutmann DH, Aylsworth A, Carey JC et al (1997) The diagnostic evaluation and multidisciplinary management of neurofibromatosis 1 and neurofibromatosis 2. JAMA 278(1):51–57
10. Frahm S, Mautner VF, Brems H et al (2004) Genetic and phenotypic characterization of tumor cells derived from malignant peripheral nerve sheath tumors of neurofibromatosis type 1 patients. Neurobiol Dis 16(1):85–91
11. Bihorel S, Camenisch G, Gross G et al (2006) Influence of hydroxyurea on imatinib mesylate (gleevec) transport at the mouse blood-brain barrier. Drug Metab Dispos 34(12):1945–1949
12. Weisberg E, Catley L, Wright RD et al (2007) (2007) Beneficial effects of combining nilotinib and imatinib in preclinical models of BCR-ABL + leukemias. Blood 109(5):2112–2120
13. Babovic-Vuksanovic D, Petrovic L, Knudsen BE, Plummer TB, Parisi JE, Babovic S, Platt JL (2004) Survival of human neurofibroma in immunodeficient mice and initial results of therapy with pirfenidone. J Biomed Biotechnol 2004(2):79–85
14. Lee JK, Sobel RA, Chiocca EA, Kim TS, Martuza RL (1992) Growth of human acoustic neuromas, neurofibromas and schwannomas in the subrenal capsule and sciatic nerve of the nude mouse. J Neurooncol 14(2):101–112

15. Perrin GQ, Fishbein L, Thomson SA et al (2007) Plexiform-like neurofibromas develop in the mouse by intraneural xenograft of an NF1 tumor-derived Schwann cell line. J Neurosci Res 85(6):1347–1357

16. Lasater EA, Bessler WK, Mead LE et al (2008) Nf1+/− mice have increased neointima formation via hyperactivation of a gleevec sensitive molecular pathway. Hum Mol Genet 17(15): 2336–2344

PHYTOTHERAPY RESEARCH
Phytother. Res. (2008)
Published online in Wiley InterScience
(www.interscience.wiley.com) **DOI**: 10.1002/ptr.2594

CAPE (Caffeic Acid Phenethyl Ester)-based Propolis Extract (Bio 30) Suppresses the Growth of Human Neurofibromatosis (NF) Tumor Xenografts in Mice

M. Demestre[1], S. M. Messerli[2], N. Celli[3], M. Shahhossini[1], L. Kluwe[1], V. Mautner[1] and H. Maruta[1]*

[1]UKE (Universitaets Klinikum Eppendorf), Hamburg 20246, Germany
[2]MBL (Marine Biological Laboratory), Woods Hole, MA 02543, USA
[3]Consorzio Mario Negri Sud, Via Nazionale, Chieti 66030, Italy

Dysfunction of the *NF1* gene coding a RAS GAP is the major cause of neurofibromatosis type 1 (NF1), whereas neurofibromatosis type 2 (NF2) is caused primarily by dysfunction of the *NF2* gene product called merlin that inhibits directly PAK1, an oncogenic Rac/CDC42-dependent Ser/Thr kinase. It was demonstrated previously that PAK1 is essential for the growth of both NF1 and NF2 tumors. Thus, several anti-PAK1 drugs, including FK228 and CEP-1347, are being developed for the treatment of NF tumors. However, so far no effective NF therapeutic is available on the market. Since propolis, a very safe healthcare product from bee hives, contains anticancer ingredients called CAPE (caffeic acid phenethyl ester) or ARC (artepillin C), depending on the source, both of which block the oncogenic PAK1 signaling pathways, its potential therapeutic effect on NF tumors was explored *in vivo*. Here it is demonstrated that Bio 30, a CAPE-rich water-miscible extract of New Zealand (NZ) propolis suppressed completely the growth of a human NF1 cancer called MPNST (malignant peripheral nerve sheath tumor) and caused an almost complete regression of human NF2 tumor (Schwannoma), both grafted in nude mice. Although CAPE alone has never been used clinically, due to its poor bioavailability/water-solubility, Bio 30 contains plenty of lipids which solubilize CAPE, and also includes several other anticancer ingredients that seem to act synergistically with CAPE. Thus, it would be worth testing clinically to see if Bio 30 and other CAPE-rich propolis are useful for the treatment of NF patients. Copyright © 2008 John Wiley & Sons, Ltd.

Keywords: propolis; CAPE; neurofibromatosis; NF1; NF2; Bio 30; MM; AIDS; Fragile X syndrome.

INTRODUCTION

Propolis from bee hives (also called 'bee wax') contains a 100 million years of wisdom of bee colonies protecting their larva from a variety of diseases. Propolis has been used since ancient Egypt times as a traditional/folk medicine for the treatment of infection, wound and inflammation as well as for preparing mummies. Entering our modern era, propolis was first identified as an anticancer remedy in the late 1980s when Dezider Grunberger's group at Columbia University found that CAPE (caffeic acid phenethyl ester) was the major anticancer ingredient in a propolis sample from Israel (Grunberger *et al.*, 1988). CAPE is a derivative of caffeic acid (CA) that down-regulates the GTPase Rac, a direct activator of the kinase PAK1 (Xu *et al.*, 2005). As a consequence, CAPE eventually inactivates PAK1. Interestingly, a propolis from New Zealand (NZ) reportedly showed the highest CAPE content (6–7% of extract) of a variety of propolis samples from around the world, whereas Brazilian green propolis contains another anticancer ingredient called ARC (artepillin C), instead of CAPE, which also inactivates PAK1 (Maruta and Ohta, 2008).

Recently we and others have shown that more than 70% of human cancers and all NF (neurofibromatosis) tumors are highly dependent on PAK1 for their growth, but not normal cells (Sasakawa *et al.*, 2003; Hirokawa *et al.*, 2004, 2005a, 2005b; Maruta and Ohta, 2008). Dysfunction of the *NF1* gene coding a RAS GAP is the major cause of type 1 NF, whereas type 2 NF is caused primarily by dysfunction of the *NF2* gene product called merlin that inhibits directly PAK1, a Rac/CDC42-dependent Ser/Thr kinase (Hirokawa *et al.*, 2004). Several years ago, *NF1*-deficient tumors were shown to require PAK1 for their growth *in vivo*, and more recently it was found that *NF2*-deficient tumors also require the same kinase for their growth *in vitro* (Hirokawa *et al.*, 2004). However, so far no effective NF therapeutic is available on the market. Thus, we have been developing a series of anti-PAK1 drugs which would be useful for the treatment of these PAK1-dependent cancers or tumors. Of the anti-PAK1 drugs/ingredients that have been identified or developed for the treatment of NF1

* Correspondence to: Hiroshi Maruta, NF Cure Japan, 6 Shiel Street, North Melbourne, Australia 3051.
E-mail: maruta19420@hotmail.com
Contract/grant sponsor: DFG (Deutsche Forschungsgemeinschaft).
Contract/grant sponsor: NF CURE Japan.
Contract/grant sponsor: US DOD; contract/grant number: NF050145.
Contract/grant sponsor: The Peterson Foundation in Philadelphia.
Contract/grant sponsor: NIH Biocurrents Research Center at MBL; contract/grant number: P41 RR001395.

Received 10 February 2008
Revised 12 April 2008
Accepted 9 May 2008

and NF2 tumors, a natural ring peptide FK228 appears to be the most potent both *in vitro* and *in vivo*. The IC_{50} for NF tumor cells is around 5 pM *in vitro*, and causes the complete regression of *NF1*-deficient MPNST xenograft in mice (Hirokawa *et al.*, 2005b). Its direct target is an HDAC (histone deacetylase), and it activates a specific set of tumor suppressor genes such as p21 (a CDK inhibitor) and RAP1a (a RAS antagonist), which eventually block both up-stream and down-stream of PAK1 (Hirokawa *et al.*, 2005a). Unfortunately, FK228 is still in clinical trials (phase 2) for cancers, but not for NF, and it would take several more years for this powerful drug to enter NF trials, and eventually to give any benefit to NF patients.

So we have recently started developing anti-PAK1 ingredients from natural products which are inexpensively available on the market, hoping to give the immediate benefit to NF patients. The first natural anti-PAK1 ingredient(s) was found in an ethanol extract of Chinese (Sichuan) pepper which selectively blocks PAK1 activation, but not another kinase called AKT (Hirokawa *et al.*, 2006). This extract suppresses the growth of *NF1*-deficient cancer xenografts in mice by 50%. More recently we found there was a much more potent natural anti-NF therapeutic called 'Bio 30'. It is a water-miscible CAPE-rich extract of NZ (New Zealand) propolis. This study demonstrates that Bio 30 suppressed completely the growth of both NF1 and NF2 tumor xenografts in mice, suggesting the possibility that Bio 30 and other CAPE-rich propolis might serve as the first effective and very safe NF therapeutic inexpensively available on the market.

MATERIALS AND METHODS

Tumor xenografts in mice. 6-week-old female nu/nu mice (from Charles River or NCI) received 5 million MPNST (S-462) cells (Hirokawa *et al.*, 2005b, 2006) or 2–5 million *NF2*-deficient Schwannoma (HEI-193) cells (Prabhakar *et al.*, 2007; Lepont *et al.*, 2008) of human origin in 0.2 mL of 50% Matrigel per mouse subcutaneously in the flank or thigh. When the average size of the tumors reached around 5 mm diameter (length or width), groups of 5–7 mice were treated with either Bio 30 (100–300 mg/kg) alone or CAPE 60 (Bio 30 plus extra 5 mg/kg CAPE) i.p., twice a week, while the control mice were treated with the vehicle (11% propylene glycol and 26% DMSO in PBS). The size of each tumor (both the original and metastasized) was measured twice a week by calliper. None of these treatments caused any adverse effect on the mice.

Cell culture. 10^3 cells of MPNST or Schwannoma cell lines were seeded per well, and cultured for 3–6 days, in the presence or absence of Bio 30, CAPE or ARC at various concentrations and the growth was monitored by either directly counting viable cells with a hemocytometer or MTT method (measuring the optical density at 550 nm) as described previously (Mosmann, 1983; Hirokawa *et al.*, 2006).

Polyphenol content analysis of Bio 30. The Bio 30 (alcohol-free liquid) sample was extracted by ethyl acetate and subjected to liquid chromatography to analyse its major polyphenols including CAPE by the tandem mass spectrometric method described previously (Celli *et al.*, 2004).

RESULTS AND DISCUSSION

Effect of Bio 30 on the growth of NF1 and NF2 tumor cells *in vitro*

Since it was found that Bio 30 (Manuka Health, NZ) was more potent than the Chinese pepper extract (Hirokawa *et al.*, 2006) in inhibiting the growth of PAK1-dependent pancreatic and breast cancer cell lines both *in vitro* and *in vivo* (Y. Hirokawa and H. Maruta, unpublished observation), its effect on NF tumor cell lines was examined *in vitro* to begin with. The IC_{50} of Bio 30 for NF2 tumor (HEI-193) and NF1 cancer (MPNST/ S-462) cells turned out to be around 1.5 μg/mL and 8 μg/mL, respectively (see Fig. 1).

Effects of Bio 30 on the growth (or metastasis) of NF tumor xenografts in mice

Effect on the growth of *NF1*-deficient MPNST. Bio 30 (100 mg/kg, i.p., twice a week) suppressed completely

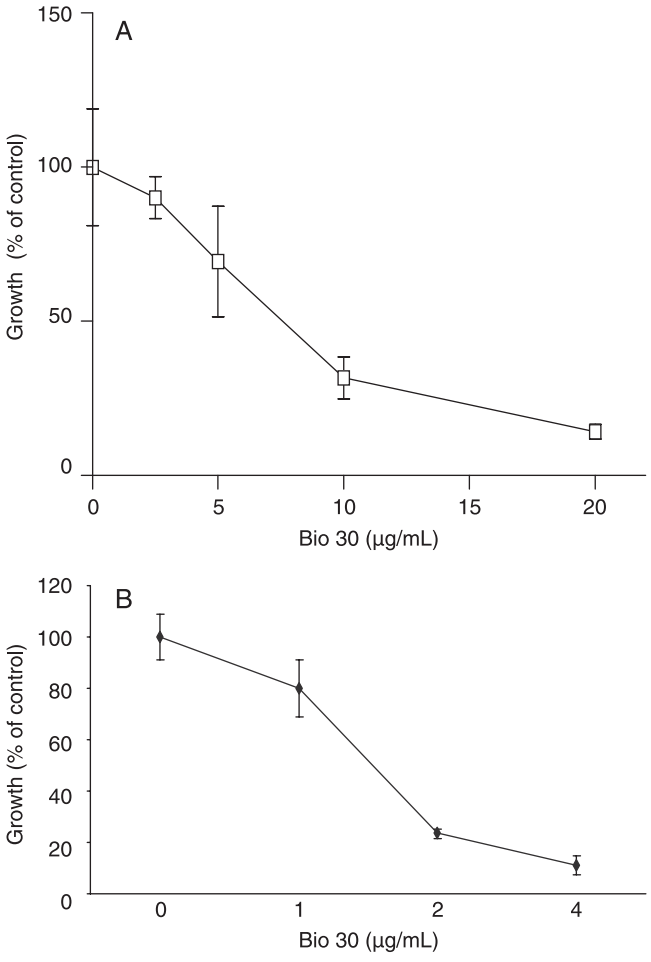

Figure 1. Bio 30 inhibits the growth of NF tumor cells MPNST (A) and Schwannoma (B) cells cultured for 6 days in the presence or absence of Bio 30 at the concentrations indicated as described under Materials and Methods.

DOI: 10.1002/ptr

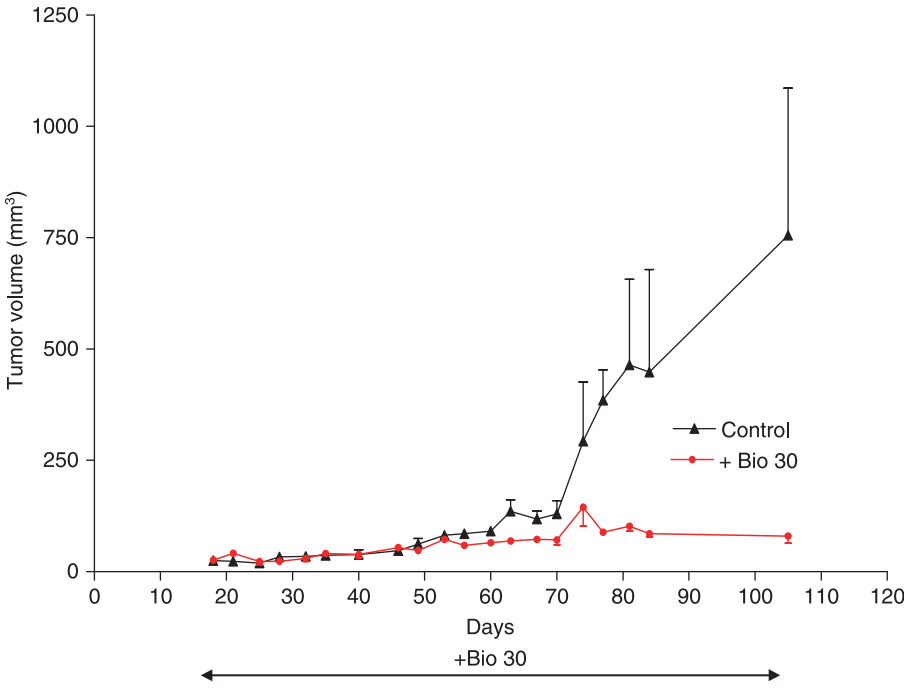

Figure 2. Bio 30 suppresses the growth of MPNST *in vivo* in nude mice bearing MPNST on the flank were treated with Bio 30 (100 mg/kg), i.p., twice a week during days 19–100, as described under Materials and Methods. Each group consisted of five mice.

the slow growth of MPNST /S-462 xenograft in mice over 100 days (see Fig. 2). Since this MPNST is poorly angiogenic, it remains dormant for the first 10 weeks until the blood vessel forms sufficiently around a tiny tumor (around 5–6 mm in a diameter). Then tumors in the control mice burst to growth. However, tumors in the Bio 30-treated mice failed to grow, probably because the CAPE-rich propolis blocked the angiogenesis, in addition to cell division and metastasis of the MPNST cells.

Effects on the highly metastatic *NF1*-deficient MPNST. It was found that the MPNST became highly metastatic and grew much more slowly if MPNST cells were inoculated in the thigh of a back leg, instead of the flank. This provided a good opportunity to examine the antimetastatic effect of Bio 30 (100 mg/kg) alone or its combination with an extra CAPE (5 mg/kg) called 'CAPE 60' (containing 60 mg of CAPE, instead of 12 mg of CAPE, per g of Bio 30 extract) on the MPNST. At around 6 weeks, the metastasis of tumors began in the control mice (Fig. 3). However, in the Bio 30 (alone)-treated mice, the total number of metastasized tumors was reduced significantly. Furthermore, extra CAPE significantly delayed the onset of metastasis and enhanced the antimetastatic effect of Bio 30. In addition, Bio 30 alone or its combination with extra CAPE (CAPE 60) caused the regression of MPNST: while all the control mice bore tumors, a third of Bio 30-treated mice and two thirds of CAPE 60-treated mice lost the tumors completely over 10 weeks. PAK1 is known to be essential for anchorage-independent growth, mestastasis

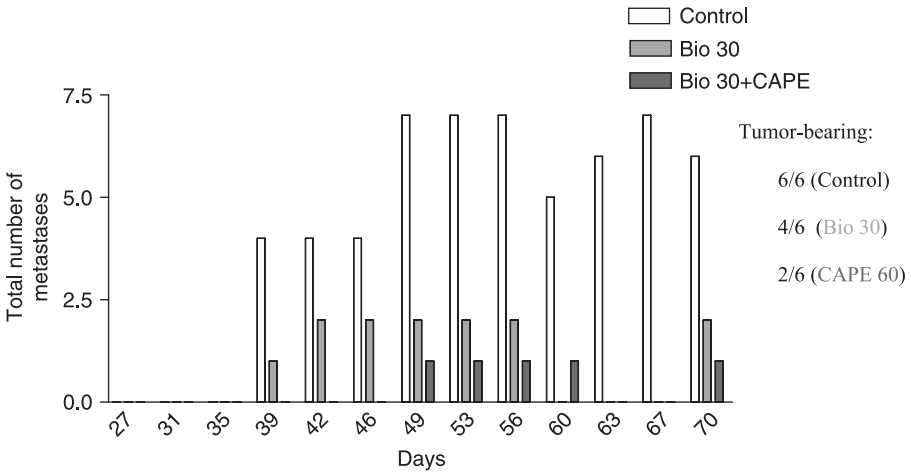

Figure 3. Bio 30 alone or its combination CAPE 60 blocks metastasis of MPNST in nude mice bearing MPNST on the thigh treated with either Bio 30 (100 mg/kg) alone or CAPE 60, i.p., twice a week during days 27–63, as described under Materials and Methods. Each group consisted of six mice. While all the control mice continued carrying tumors, the Bio 30 alone-treated mice lost two original tumors, and the CAPE-treated mice lost four original tumors by day 63. The number of metastasized tumors represents the total number of those in each group, and not the average per mouse of each group.

DOI: 10.1002/ptr

and angiogenesis of cancers in general (Kiosses *et al.*, 2002; Maruta and Ohta, 2008). These observations together strongly suggest that CAPE is the limiting antitumor ingredient of Bio 30, and extra CAPE would boost both its antimetastatic and antimitotic (or/and antiangiogenic) effects on the MPNST. The richer in CAPE, the more therapeutic a propolis might be (on NF tumors).

Effect on the growth of *NF2*-deficient Schwannoma

Bio 30 alone (100 mg/kg, i.p., twice week) caused an almost complete regression of the fast-growing human *NF2*-deficient Schwannoma (HEI-193) xenograft in mice over 30 days (see Fig. 4A). This regression occurred only when the drug treatment started at an early stage of tumor growth (with the average volume of tumors being around 150 mm^3).

However, if the treatment started after the tumor size reached around 400 mm^3, the therapeutic effect of Bio 30 was hardly observed at this dose (data not shown). With the tripled dose (300 mg/kg), even if the drug treatment started when the tumor size reached over 600 mm^3, Bio 30 alone could suppress the growth of Schwannoma almost completely for 30 days (see Fig. 4B). This size

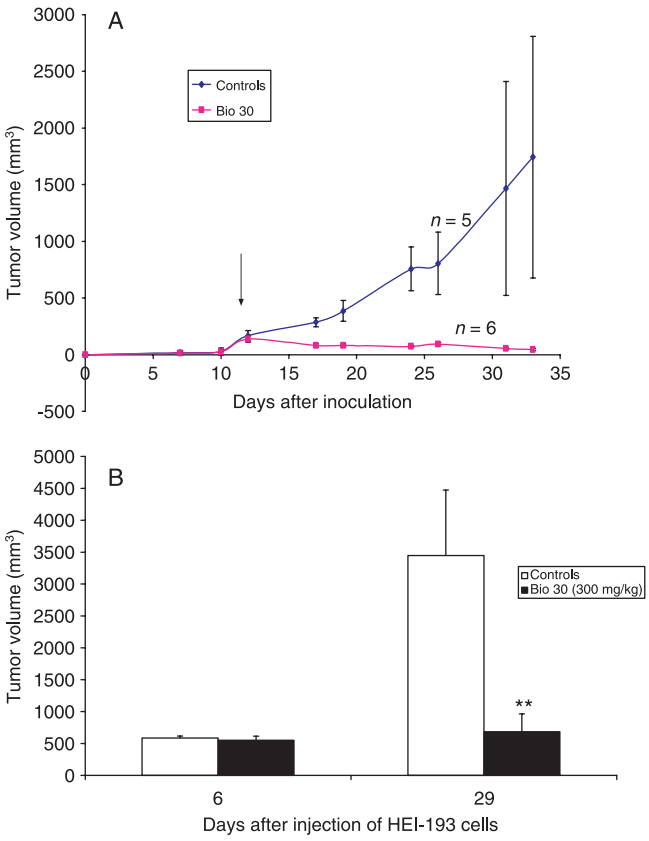

Figure 4. Bio 30 alone suppresses the growth of Schwannoma *in vivo* in nude mice bearing Schwannoma on the flank treated with (A) Bio 30 (100 mg/kg), during days 14–31, or (B) Bio 30 (300 mg/kg), during days 6–27, i.p., twice a week as described under Materials and Methods. (A) drug-treatment began when the average volume of tumors was around 150 mm^3, and (B) the treatment began when the tumor volume was just over 600 mm^3. Histogram (B): the control (blank, $n = 7$), and the Bio 30 treated (filled, $n = 7$).

Table 1. Major polyphenol content of Bio 30

Compound	mg/g
Pinocembrin	110
Galangin[a]	60
Chrysin[a]	30
CAPE[a]	12
CA[a]	12
Apigenin[a]	12

The ethyl acetate extract of Bio 30 was analysed as described under Materials and Methods.
The source of Bio 30 was Manuka Health, Auckland, New Zealand.
[a]Anticancer compounds.

of NF2 tumors in mice (weighing around 20 g) is equivalent to that of a fairly large NF2 tumor (over 1.5 kg) for people (weighing around 50 kg). These observations seem to parallel the clinical situation in that the earlier the treatment begins, the better the chance of complete tumor regression.

CAPE alone versus Bio 30

Propolis such as Bio 30 contains plenty of lipids which solubilize CAPE and a few other anticancer polyphenols such as galangin, chrysin and apigenin (see Table 1). Furthermore, CAPE appears to work synergistically with these other polyphenols in Bio 30 to suppress the growth of these NF tumor cells at least *in vitro*. For instance, as mentioned before, the IC_{50} of Bio 30 for the Schwannoma cell line is around 1.5 μg/mL. Since the CAPE content of this propolis extract is only 1.2% (12 mg/g of extract), the contribution of CAPE alone to 1.5 μg/mL of Bio 30 is only around 18 ng/mL, that is to say, around 60 nM. The IC_{50} of CAPE alone for the same cells is as high as about 36 μM (see Fig. 5) which

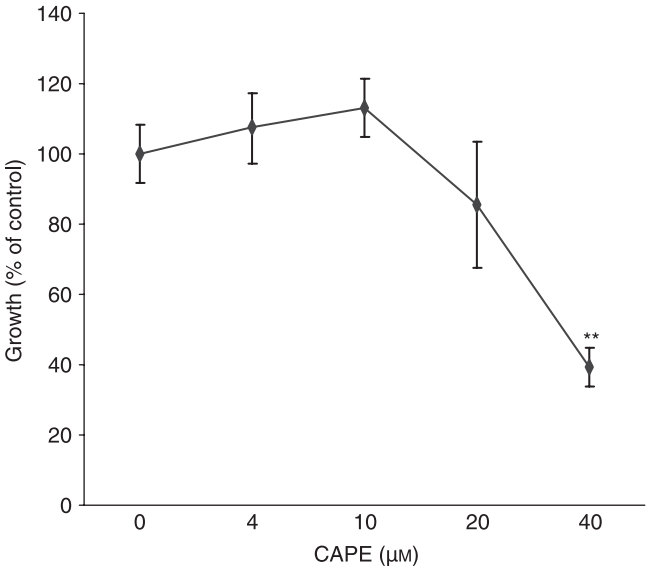

Figure 5. IC_{50} of CAPE alone for the growth of Schwannoma cells. Cells were cultured for 6 days in the presence or absence of CAPE at the indicated concentrations, and the cell growth was monitored as described in Fig. 1B.

DOI: 10.1002/ptr

is around 600 times higher than 60 nM. Since the IC_{50} of a few other anticancer ingredients such as galangin, chrysin and apigenin is known to be around a similar range (10–40 μM) for various cancer cells (Murray *et al.*, 2006; Maruta and Ohta, 2008), it is most likely that CAPE acts synergistically (rather than simply additively) with these anticancer ingredients in Bio 30. In other words, the water-miscible Bio 30 would be far more effective than the water-insoluble CAPE alone for the treatment of NF tumors. Besides propolis in general is known to have an additional (indirect) anticancer function that boosts the immune system, in particular the lytic action of natural killers against tumor cells, and the antibody production (Sforcin, 2007).

Bio 30 trials

Since Bio 30 is a very safe healthcare food supplement, a trial is being conducted of Bio 30 (daily oral treatment with a dose of 25 mg/kg) for, so far, around 70 patients of body weight over 25 kg (or over 10 years old) who are suffering from either NF or formidable cancers such as melanoma and pancreatic cancers in which RAS is mutated and therefore PAK1 is abnormally activated. Its daily cost per person (adult) is only a dollar. The only minor potential problem with CAPE-based propolis such as Bio 30 is that less than 5% of people are allergic to CAPE. In our Bio 30 trial, so far only one person has shown an allergic skin rash, and switched to ARC-based Brazilian green propolis which does not cause any allergy but costs around 10 times as much as Bio 30.

Although our trial is still at a very early stage (less than 12 months for NF1 patients and 6 months for NF2 and a few other cancer patients), so far the majority of these patients showed a positive outcome from Bio 30, namely no further growth of their tumors.

It is our hope that this work will set the stage, a milestone for much more sophisticated and comprehensive clinical studies in the future for testing the effect of Bio-30 not only on the growth of NF tumors and PAK1-dependent formidable cancers such as pancreatic cancers, melanomas and MM (multiple myeloma), but also several other PAK1-dependent diseases such as AIDS (HIV-infection) and Fragile X mental retardation syndrome (Nguyen *et al.*, 2006; Hayashi *et al.*, 2007; Porchia *et al.*, 2007; Zhang *et al.*, 2007; Maruta and Ohta, 2008).

Acknowledgement

This work was supported in part by funds from DFG (Deutsche Forschungsgemeinschaft) to HM, NF CURE Japan to VM and SMM, and US DOD (No. NF050145) to VM, and The Peterson Foundation in Philadelphia to SMM. Support was also received from the NIH Biocurrents Research Center at MBL (P41 RR001395). Bio 30 was kindly provided by Manuka Health, New Zealand.

REFERENCES

Celli N, Mariani B, Dragani LK *et al.* 2004. Development and validation of a liquid chromatographic-tandem mass spectrometric method for the determination of caffeic acid phenethyl ester in rat plasma and urine. *J Chromatogr B Analyt Technol Biomed Life Sci* **810**: 129–136.

Grunberger D, Banerjee R, Eisinger K *et al.* 1988. Preferential cytotoxicity on tumor cells by caffeic acid phenethyl ester isolated from propolis. *Experientia* **44**: 230–232.

Hayashi ML, Rao BS, Seo JS *et al.* 2007. Inhibition of p21-activated kinase rescues symptoms of fragile X syndrome in mice. *Proc Natl Acad Sci USA* **104**: 11489–11494.

Hirokawa Y, Arnold M, Nakajima H *et al.* 2005a. Signal therapy of breast cancer xenograft in mice by the HDAC inhibitor FK228 that blocks the activation of PAK1 and abrogates the tamoxifen-resistance. *Cancer Biol Ther* **4**: 956–960.

Hirokawa Y, Nakajima H, Hanemann O *et al.* 2005b. Signal therapy of NF1-deficient tumor xenograft in mice. *Cancer Biol Ther* **4**: 379–381.

Hirokawa Y, Nheu T, Grimm K *et al.* 2006. Sichuan pepper extracts block the PAK1/Cyclin D1 pathway and the growth of NF1-deficient cancer xenograft in mice. *Cancer Biol Ther* **5**: 305–309.

Hirokawa Y, Tikoo A, Huynh J *et al.* 2004. A clue to the therapy of neurofibromatosis type 2: NF2/merlin is a PAK1 inhibitor. *Cancer J* **10**: 20–26.

Kiosses WB, Hood J, Yang S *et al.* 2002. A dominant-negative p65 PAK peptide inhibits angiogenesis. *Circ Res* **90**: 697–702.

Lepont P, Stickney JT, Foster LA *et al.* 2008. Point mutation in the NF2 gene of HEI-193 human Schwannoma cells results in the expression of a merlin isoform with attenuated growth suppressive activity. *Mutat Res* **637**: 142–151.

Maruta H, Ohta T. 2008. Signal therapy: propolis and pepper extracts as cancer therapeutics. In *Complementary and Alternative Therapies and the Aging Population*, Watson RR (ed.). Elsevier Inc: San Diego, in press.

Mosmann T. 1983. Rapid colorimetric assay for cellular growth and survival: application to proliferation and cytotoxicity assays. *J Immunol Methods* **65**: 55–63.

Murray TJ, Yang X, Sherr DH. 2006. Growth of a human mammary tumor cell line is blocked by galangin, a naturally occurring bioflavonoid, and is accompanied by down-regulation of cyclins D3, E, and A. *Breast Cancer Res* **8**: R17.

Nguyen DG, Wolff KC, Yin H *et al.* 2006. 'UnPAKing' human immunodeficiency virus (HIV) replication: using small interfering RNA screening to identify novel cofactors and elucidate the role of group I PAKs in HIV infection. *J Virol* **80**: 130–137.

Porchia LM, Guerra M, Wang YC *et al.* 2007. 2-Amino-N-{4-[5-(2-phenanthrenyl)-3-(trifluoromethyl)-1H-pyrazol-1-yl]-phenyl} acetamide (OSU-03012), a celecoxib derivative, directly targets p21-activated kinase. *Mol Pharmacol* **72**: 1124–1131.

Prabhakar S, Messerli S, Stemmer-Rachamimov A *et al.* 2007. Treatment of implantable NF2 Schwannoma tumor models with oncolytic herpes simplex virus G47Delta. *Cancer Gene Ther* **14**: 460–467.

Sasakawa Y, Naoe Y, Inoue T, Sasakawa T *et al.* 2003. Effects of FK228, a novel histone deacetylase inhibitor, on tumor growth and expression of p21 and c-myc genes *in vivo*. *Cancer Lett* **195**: 161–168.

Sforcin JM. 2007. Propolis and the immune system: a review. *J Ethnopharmacol* **113**: 1–14.

Xu JW, Ikeda K, Kobayakawa A *et al.* 2005. Down-regulation of Rac1 activation by caffeic acid in aortic smooth muscle cells. *Life Sci* **76**: 2861–2872.

Zhang S, Suvannasankha A, Crean CD *et al.* 2007. OSU-03012, a novel celecoxib derivative, is cytotoxic to myeloma cells and acts through multiple mechanisms. *Clin Cancer Res* **13**: 4750–4758.

Carcinogenesis vol.27 no.3 pp.664–671, 2006
doi:10.1093/carcin/bgi273
Advance Access publication December 15, 2005

Mutation and expression of *PDGFRA* and *KIT* in malignant peripheral nerve sheath tumors, and its implications for imatinib sensitivity

Nikola Holtkamp*, Ali Fuat Okuducu, Jana Mucha, Anastasia Afanasieva, Christian Hartmann, Isis Atallah, Lope Estevez-Schwarz[1], Christian Mawrin[2], Reinhard E.Friedrich[3], Victor-F.Mautner[3] and Andreas von Deimling

Institute of Neuropathology, Charité — Universitätsmedizin Berlin, Germany, [1]Department of Surgery and Surgical Oncology, Robert-Rössle-Hospital, Berlin, Germany, [2]Department of Neuropathology, Otto-von-Guericke-University, Magdeburg, Germany and [3]Department of Oral and Maxillofacial Surgery, University Hospital Eppendorf, Hamburg, Germany

*To whom correspondence should be addressed. Tel: +49 30 450 536042; Fax: +49 30 450 536940;
Email: nikola.holtkamp@charite.de

Platelet-derived growth factor receptor alpha (PDGFRα) and c-Kit are receptor tyrosine kinases. Both are targets of the tyrosine kinase inhibitor imatinib mesylate which is approved for treatment of some cancers. In order to assess the role of PDGFRα and c-Kit in malignant peripheral nerve sheath tumours (MPNST) we examined human tumours for structural alterations, protein and ligand expression. We investigated 34 MPNST, 6 corresponding plexiform neurofibromas (pNF) and 1 MPNST cell culture from 31 patients for mutations and polymorphisms in *PDGFRA* (exon 2–21) and *KIT* (exon 9, 11, 13, 17). *PDGFRA* was amplified in seven tumours from six patients and MPNST cell culture S462. *KIT* was amplified in five tumours from four patients and in the cell culture. Two MPNST carried somatic *PDGFRA* mutations in exons coding for the extracellular domain. In addition we detected several polymorphisms in *PDGFRA*. No point mutations or polymorphisms were detected in the four *KIT* exons analysed. PDGFRα expression was present in 21 of 28 MPNST patients (75%) and the MPNST cell culture. Expression analysis of PDGFRα ligands in MPNST and neurofibromas revealed that PDGF-A was more widely expressed than PDGF-B. Focal c-Kit expression was detected in 2 of 29 (7%) MPNST patients. Imatinib treatment of MPNST cell culture S462 exerted a growth inhibitory effect and prevented PDGF-AA induced PDGFRα phosphorylation. In summary, *PDGFRA*, *PDGF* and *KIT* dysregulation as well as growth inhibition of cell culture S462 by imatinib may suggest that MPNST patients benefit from treatment with imatinib.

Introduction

Malignant peripheral nerve sheath tumours (MPNST) are very aggressive tumours with poor prognosis. Approximately half of the MPNST occur in the setting of Neurofibromatosis type 1 (NF1), a hereditary tumour syndrome with an incidence of 1:3500 (1). MPNST in NF1 patients is the major cause for reduced life expectancy with only 21% of NF1 patients surviving longer than 5 years after diagnosis of MPNST (2).

The *NF1* gene on chromosome 17q11.2 encodes the large protein neurofibromin, which acts as negative regulator of ras. Functional neurofibromin is lost in NF1 associated nerve sheath tumours. However, not much is known about additional molecular aberrations underlying transformation or malignant progression of nerve sheath tumours. However, *TP53* and *CDKN2A* have been shown to harbour mutations in a subgroup of MPNST (3–5). In addition, gene amplification and increased transcription of *EGFR* have been detected in MPNST (6,7). MPNST in NF1 patients frequently arise from malignant progression of plexiform neurofibromas (pNF). Dermal neurofibromas (dNF), which develop in nearly all NF1 patients, virtually have no risk of malignant transformation. With the exception of *NF1* loss, little is known about genetic aberrations in neurofibromas.

We have recently demonstrated higher expression of platelet-derived growth factor receptor alpha (PDGFRα) in MPNST than in benign nerve sheath tumours (8). Because ligands of PDGFRα are powerful mitogens for Schwann cells (9), the PDGF system might contribute to malignant progression of nerve sheath tumours. The PDGF system is complex with two receptor genes forming three receptor types (PDGFRα and PDGFRβ homodimers and PDGFRαβ heterodimers). These receptors may bind ligands encoded by four genes building at least five different dimers (PDGF-AA, PDGF-AB, PDGF-BB, PDGF-CC and PDGF-DD) with different receptor-binding specificities (10). Expression of c-Kit and its ligand stem cell factor was found in MPNST cell cultures (11,12) and c-Kit expression was documented in an MPNST (13).

PDGFRα and c-Kit belong to the type III subfamily of receptor tyrosine kinases. Both have been reported to be strongly expressed and/or mutated in gastrointestinal stromal tumours (GIST) and gliomas (14,15).

PDGFRA and *KIT* have attracted special attention since it became evident that their protein products were among the tyrosine kinases inhibited by imatinib mesylate (Glivec®, STI571). Imatinib treatment yields high response rates in patients with GIST and chronic myeloid leukemia (CML) (16,17). The major target of imatinib in GIST is mutant c-Kit, whereas the inhibited kinase in CML is the Bcr–Abl fusion protein. Successful treatment with imatinib has also been reported for patients with dermatofibrosarcoma protuberans. This disease is characterized by a chromosomal translocation leading to overexpression of PDGF-B, which is bound by all 3 PDGF receptor types (18).

Our previous findings of increased PDGFRα levels in MPNST led us to examine MPNST for activating mutations or amplifications. Activation of PDGFRα and c-Kit would

Abbreviations: DMSO, dimethylsulfoxide; GIST, gastrointestinal stromal tumours; MPNST, malignant peripheral nerve sheath tumours; NF1, neurofibromatosis type 1; PDGFRα, platelet-derived growth factor receptor alpha; pNF, plexiform neurofibromas.

Table I. Primer sequences and product size

	Forward	Reverse	Product size in bp
DNA primer			
KIT exon 9a	TTTCCTAGAGTAAGCCAGGGC	GTTGTAAGCCTTACATTCAACCG	180
KIT exon 9b	AGTGCATTCAAGCACAATGG	GACAGAGCCTAAACATCCCC	146
KIT exon 11	CTATTTTTCCCTTTCTCCCC	TACCCAAAAAGGTGACATGG	193
KIT exon 13	TTTGCCAGTTGTGCTTTTTG	CAGCTTGGACACGGCTTTAC	176
KIT exon 17	TGGTTTTCTTTTCTCCTCCAA	TGCAGGACTGTCAAGCAGAG	185
PDGFRA exon 2	TCCAGGGTTGTTTCTATTTGC	GACACCCAAACAAGGAACTCA	157
PDGFRA exon 3/1	CCTATTCAGAGCGTGCTTCC	AGGCCGCTGTTGTTTTCTT	218
PDGFRA exon 3/2	GGGGAGAGTGAAGTGAGCTG	CCAACTCACCTGGCACATAG	226
PDGFRA exon 4/1	TCTGGATTTATGTGTAAAGGTGAAA	TCCCATTAAAGCCCTGTCTG	239
PDGFRA exon 4/2	TCCCGAGACTCCTGTAACCTT	CACGCACCTTATGATTTTGC	229
PDGFRA exon 5	TGTGGATTTTTAGGCCCTTG	CATTGCACGTTTTGAGGGTA	195
PDGFRA exon 6	GGTTTTCTTCCCCTTTTGCT	GCAGCATGGACAACTGACAT	235
PDGFRA exon 7	CTCGGGATCCATATGTGGTAA	CGCCTCTGATGCACACTAAA	295
PDGFRA exon 8	TGCTTGTTGAAACAAAATCCTTT	CACTCATCTACAGAGCTAGCATTATC	194
PDGFRA exon 9	TCTGGGACACGAGCTATTCC	CTGACCACGAAAGAAGAAGACA	212
PDGFRA exon 10	GGCCCTATACTTAGGCCCTTT	TCCTGACTGTTGAGGAACTCAC	247
PDGFRA exon 11	GCATGTCTGCCAGGAAACTT	TGCTTGTTCTCATTGGCTTC	197
PDGFRA exon 12	TCCAGTCACTGTGCTGCTTC	GCAAGGGAAAAGGGAGTCTT	261
PDGFRA exon 13	CGTCTGGAGTTTTTGGGTGT	CCCCAGGAAGGAGCACTTAC	167
PDGFRA exon 14	GCTCAGCTGGACTGATATGTGA	CCAGTGAAAATCCTCACTCCA	185
PDGFRA exon 15	ACCCATCTCCTAACGGCTTT	CAGCAACATCTCTCTTTGCAC	210
PDGFRA exon 16	GGCACCCTGGGTAAGATTTC	CACTGGAAAGTCCCAACACC	248
PDGFRA exon 17	CCTGCCAGCACCAATACAT	GGGTCTAAAAAGGTCTGTGTTCC	186
PDGFRA exon 18	ACCATGGATCAGCCAGTCTT	TGAAGGAGGATGAGCCTGACC	252
PDGFRA exon 19	AACTGTCTCCCTCCTTCCTTG	GCCCAAATAAGCAGCAATGT	167
PDGFRA exon 20	TGGTGTTTTATTGTTTGGCTTTT	CCCCCTAGACCCACAGACT	180
PDGFRA exon 21	TCTTGAGTTCTGTCCCCACA	CACCCACAGATCCAAACACA	148
Desmin exon 8	ACTCCCAGCCCCTGGTATAG	AGGGTAAGGAGCCCAGACAG	180
cDNA primer			
PDGFRA fragment 1	GACTTCCCATCCGGCGTTC	TTGACCTCCCTGGTAGCCT	894
PDGFRA fragment 2	TGGAGATTACGAATGTGCTG	CCAAGCACTAGTCCATCTCT	933
PDGFRA fragment 3	CTTATGACTCAAGATGGGAG	CAGACATCACTCAGTGTGGT	954
PDGFRA fragment 4	CTCCTGAGAGCATCTTTGAC	AAGTGGAAGGAACCCCTCGA	712
PDGFA	ACACGAGCAGTGTCAAGTGC	GGCTCATCCTCACCTCACAT	200
PDGFB	GGCATGCAAGTGTGAGACAG	GTCTTGTCATGCGTGTGCTT	171
RPS3	CTGGGCATCAAGGTGAAGAT	AGACCCTGTTATGCTGTGGG	205

render MPNST attractive candidates for imatinib treatment. Since there are only limited treatment options for MPNST patients new treatment possibilities are required.

Materials and methods

Tumour tissue, DNA and RNA extraction

Tumour samples were collected from University Hospital Eppendorf (Hamburg, Germany), Robert-Rössle-Hospital (Berlin, Germany), Otto-von-Guericke-University (Magdeburg, Germany) and Charité University Hospital (Berlin, Germany). The study contained 40 nerve sheath tumours (34 MPNST and 6 pNF) from 31 patients and MPNST cell culture S462, which was established from MPNST 24472 (19). Twenty-six patients were diagnosed with NF1. Following initial diagnosis in local neuropathologies, all tumour samples were reviewed by the same pathologist (A.F.O.). Histopathological examination was based on the modified FNCLCC system (20). Eleven tumour samples have already been analysed for gene expression profiles (6). Before extraction of DNA, RNA and protein tumour samples were examined by histology to exclude contaminating non-tumourous portions. In case of frozen material DNA and RNA was extracted using TRIzol reagent from Invitrogen (Karlsruhe, Germany). DNA extraction from paraffin embedded material was carried out according to the QIAamp DNA Mini Kit protocol (Qiagen, Hilden, Germany). Four MPNST (24626, 24772, 24776 and 24324) contained adjacent pNF tissue. DNA from pNF and MPNST areas were separately extracted. A c-Kit positive GIST was kindly provided by Prof. Gottschalk (Hamburg) and served as positive control for immunohistochemistry. Microdissection of skeletal muscle and vascular endothelial cells was performed with two cases (24748 and 24772) because blood was not available. The PALM Laser Microbeam System (Bernried, Germany) was employed to dissect ~2000 cells from paraffin sections stained with toluidine blue as described previously (21). The investigations were carried out with the informed consent of the patients.

SSCP and sequencing

Electrophoresis of PCR products of *PDGFRA* exon 2–21 and *KIT* exon 9, 11, 13, 17 was performed on polyacrylamid gels applying 500 V and 6 mA for 18 h. All PCR products showing a mobility shift were confirmed by an independent PCR and compared with PCR products of corresponding normal tissue (blood or microdissected normal cells). Aberrantly migrating SSCP bands were excised and the DNA was extracted. After reamplification, PCR products were sequenced bidirectionally on a semiautomated sequencer (model 377; Applied Biosystems, Foster City, CA). Sequences were compared to *PDGFRA* NM_006206 and *KIT* X06182. Primer sequences are compiled in Table I. Amplification and gel conditions are available on request.

Gene amplification analysis by real-time PCR

Quantitative real-time PCR was performed with SYBR green I (1:5000 dilution, Molecular Probes, The Netherlands) using the ABI Prism 7700 Sequence Detection System (Applied Biosystems). PCR products of the target genes *KIT* (Exon 17, PCR product of 185 bp) and *PDGFRA* (Exon 21, PCR product of 148 bp) were compared to the reference gene *DES* (Exon 8, PCR product of 180 bp) on chromosome 2q35 encoding desmin. This region appears not to have gains of chromosomal material in MPNST (22). Primer sequences are given in Table I. PCR efficiency, determined by serial dilution of DNA, demonstrated similar results for target and reference genes. All samples were analysed in duplicate in 25 μl reaction mixes containing 1.25 U of Platinum *Taq* DNA Polymerase (Invitrogen). Amplification conditions are available on request. Evaluation of data were performed using the ΔΔCt method: $\Delta\Delta Ct = \Delta Ct$ tumour DNA $- \Delta Ct$ blood DNA. ΔCt (threshold cycles) is the Ct of the reference gene minus the Ct of the target gene. Fold increase of the target genes (*PDGFRA* and *KIT*) was calculated by $2^{(\Delta\Delta Ct)}$ and values of ≥ 1.7 were defined

as gene amplification. Tumours conspicuous for gene amplification were verified in an independent PCR run. DNAs from glioblastomas with known *PDGFRA* amplification served as positive controls (15).

RT–PCR analysis

RT of 2 μg DNA free RNA was achieved with the SuperScript™ First-Strand Synthesis System (Invitrogen). PCR were performed in a volume of 20 μl containing cDNA transcripts equivalent to 45 ng RNA. For the detection of large deletions in *PDGFRA* 10 MPNST (21852, 24784, 26580, 26582, 26584, 26586, 26588, 26592, 24472, 21914) and the cell culture S462 were analysed using four overlapping primer pairs covering the whole coding region of *PDGFRA*. Primer sequences are given in Table I. PCR fragments were separated on 1.5% agarose gels allowing size differences of 50 bp to be visualized. For semi-quantitative ligand determination 35 PCR cycles were performed for *PDGFA* and *PDGFB*, and 32 cycles were performed for the reference gene *RPS3*. Amplification conditions are available on request.

Immunohistochemistry and scoring

Immunohistochemistry was performed with a Ventana Benchmark™ automate (Ventana, Strasbourg, France). The antibodies against PDGFRα (C-20, dilution 1:100) and PDGF-A (N-30, dilution 1:50) were obtained from Santa Cruz Biotechnology (Heidelberg, Germany). The c-Kit antibody (A4502, dilution 1:400) was obtained from Dako (Hamburg, Germany). Antigen retrieval was enhanced by heating. Primary antibodies were incubated for 30 min at 40°C. Negative controls without primary antibodies were carried out and did not produce signals. Scoring was performed according to the percentage of positive cells: <5% was classified as negative (−), 6–100% was classified as positive. Positive cells (6–30%) were scored with +, 31–60% with ++, >60% with +++. A repeated test (blinded) gave similar results.

Immunocytochemistry

MPNST cells (2×10^4) per well were seeded on Permanox chamberslides (Nunc, Wiesbaden, Germany). Cells were fixed with acetone the following day. The same antibodies used for immunohistochemistry were applied in a 1:50 dilution. Incubation of primary antibodies was performed for 2 h at room temperature. Visualization was performed with Cy3- (Dianova, Hamburg, Germany) or Alexa488- (Invitrogen) conjugated anti-rabbit antibodies (dilution 1:100). Negative controls without primary antibodies were carried out and did not produce signals.

Western blot

Tumour lysates were heat denaturated and loaded on to 7.5% acrylamide gels for subsequent protein separation. After transfer of proteins to nitrocellulose membranes, the membranes were blocked in 3% non-fat dry milk with 0.05% Tween-TBS for 1 h and incubated overnight at 4°C with anti-PDGFRα antibody (C-20, dilution 1:200). After washing, the membranes were incubated for 1 h with biotin-conjugated second antibodies, washed and incubated 1 h with ExtrAvidin from Sigma (dilution 1:2000). Visualization was performed with ECL (Amersham Biosciences, Freiburg, Germany). Lysates were adjusted to β-actin expression levels which were determined with the anti-β-actin antibody AC-15 (dilution 1:6.000) from Sigma (Munich, Germany). Phosphorylation was detected with anti-p-Tyr (PY99, dilution 1:10.000) from Santa Cruz Biotechnology.

Cell culture assays

During imatinib inhibition the MPNST cell culture S462 (<18 passages) was maintained in DMEM Glutamax-I with 5% FBS from Invitrogen (Karlsruhe, Germany). Imatinib mesylate was kindly provided by Novartis Pharma AG (Basel, Switzerland) and dissolved in dimethyl sulphoxide (DMSO). Cells (2×10^3) were seeded in 300 μl medium into 24 well plates and were allowed to adhere. Imatinib was added in 100 μl to final concentrations of 2 μM and 10 μM with no more than 0.1% DMSO. Negative controls contained 0.1% DMSO only. The 300 μl of medium containing respective imatinib or DMSO concentrations were exchanged on day 3 and 5. Cell proliferation was evaluated on day 4 and 7 post-imatinib treatment with the CellTiter 96 AQueous One Solution Cell Proliferation Assay from Promega (Mannheim, Germany) by measurement of absorbance at 490 nm. The experiments were performed in duplicate and repeated thrice with comparable results.

Imatinib effect on PDGFRα phosphorylation was determined in 6 well plates in duplicates. Cells (5×10^5) were seeded per well in DMEM with 10% FBS. The next day medium was changed to serum-free DMEM. After 24 h imatinib or DMSO was added and cells were incubated for 30 min. Cells were then stimulated with PDGF-AA (50 ng/ml) for 10 min, washed with phosphate-buffered saline (PBS), scraped, centrifuged and resuspended in lysis buffer [1% Triton X-100, 100 mM NaCl, 50 mM Tris–HCl (pH 7.5) and 5 mM EDTA]. Protease inhibitor cocktail (Roche, Penzberg, Germany) and phosphatase inhibitor cocktail 2 (Sigma, Saint Louis, Missouri) were added.

Stimulation with PDGF-AA and PDGF-BB (Oncogene, San Diego, CA) was performed in 6 well plates with 50 ng PDGF per ml serum-free DMEM for 48 h. Each well contained 10^5 cells seeded in DMEM with 10% FBS. The next day medium was switched to serum-free DMEM. Cell line ST88-14 and DBTRG (kindly provided by A. Kurtz and E. Elstner) were cultured in DMEM Glutamax-I with 10% FBS.

Results

Mutations and polymorphisms

We investigated 34 MPNST, 6 pNF and 1 MPNST cell culture from 31 patients for *PDGFRA* mutations (exon 2–21) and *KIT* mutations (exon 9, 11, 13, 17). Because *KIT* mutations in GIST mostly occur in exon 9 and 11 but also in exon 13 and 17 we restricted our analysis to these four exons (23). We detected somatic *PDGFRA* mutations in 2 MPNST (Figure 1A and B). MPNST 24748 had a mutation in exon 4 (CCT>TCT, codon 130) leading to the non-conservative amino acid exchange from proline to serine. MPNST 24740 harboured a somatic mutation in exon 10 (GTC>GCC, codon 469) leading to an exchange from valine to alanine.

Because a transforming PDGFRα deletion mutant (loss of exon 8 and 9) was reported in a glioblastoma (24) we examined *PDGFRA* cDNA in order to detect large deletions that would not be recognized by SSCP. Analysis of 10 MPNST and cell culture S462 did not reveal large deletions (data not shown).

We found six different single nucleotide polymorphisms in *PDGFRA* which are listed in Table II. Three of 31 MPNST from individual patients were heterozygous for the 478Pro allel and exhibited allel frequencies of $f(Ser^{478}) = 0.950$ and $f(Pro^{478}) = 0.050$. To determine the allel frequency in the general population we investigated 150 blood samples. The allel frequency was $f(Ser^{478}) = 0.873$ and $f(Pro^{478}) = 0.127$. Individuals with the 478Pro variant in exon 10 also carried the silent polymorphism in exon 7. Recently, we detected the 478Pro polymorphism in 14 of 103 gliomas (13 heterozygous and 1 homozygous) (25). The allel frequency in glioma was $f(Ser^{478}) = 0.927$ and $f(Pro^{478}) = 0.073$.

The pNF 28572 and corresponding normal cells carried an allelic variant lacking 18 bp in exon 7. The 18 bp deletion variant seen in a single patient has not been reported before and we did not find it in 150 control individuals (data not shown). The four *KIT* exons analysed did not harbour mutations or polymorphisms.

Gene amplification of PDGFRA and KIT

PDGFRA and *KIT* amplification was investigated by real-time PCR. Eight samples (seven solid tumours and cell culture S462) from six patients showed *PDGFRA* amplification by a factor of 1.8 or more relative to the normal gene dose. *KIT* amplifications were detected in six samples (five tumours and cell culture S462) from four patients. Five samples (24472, 24784, 21914, 22318, cell culture S462) showed amplification of both, *PDGFRA* and *KIT*. Gene amplification results are summarized in Table III.

Expression of receptors PDGFRα and c-Kit

PDGFRα expression was determined in 32 MPNST from 28 patients. Immunoreactivity was observed on sections from 21 of 28 MPNST patients (75%). Twelve MPNST (38%) expressed PDGFRα in >60% of tumour cells, 7 MPNST (22%) in 31–60% of the tumour cells and 4 MPNST (13%) in 6–30% of the tumour cells. Five pNF were also evaluated

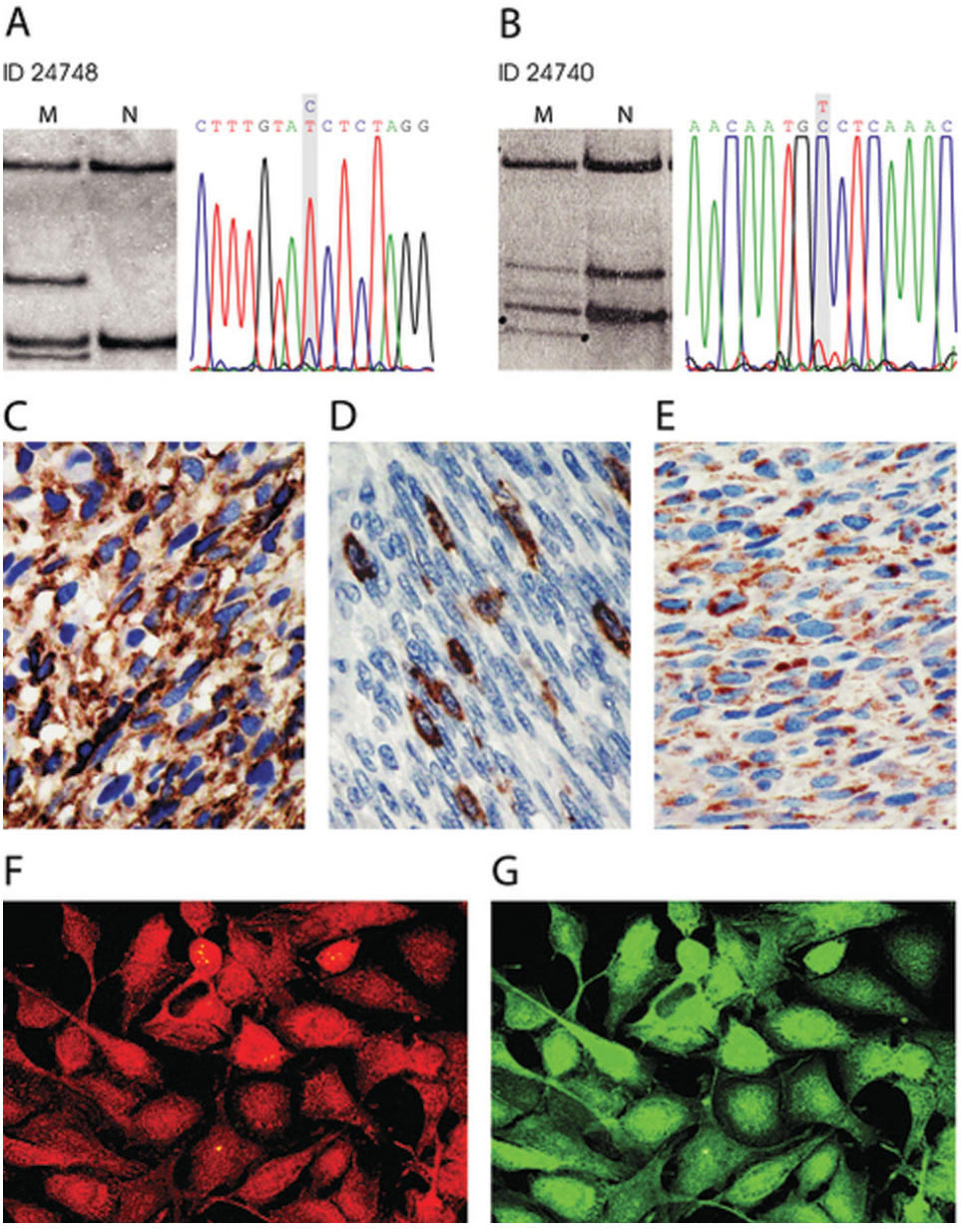

Fig. 1. Mutation and expression in MPNST. (**A**) and (**B**) SSCP gels and sequences of the shifted *PDGFRA* bands. MPNST 24748 shows a T to the wild-type C exchange and MPNST 24740 a C to the wild-type T exchange. (C–E) Immunohistochemistry. PDGFRα expression in MPNST 21852 (**C**), c-Kit expression in MPNST 24694 (**D**), PDGF-A expression in MPNST 24748 (**E**). (**F**) and (**G**) shows cell culture S462 double stained with antibodies to PDGF-A red, (F) and PDGFRα green, (G). Original magnification: 400×.

and 4 showed PDGFRα expression. Three of these pNF localized adjacent to MPNST and 2 of them showed lower PDGFRα expression than the MPNST areas (MPNST 24626/pNF 28578 and MPNST 24772/pNF 28572). MPNST 24324 and corresponding pNF 28580 contained >60% PDGFRα positive tumour cells in both parts of the tumour. An example of immunohistochemistry is shown in Figure 1C. Results are compiled in Table III. Examination of 5 MPNST and cell culture S462 for PDGFRα expression by western blot revealed bands at the expected size of 185 kDa in four samples (Figure 2). Further 6 neurofibromas analysed by western blotting showed little or no PDGFRα signals (data not shown). The western blot results were in accordance with immunohistochemistry. All tumour samples positive for PDGFRα in western blot (21914, 21852, 24472 and corresponding cell culture S462) were also positive in immunohisto- and cytochemistry (Figure 1C and G). No signals were detected in MPNST 24480 and 24784. Accordingly, these tumours were negative or showed PDGFRα expression in only a minority of cells. With the exception of pNF 28578, all tumours with *PDGFRA* amplification expressed PDGFRα.

Immunohistochemistry revealed focal c-Kit expression in 2 MPNST (Figure 1D). C-Kit positive mast cells within the tumours and a c-Kit expressing GIST served as controls.

Expression of growth factors PDGFA and PDGFB

In order to examine PDGFRα ligand expression in neurofibromas and MPNST we performed RT–PCR for *PDGFA* and *PDGFB* in 5 dNF, 3 pNF, 8 MPNST and 2 MPNST cell cultures and the glioblastoma cell line DBTRG. *PDGFA* was expressed in most tumours whereas *PDGFB* was detected in only 1 pNF but the majority of MPNST (Figure 3).

PDGF-A expression was determined in 30 MPNST from 26 patients. Immunoreactivity was observed on sections from 21 of 26 MPNST patients (81%). Fifteen MPNST (50%) expressed PDGF-A in >60% of tumour cells, 3 MPNST (10%) in 31–60% of the tumour cells and 5 MPNST (17%) in 6–30% of the tumour cells. Five pNF were also evaluated and 4 showed PDGF-A expression. Immunocytochemistry revealed strong PDGF-A expression in MPNST cell culture S462 (Figure 1F). Results for individual tumours are given in Table III.

Table II. Allelic variants of *PDGFRA* in MPNST

Exon	Codon	Triplett	Amino acid	Patient ID
3	79	GGC>GAC	G>N	26592
7	Del 348–353	Del 18 bp	Deletion of SWLKNN	24772
7	313	GGT>GGG	Silent	24308, 24624/24626, 26586, 27724
10	478	TCC>CCC	S>P	24308, 24624/ 24626, 26586
13	603	GCG>GCA	Silent	26586
16	764	CGT>CAT	R>H	24740
18	824	GTC>GTT	Silent	24308, 26586, 26588

Inhibition of MPNST cell culture proliferation and phosphorylation of PDGFRα by imatinib

The inhibitory effect of imatinib was tested with concentrations of 2 and 10 μM. Use of 2 μM imatinib led to an 11% reduction in proliferation on day 4 and a reduction of 39% on day 7 as compared to untreated control cells. The effect of 10 μM imatinib was more pronounced with 58% inhibition on day 4 and 66% on day 7 post-exposure (Figure 4A). This corresponds to a biologic IC_{50} of <10 μM. Next, we evaluated if concentrations of 2 μM and 10 μM imatinib would inhibit ligand induced phosphorylation of PDGFRα. In fact, both imatinib concentrations prevented PDGF-AA induced phosphorylation in S462 cells which corresponds to a pharmacologic IC_{50} <2 μM (Figure 4B).

Stimulation with PDGF-AA and PDGF-BB increased proliferation of S462 cells under serum-free conditions by a

Table III. Mutation and protein expression of *KIT* and *PDGFRA* in peripheral nerve sheath tumors

No.	Patient ID	Tumour entity	Grade	NF1	PDGFRA mutation	PDGFRα IHC	PDGFRα WB	PDGF-A IHC	KIT mutation	c-Kit IHC
1	24256¥	MPNST	3	Yes	–	+++	nd	++	–	–
2	24740¥	MPNST	3	Yes	Codon 469 GTC>GCC	+	nd	+++	–	–
3	24304	MPNST	1	Yes	–	nd	nd	nd	–	–
4	24326	MPNST	2	Yes	–	++	nd	+++	–	–
5	24624*	pNF	1	Yes	–	++	nd	+	–	–
6	24626*	MPNST	2	Yes	2.8amp	+++	nd	+++	–	–
7	28578*	pNF	1	Yes	2.4amp	–	nd	++	–	–
8	24534	MPNST	3	Yes	–	–	nd	+++	–	–
9	24668	MPNST	3	Yes	–	++	nd	+	–	–
10	24670	MPNST	3	Yes	–	+++	nd	+	–	–
11	24748	MPNST	3	Yes	Codon 130 CCT>TCT	++	nd	+++	–	–
12	24772+	MPNST	2	Yes	–	+++	nd	+	–	+ focal
13	28572+	pNF	1	Yes	–	+	nd	–	–	–
14	24776∼	MPNST	1	Yes	–	+++	nd	+	–	–
15	28576∼	pNF	1	Yes	–	nd	nd	nd	–	nd
16	24472#	MPNST	3	Yes	10.3amp	++	+	+++	5.5amp	–
17	S462#	Cell line	–	Yes	5.1amp	+++	+	+++	7.9amp	–
18	24480	MPNST	2	Yes	–	–	–	nd	–	–
19	24484	MPNST	3	Yes	3.7amp	nd	nd	nd	–	nd
20	24476	MPNST	2	Yes	–	–	nd	+++	–	–
21	22476$	pNF	1	Yes	–	+	nd	+++	9.3amp	–
22	24784$	MPNST	1	Yes	2.7amp	+	–	+++	9.6amp	–
23	21914	MPNST	2	Yes	5.9amp	++	+	+	1.8amp	–
24	21852§	MPNST	2	Yes	–	+++	+	+++	–	–
25	22318§	MPNST	3	Yes	2.0amp	+	nd	–	3.3amp	–
26	24308	MPNST	3	Yes	–	+	nd	+++	–	–
27	24310	MPNST	2	Yes	–	–	nd	nd	–	–
28	24324%	MPNST	1	Yes	–	+++	nd	+++	–	–
29	28580%	pNF	1	Yes	–	+++	nd	+++	–	–
30	24332	MPNST	2	Yes	–	+	nd	++	–	–
31	24354$	MPNST	1	Yes	–	++	nd	+++	–	–
32	24694	MPNST	2	Yes	–	–	nd	–	–	+ focal
33	26592	MPNST	2	Yes	–	+++	nd	–	–	–
34	28650	MPNST	2	Yes	–	++	nd	++	–	–
35	28652	MPNST	1	Yes	–	–	nd	+++	–	–
36	27724	MPNST	3	Yes	–	–	nd	+++	–	–
37	26580	MPNST	3	No	–	nd	nd	nd	–	nd
38	26582	MPNST	3	No	–	+++	nd	–	–	–
39	26584	MPNST	2	No	–	+++	nd	+++	–	–
40	26586	MPNST	2	No	–	+++	nd	–	–	–
41	26588	MPNST	3	No	–	+++	nd	–	–	–

Amplification status (amp) is indicated by fold increase relative to the normal gene dose. ID: tumour identification number. NF1: NF1 status of the tumour patient. IHC: immunohistochemistry. WB: western blot. symbols ¥, $, %, #, §, *, + indicate tumours belonging to the same patient. nd: not determined (lack of material). Tumours were graded according to the modified FNCLCC system.

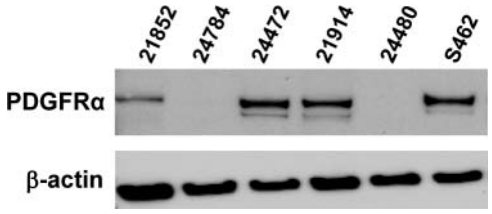

Fig. 2. Western blot of primary MPNST and MPNST cell culture S462 with antibodies to PDGFRα and β-actin.

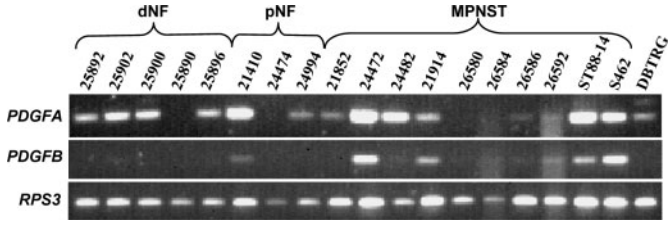

Fig. 3. Expression of *PDGFA* and *PDGFB* in dermal neurofibromas (dNF), plexiform neurofibromas (pNF), MPNST, MPNST cell lines and the glioblastoma cell line DBTRG. *RPS3* served as reference gene.

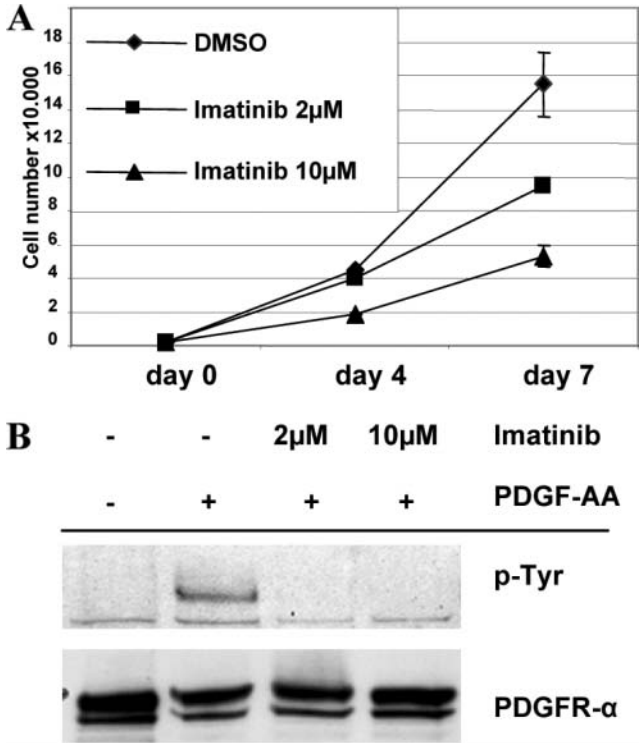

Fig. 4. (**A**) Effect of imatinib on proliferation of MPNST cell culture S462. (**B**) Inhibition of PDGF-AA induced phosphorylation of PDGFRα by 2 and 10 μM imatinib. Lysates of treated cells were resolved by electrophoresis and transferred to membranes. Membranes were probed with the indicated antibodies.

factor of four in comparison to the untreated controls (data not shown).

Discussion

This study is the first to demonstrate molecular aberrations of receptor tyrosine kinase genes *PDGFRA* and *KIT* in MPNST. We detected gene amplification of *PDGFRA* in 6 and somatic point mutations in 2 of 31 patients with MPNST. Structural alterations of *PDGFRA* were therefore present in 8 of 31 (26%) patients with MPNST. The 2 point mutations localized to exon 4 and exon 10 of *PDGFRA*, which encode parts of the extracellular domain of PDGFRα. *PDGFRA* exon 10 corresponds to *KIT* exon 9 which is the second most mutated *KIT* exon in GIST (23). We found valine substituted by alanine in codon 469. This valine, located in the Ig-like domain of the receptors, is conserved in c-Kit and corresponds there to codon 459. Mutations in the extracellular domain may modulate ligand-binding and dimerization, thereby indirectly influencing tyrosine kinase activity. Finally, mutations of *PDGFRA* in MPNST occur as frequent as *EGFR* amplifications, which have also been found in 26% of MPNST (7). Other frequent alterations in MPNST include *NF1*, *CDKN2A* and *TP53* deletions and/or mutations (5,7,19,26). Until today not many tumour entities with mutations in *PDGFRA* have been described. Recently it was shown, that a subset of about 35% of GISTs lacking *KIT* mutations carried mutations in *PDGFRA* (27,28) indicating that either *KIT* or *PDGFRA* aberrations contribute to the development of these tumours.

We detected 7 allelic variants of *PDGFRA* present in both, tumour and reference tissues. Three of them led to an amino acid exchange and one to a truncated protein. The 478Pro variant has been described before and functional analysis revealed no constitutive phosphorylation like 2 PDGFRα gain-of-function mutants (25,28). We found a variant of *PDGFRA* with an 18 bp deletion resulting in a truncated protein lacking the 6 amino acids SWLKNN in a single patient (Table II). This deletion is located in the extracellular Ig-like domain IV and may, therefore, modulate ligand-binding. Protein extracts for western blotting were available from 5 MPNST patients. Three samples showed expression of PDGFRα, 2 of which were detected with amplification. Two samples with weak PDGFRα expression were derived from one patient with, and one without, gene amplification. Immunohistochemistry demonstrated PDGFRα expression in the majority of MPNST patients (75%). A cell culture established from MPNST 24472 exhibited similar features regarding *PDGFRA* amplification and PDGFRα expression as the native tumour. Gene amplification of *KIT* was detected in 4 of 31 patients. No point mutations were observed. Immunohistochemistry revealed c-Kit expression in 2 of 29 patients (7%). Both patients with focal c-Kit expression did not harbour *KIT* amplifications. Our data demonstrating limited c-Kit expression in MPNST are in accordance with a recent study that found weak c-Kit expression in 1 of 18 MPNST (29).

With the exception of pNF 22476, all tumours with *KIT* amplification also exhibited *PDGFRA* amplification. Notably, *PDGFRA* and *KIT* map next to each other with a distance of 359 kb on the chromosomal segment 4q12. Thus, the amplicon in the majority of the MPNST in our series contains more than one gene. Amplicons containing several genes have been described previously such as the frequent amplicons on chromosomal segment 12q13–q15 in glioblastoma containing *MDM2*, *SAS*, *CDK4* and in some cases also *GADD153*, *GLI*, *RAP1B*, *A2MR* and *IFNG* (30). In MPNST the amplification of both *PDGFRA* and *KIT* may have profound effects on signal transduction. However, our observation of higher frequency of *PDGFRA* aberrations and stronger expression of PDGFRα may suggest that this gene provides a major selective advantage for MPNST tumour cells and that *KIT*, due to infrequent

expression of the protein, may be co-amplified as an 'innocent bystander'.

Because point mutations in *PDGFRA* appear to be infrequent in MPNST we suggest that an autocrine loop of the PDGF system supports proliferation and angiogenesis. We could show, that expression of PDGFR ligands PDGF-A and PDGF-B is common to nerve sheath tumours. *PDGFA* was more widely expressed than *PDGFB* especially in neurofibromas. Similar mechanisms are known to play a role in gliomas (31,32). In addition to an autocrine loop, paracrine stimulation of the PDGF system may also contribute to tumour proliferation because fibroblasts are known to be a source for PDGF. There is evidence for a direct link between NF1 and PDGF. It was shown that Schwann cells derived from Nf1−/− mice expressed *PDGFB* which was absent in Nf1+/+ mice (33).

Patients with GIST respond to treatment with imatinib, an inhibitor of the protein tyrosin kinase c-Kit (16). Imatinib does not selectively inhibit c-Kit but also interferes with other receptor tyrosine kinases such as PDGFRα (34,35). We therefore analysed growth of MPNST cells at imatinib concentrations of 2 and 10 μM employing cell culture S462, which was shown to harbour loss of heterozygosity in genes encoding neurofibromin, p53 and p16 (19). S462 showed a dose-dependent reduction of cell growth *in vitro* (Figure 4A). Ligand induced phosphorylation of PDGFRα was completely inhibited at both concentrations of imatinib (Figure 4B). The effect of imatinib on PDGFRα positive tumour cells has recently been shown in ovarian cancer cells. Only PDGFRα positive cell cultures were inhibited while cell lines lacking PDGFRα expression were not affected (36). In patients, a mean plasma concentration of up to 4.6 μM imatinib after oral administration of 400 mg (1.46 μM after 24 h) has been reported (17). Therefore, the concentration of imatinib inhibiting MPNST cell culture is similar to that in patient plasma. Further support for the potential sensitivity to imatinib is derived from the observation, that a majority of MPNST patients with *PDGFRA* amplification also exhibit amplification of *KIT*, although the latter seems not to be strongly expressed in tumour cells. However, c-Kit positive mast cells within the tumour are thought to contribute to its development (37). Therefore, MPNST carry at least two targets of imatinib. These data may indicate that patients with MPNST benefit from imatinib treatment.

In conclusion, we describe frequent mutations of *PDGFRA* in MPNST often associated with coamplification of *KIT*. *In vitro* growth of an MPNST cell line could be inhibited by the tyrosin kinase inhibitor imatinib which is known to target both PDGFRα and c-Kit. PDGFRα should therefore be considered as candidate for targeted therapy of MPNST.

Acknowledgements

We thank Kathrein Stichling and Petra Matylewski for their technical assistance and Prof. Karl Riabowol for critically reading the manuscript. This work was supported by Deutsche Krebshilfe (70-2794-De1) and the US army grant NF050145.

Conflict of Interest Statement: None declared.

References

1. Huson,S.M. (1994) Neurofibromatosis 1: a clinical and genetic overview. In Huson,S.M. and Hughes,R.A.C. (eds) *The Neurofibromatoses*. Chapman and Hall Medical, London, pp. 160–203.
2. Evans,D.G., Baser,M.E., McGaughran,J., Sharif,S., Howard,E. and Moran,A. (2002) Malignant peripheral nerve sheath tumours in neurofibromatosis 1. *J. Med. Genet.*, **39**, 311–314.
3. Menon,A.G., Anderson,K.M., Riccardi,V.M. *et al.* (1990) Chromosome 17p deletions and p53 gene mutations associated with the formation of malignant neurofibrosarcomas in Recklinghausen neurofibromatosis. *Proc. Natl Acad. Sci. USA*, **87**, 5435–5439.
4. Legius,E., Dierick,H., Wu,R., Hall,B.K., Marynen,P., Cassiman,J.J. and Glover,T.W. (1994) TP53 mutations are frequent in malignant NF1 tumors. *Genes Chromosomes Cancer*, **10**, 250–255.
5. Kourea,H.P., Orlow,I., Scheithauer,B.W., Cordon-Cardo,C. and Woodruff,J.M. (1999) Deletions of the INK4A gene occur in malignant peripheral nerve sheath tumors but not in neurofibromas. *Am. J. Pathol.*, **155**, 1855–1860.
6. Holtkamp,N., Reuss,D.E., Atallah,I. *et al.* (2004) Subclassification of nerve sheath tumors by gene expression profiling. *Brain Pathol.*, **14**, 258–264.
7. Perry,A., Kunz,S.N., Fuller,C.E., Banerjee,R., Marley,E.F., Liapis,H., Watson,M.A. and Gutmann,D.H. (2002) Differential NF1, p16, and EGFR patterns by interphase cytogenetics (FISH) in malignant peripheral nerve sheath tumor (MPNST) and morphologically similar spindle cell neoplasms. *J. Neuropathol. Exp. Neurol.*, **61**, 702–709.
8. Holtkamp,N., Mautner,V.F., Friedrich,R.E., Harder,A., Hartmann,C., Theallier-Janko,A., Hoffmann,K.T. and von Deimling,A. (2004) Differentially expressed genes in neurofibromatosis 1-associated neurofibromas and malignant peripheral nerve sheath tumors. *Acta Neuropathol. (Berl)*, **107**, 159–168.
9. Weinmaster,G. and Lemke,G. (1990) Cell-specific cyclic AMP-mediated induction of the PDGF receptor. *EMBO J.*, **9**, 915–920.
10. Betsholtz,C., Karlsson,L. and Lindahl,P. (2001) Developmental roles of platelet-derived growth factors. *Bioessays*, **23**, 494–507.
11. Ryan,J.J., Klein,K.A., Neuberger,T.J., Leftwich,J.A., Westin,E.H., Kauma,S., Fletcher,J.A., DeVries,G.H. and Huff,T.F. (1994) Role for the stem cell factor/KIT complex in Schwann cell neoplasia and mast cell proliferation associated with neurofibromatosis. *J. Neurosci. Res.*, **37**, 415–432.
12. Badache,A., Muja,N. and De Vries,G.H. (1998) Expression of Kit in neurofibromin-deficient human Schwann cells: role in Schwann cell hyperplasia associated with type 1 neurofibromatosis. *Oncogene*, **17**, 795–800.
13. Leroy,K., Dumas,V., Martin-Garcia,N. *et al.* (2001) Malignant peripheral nerve sheath tumors associated with neurofibromatosis type 1: a clinicopathologic and molecular study of 17 patients. *Arch Dermatol.*, **137**, 908–913.
14. Heinrich,M.C., Corless,C.L., Duensing,A. *et al.* (2003) PDGFRA activating mutations in gastrointestinal stromal tumors. *Science*, **299**, 708–710.
15. Hermanson,M., Funa,K., Koopmann,J. *et al.* (1996) Association of loss of heterozygosity on chromosome 17p with high platelet-derived growth factor alpha receptor expression in human malignant gliomas. *Cancer Res.*, **56**, 164–171.
16. Demetri,G.D., von Mehren,M., Blanke,C.D. *et al.* (2002) Efficacy and safety of imatinib mesylate in advanced gastrointestinal stromal tumors. *N. Engl. J. Med.*, **347**, 472–480.
17. Druker,B.J., Talpaz,M., Resta,D.J. *et al.* (2001) Efficacy and safety of a specific inhibitor of the BCR-ABL tyrosine kinase in chronic myeloid leukemia. *N. Engl. J. Med.*, **344**, 1031–1037.
18. Price,V.E., Fletcher,J.A., Zielenska,M., Cole,W., Viero,S., Manson,D.E., Stuart,M. and Pappo,A.S. (2005) Imatinib mesylate: an attractive alternative in young children with large, surgically challenging dermatofibrosarcoma protuberans. *Pediatr. Blood Cancer*, **44**, 511–515.
19. Frahm,S., Mautner,V.F., Brems,H., Legius,E., Debiec-Rychter,M., Friedrich,R.E., Knofel,W.T., Peiper,M. and Kluwe,L. (2004) Genetic and phenotypic characterization of tumor cells derived from malignant peripheral nerve sheath tumors of neurofibromatosis type 1 patients. *Neurobiol. Dis.*, **16**, 85–91.
20. Coindre,J.M., Trojani,M., Contesso,G., David,M., Rouesse,J., Bui,N.B., Bodaert,A., De Mascarel,I., De Mascarel,A. and Goussot,J.F. (1986) Reproducibility of a histopathologic grading system for adult soft tissue sarcoma. *Cancer*, **58**, 306–309.
21. Okuducu,A.F., Janzen,V., Hahne,J.C., Ko,Y. and Wernert,N. (2003) Influence of histochemical stains on quantitative gene expression analysis after laser-assisted microdissection. *Int. J. Mol. Med.*, **11**, 449–453.
22. Plaat,B.E., Molenaar,W.M., Mastik,M.F., Hoekstra,H.J., te Meerman,G.J. and van den Berg,E. (1999) Computer-assisted cytogenetic analysis of 51 malignant peripheral-nerve-sheath tumors: sporadic vs. neurofibromatosis-type-1-associated malignant schwannomas. *Int. J. Cancer*, **83**, 171–178.

23. Duensing,A., Heinrich,M.C., Fletcher,C.D. and Fletcher,J.A. (2004) Biology of gastrointestinal stromal tumors: KIT mutations and beyond. *Cancer Invest*., **22**, 106–116.
24. Clarke,I.D. and Dirks,P.B. (2003) A human brain tumor-derived PDGFR-alpha deletion mutant is transforming. *Oncogene*, **22**, 722–733.
25. Hartmann,C., Xu,X., Bartels,G., Holtkamp,N., Gonzales,I.A., Tallen,G. and von Deimling,A. (2004) Pdgfr-alpha in 1p/19q LOH oligodendrogliomas. *Int. J. Cancer*, **112**, 1081–1082.
26. Lothe,R.A., Smith-Sorensen,B., Hektoen,M., Stenwig,A.E., Mandahl,N., Saeter,G. and Mertens,F. (2001) Biallelic inactivation of TP53 rarely contributes to the development of malignant peripheral nerve sheath tumors. *Genes Chromosomes Cancer*, **30**, 202–206.
27. Heinrich,M.C., Corless,C.L., Demetri,G.D. *et al.* (2003) Kinase mutations and imatinib response in patients with metastatic gastrointestinal stromal tumor. *J. Clin. Oncol*., **21**, 4342–4349.
28. Hirota,S., Ohashi,A., Nishida,T., Isozaki,K., Kinoshita,K., Shinomura,Y. and Kitamura,Y. (2003) Gain-of-function mutations of platelet-derived growth factor receptor alpha gene in gastrointestinal stromal tumors. *Gastroenterology*, **125**, 660–667.
29. Sato,O., Wada,T., Kawai,A. *et al.* (2005) Expression of epidermal growth factor receptor, ERBB2 and KIT in adult soft tissue sarcomas: a clinicopathologic study of 281 cases. *Cancer*, **103**, 1881–1890.
30. Reifenberger,G., Ichimura,K., Reifenberger,J., Elkahloun,A.G., Meltzer,P.S. and Collins,V.P. (1996) Refined mapping of 12q13–q15 amplicons in human malignant gliomas suggests CDK4/SAS and MDM2 as independent amplification targets. *Cancer Res*., **56**, 5141–5145.
31. Hermanson,M., Nister,M., Betsholtz,C., Heldin,C.H., Westermark,B. and Funa,K. (1988) Endothelial cell hyperplasia in human glioblastoma: coexpression of mRNA for platelet-derived growth factor (PDGF) B chain and PDGF receptor suggests autocrine growth stimulation. *Proc. Natl Acad. Sci. USA*, **85**, 7748–7752.
32. Guha,A., Dashner,K., Black,P.M., Wagner,J.A. and Stiles,C.D. (1995) Expression of PDGF and PDGF receptors in human astrocytoma operation specimens supports the existence of an autocrine loop. *Int. J. Cancer*, **60**, 168–173.
33. Mashour,G.A., Ratner,N., Khan,G.A., Wang,H.L., Martuza,R.L. and Kurtz,A. (2001) The angiogenic factor midkine is aberrantly expressed in NF1-deficient Schwann cells and is a mitogen for neurofibroma-derived cells. *Oncogene*, **20**, 97–105.
34. Buchdunger,E., Cioffi,C.L., Law,N., Stover,D., Ohno-Jones,S., Druker,B.J. and Lydon,N.B. (2000) Abl protein-tyrosine kinase inhibitor STI571 inhibits *in vitro* signal transduction mediated by c-kit and platelet-derived growth factor receptors. *J. Pharmacol. Exp. Ther*., **295**, 139–145.
35. Trempat,P., Villalva,C., Laurent,G., Armstrong,F., Delsol,G., Dastugue,N. and Brousset,P. (2003) Chronic myeloproliferative disorders with rearrangement of the platelet-derived growth factor alpha receptor: a new clinical target for STI571/Glivec. *Oncogene*, **22**, 5702–5706.
36. Matei,D., Chang,D.D. and Jeng,M.H. (2004) Imatinib mesylate (Gleevec) inhibits ovarian cancer cell growth through a mechanism dependent on platelet-derived growth factor receptor alpha and Akt inactivation. *Clin. Cancer Res*., **10**, 681–690.
37. Viskochil,D.H. (2003) It takes two to tango: mast cell and Schwann cell interactions in neurofibromas. *J. Clin. Invest*., **112**, 1791–1793.

Received September 20, 2005; revised November 3, 2005; accepted November 12, 2005

EGFR and erbB2 in malignant peripheral nerve sheath tumors and implications for targeted therapy

Nikola Holtkamp, Elke Malzer, Jan Zietsch, Ali Fuat Okuducu, Jana Mucha, Christian Mawrin, Victor-F. Mautner, Hans-Ulrich Schildhaus, and Andreas von Deimling

Institute of Neuropathology, Charité-Universitätsmedizin Berlin, Berlin (N.H., E.M., J.Z.); Institute of Pathology, Helios-Klinikum Emil von Behring, Berlin (A.F.O.); Department of Neuropathology, Ruprecht-Karls-University Heidelberg, and Deutsches Krebsforschungszentrum Heidelberg, Heidelberg (J.M., A.V.); Department of Neuropathology, Friedrich-Schiller-University Jena, Jena, and Department of Neuropathology, Otto-von-Guericke University, Magdeburg (C.M.); Department of Maxillofacial Surgery, University Hospital Eppendorf, Hamburg (V.-F.M.); Institute of Pathology, University Hospital Bonn, Bonn (H.-U.S.); Germany

Malignant peripheral nerve sheath tumors (MPNSTs) are sarcomas with poor prognosis and limited treatment options. Evidence for a role of epidermal growth factor receptor (EGFR) and receptor tyrosine kinase erbB2 in MPNSTs led us to systematically study these potential therapeutic targets in a larger tumor panel (*n* = 37). Multiplex ligation-dependent probe amplification and fluorescence in situ hybridization analysis revealed increased *EGFR* dosage in 28% of MPNSTs. *ERBB2* and three tumor suppressor genes (*PTEN* [phosphatase and tensin homolog deleted on chromosome 10], *CDKN2A* [cyclin-dependent kinase inhibitor 2A], and *TP53* [tumor protein p53]) were frequently lost or reduced. Reduction of *CDKN2A* was linked to appearance of metastasis. Comparison of corresponding neurofibromas and MPNSTs revealed an increase in genetic lesions in MPNSTs. No somatic mutations were found within tyrosine-kinase–encoding exons of *EGFR* and *ERBB2*. However, at the protein level, expression of EGFR and erbB2 was frequently detected in MPNSTs. EGFR expression was significantly associated with increased *EGFR* gene dosage. The EGFR ligands transforming growth factor α and EGF were more strongly expressed in MPNSTs than in neurofibromas. The effects of the drugs erlotinib and trastuzumab, which target EGFR and erbB2, were determined on MPNST cell lines. In contrast to trastuzumab, erlotinib mediated dose-dependent inhibition of cell proliferation. EGF-induced EGFR phosphorylation was attenuated by erlotinib. Summarized, our data indicate that EGFR and erbB2 are potential targets in treatment of MPNST patients. *Neuro-Oncology 10, 946–957, 2008 (Posted to Neuro-Oncology [serial online], Doc. D07-00250, July 23, 2008. URL http://neuro-oncology.dukejournals.org; DOI: 10.1215/15228517-2008-053)*

Keywords: EGFR, ERBB2, MPNST, targeted therapy, tumor suppressor gene

Approximately half of malignant peripheral nerve sheath tumors (MPNSTs) develop in the setting of neurofibromatosis type 1 (NF1), a hereditary tumor syndrome with an incidence of 1:3,500.[1] NF1-associated MPNSTs generally arise from plexiform neurofibromas (pNFs). Loss of the tumor suppressor gene *NF1* constitutes only a first step in tumorigenesis. During the course of malignant progression, further genetic and regulatory alterations, such as mutations in *TP53* (tumor protein p53), *CDKN2A* (cyclin-dependent kinase

Received December 7, 2007; accepted June 3, 2008.

Address correspondence to Nikola Holtkamp, Institute of Neuropathology, Charité-Universitätsmedizin Berlin, CVK, Augustenburger Platz 1, D-13353 Berlin, Germany (nikola.holtkamp@charite.de).

inhibitor 2A), or *PDGFRA* (platelet-derived growth factor receptor α) or upregulation of MMP-13 (matrix metalloprotease 13), are acquired.[2–6] Furthermore, *EGFR* (epidermal growth factor receptor) gene amplification and increased transcript levels have been detected.[7,8]

Currently, treatment options for MPNST patients are still unsatisfactory. Thus, a better knowledge of molecular alterations in MPNSTs is of major importance for therapeutic strategies that aim to target proteins specifically altered in tumor cells (targeted therapy).

Several observations point toward a role of the erbB family, which consists of four members (erbB1–4), in nerve sheath tumors. It has been shown that normal Schwann cells are EGFR (erbB1) negative, whereas neurofibromas and MPNSTs express EGFR.[9] Evidence for a causal role of EGFR in nerve sheath tumor formation comes from transgenic mice expressing EGFR in Schwann and other glial cells. These animals developed neurofibromas and occasionally MPNSTs.[10] EGFR and receptor tyrosine kinase erbB2 (HER2/Neu) were also expressed in sarcoma cell lines generated from an NF1 mouse model.[11] Moreover, Schwann cell tumors from animals exposed to the carcinogen *N*-ethyl-*N*-nitrosourea harbor *ERBB2* mutations.[12,13]

EGFR and erbB2 are of special therapeutic interest because drugs targeting these receptors, including erlotinib (Tarceva) and trastuzumab (Herceptin), are already available for cancer treatment. Erlotinib is a low-molecular-weight inhibitor that binds to the kinase domain of EGFR, thereby inhibiting signal transduction. Trastuzumab is a humanized antibody targeting the extracellular domain of erbB2.

Although there is cumulating evidence of a role for EGFR and erbB2 in nerve sheath tumors,[14,15] previous studies did not systematically analyze these potential therapeutic targets in larger panels of human MPNSTs. We therefore studied genetic alterations and expression of erbB2 and EGFR in a set of 37 human MPNSTs and four MPNST cell lines. We also examined the effect of trastuzumab and erlotinib treatment on MPNST cell lines.

Materials and Methods

Tumor Tissue, DNA, and RNA Extraction

Tumor samples were collected from University Hospital Eppendorf (Hamburg, Germany), Robert-Rössle-Hospital (Berlin, Germany), Otto-von-Guericke-University (Magdeburg, Germany), and Charité-Universitätsmedizin Berlin (Berlin, Germany). MPNSTs of 37 patients were analyzed for genetic alterations and receptor expression. Four patients also contributed corresponding pNFs. Frozen tissue from eight neurofibromas was used for Western blotting. In addition, DNA and lysates from cell lines S462, ST88-14, NSF-1 (kindly provided by V.M. Riccardi from the Neurofibromatosis Institute, La Crescenta, CA, USA), and low-passage culture 31002 (<8 passages) were examined. The S462 cell line was established from MPNST 24472. Twenty-nine patients were diagnosed with NF1, and one patient with NF2; seven individuals were non-NF1 patients. Following initial diagnosis by local neuropathologists, all tumor samples were reviewed by the same pathologist. Histopathological examination was based on the modified Fédération Nationale des Centres de Lutte Contre le Cancer system.[16] Tumor sections were examined histologically prior to extraction of DNA and proteins. Tumor areas were scraped from the slides for subsequent extraction. In cases of frozen tissue, DNA was extracted using Trizol reagent from Invitrogen (Karlsruhe, Germany). DNA extraction from paraffin-embedded material was carried out according to the QIAamp DNA Mini Kit protocol (Qiagen, Hilden, Germany). Adjacent pNF was available for MPNSTs 24626, 24772, 24776, and 24324. DNA from pNF and MPNST areas was separately extracted. Breast cancer sample 31842, which served as control for *ERBB2* amplification, was kindly provided by Dr. Konrad Kölble (Department of Pathology, Charité-Universitätsmedizin Berlin). The investigations were carried out with the informed consent of the patients.

Single-Strand Conformational Polymorphism and Sequencing

Electrophoresis of PCR products (ranging from 170 to 270 bp) was performed on polyacrylamide gels. To enhance sensitivity, two different gel and running conditions were applied. Detailed information on primer sequences, amplification, and gel conditions is provided in Table 1. All PCR products showing mobility shifts were confirmed by independent PCRs and compared with PCR products of corresponding normal tissue. Aberrantly migrating bands were excised, and the DNA was extracted. After reamplification, PCR products were sequenced bidirectionally (model 3730; Applied Biosystems, Foster City, CA, USA). MPNST 24776 was analyzed for only *ERBB2*, and cell line ST88-14 only for *EGFR*. Sequences were compared to accession numbers AF288738 (*EGFR*) and AC079199 (*ERBB2*).

Multiplex Ligation-Dependent Probe Amplification Performance and Analysis

The SALSA P105 Oligodendroglioma-2 kit (Vs. 03, lot 0804) containing 9 *PTEN* probes, 5 *CDKN2A* probes, 8 *TP53* probes, 3 *EGFR* probes, 2 *ERBB2* probes, and 16 control probes was employed (MRC Holland, Amsterdam, the Netherlands). Five control probes were omitted from the panel of probes used for internal normalization because of their localization to chromosomal segments that are frequently altered in MPNSTs (11q23.3, 3p22, 16q24.3, 22q11.21, and 7q31.2).

Samples suspected of harboring *EGFR* amplification were also analyzed with the new version of the P105 kit (Vs. 04, lot 0306), which contains 11 *EGFR* probes, to detect possible EGFRvIII mutants lacking exons 2–7 that are frequently found in glioblastomas (GBMs). We used 150 μg of template DNA for hybridization and performed PCR reactions in a volume of 25 μl for 30 cycles. The PCR products were analyzed on a semiautomated sequencer (ABI377, Applied Biosystems). We mixed 1 μl

Table 1. Primer sequences, amplification, and gel conditions

				Condition 1[b]		Condition 2[b]	
Primer Name	Primer Sequence (5′–3′)	Product Size	Temp (°C)[a]	Gel	Run	Gel	Run
ERBB2 Ex17f	AATCCCTGACCCTGGCTTC	196 bp	59.0	10% A	3 W; 15 h	14% A	3 W; 18 h
ERBB2 Ex17r	CGGGCTGGGAGGACTTCA						
ERBB2 Ex18f	ACCCACCACCCCCTCAC	211 bp	61.0	8% A + 10% Gly	7 W; 15 h	14% A	3 W; 18 h
ERBB2 Ex18r	CGACCACACCCCTCCA						
ERBB2 Ex19f	CCCACGCTCTTCTCACTCAT	183 bp	58.6	14% A	3 W; 18 h	8% A + 10% Gly	7 W; 15 h
ERBB2 Ex19r	GGGTCCTTCCTGTCCTCCTA						
ERBB2 Ex20f	CTCTCAGCGTACCCTTGTCC	230 bp	58.6	10% A	3 W; 15 h	14% A	3 W; 18 h
ERBB2 Ex20r	CAAAGAGCCCAGGTGCATAC						
ERBB2 Ex21f	TACATGGGTGCTTCCCATTC	204 bp	58.6	10% A	3 W; 15 h	14% A	3 W; 18 h
ERBB2 Ex21r	TCTGCTCCTTGGTCCTTCAC						
ERBB2 Ex22f	TAGCCCATGGGAGAACTCTG	243 bp	61.0	10% A	3 W; 15 h	14% A	3 W; 18 h
ERBB2 Ex22r	AGCTCTCATCCTCCCTCCAG						
ERBB2 Ex23f	ACTCCTGACCCTGTCTCTGC	200 bp	58.6	10% A	3 W; 15 h	14% A	3 W; 18 h
ERBB2 Ex23r	AGGCAGCCAGCACAGCTC						
ERBB2 Ex24f	ATGCTGACCTCCCTCCTG	170 bp	63.0	14% A + 5% Gly	6 W; 18 h	10% A	3 W, 15 h
ERBB2 Ex24r	GAGGGTGCTCTTAGCCACAG						
EGFR Ex18f	CATGGTGAGGGCTGAGGTGA	202 bp	61.0	14% A	3 W, 18 h	8% A + 10% Gly	7 W; 15 h
EGFR Ex18r	AGCCCAGAGGCCTGTGCCA						
EGFR Ex19f	CACAATTGCCAGTTAACGTC	189 bp	54.0	8% A + 10% Gly	7 W; 15 h	14% A	3 W; 18 h
EGFR Ex19r	GCCTGAGGTTCAGAGCCAT						
EGFR Ex20f	CTTCTGGCCACCATGCGAA	270 bp	56.0	14% A + 5% Gly	6 W; 20 h	14% A	3 W, 18 h
EGFR Ex20r	ATCTCCCCTCCCCGTATCT						
EGFR Ex21f	ATGATGATCTGTCCCTCACAG	222 bp	58.0	14% A	3 W; 18 h	18% A + 10% Gly	7 W; 15 h
EGFR Ex21r	TGGCTGACCTAAAGCCACCT						
EGFR Ex22f	TAGGTCCAGAGTGAGTTAAC	205 bp	57.6	10% A	3 W; 15 h	14% A	3 W; 18 h
EGFR Ex22r	AGCCAGCTTGGCCTCAGTAC						
EGFR Ex23f	GTTCATTCATGATCCCACTGCC	221 bp	60.9	10% A	3 W; 15 h	14% A	3 W; 18 h
EGFR Ex23r	AGTGTGGACAGACCCACCAG						
EGFR Ex24f	CAATGCCATCTTTATCATTTC	191 bp	54.8	10% A	3 W; 15 h	14% A	3 W; 18 h
EGFR Ex24r	CAATGGAAGCACAGACTGC						

Abbreviations: ERBB2, receptor tyrosine-protein kinase; Ex, exon; f, forward; r, reverse; EGFR, epidermal growth factor receptor.

[a]Primer annealing temperature.

[b]Gel and running condition of single-strand conformational polymorphism analysis: A, acrylamide; Gly, glycerin.

of the PCR product with 4 μl loading buffer and heat denatured it. We loaded 0.5 μl on acrylamide gels. The GeneScan 500 TAMRA size Standard (Applied Biosystems) served as molecular weight marker.

Samples were normalized by dividing each peak area by the combined peak areas of all peaks in a lane. This procedure generates proportions of individual peaks of the total peak area (relative peak value). The mean value of the 11 internal control probes was calculated, and all relative peak values were divided by the mean value of the controls. Tumor values were then divided by the values obtained from normal control DNA to calculate a ratio. Mean values of the probes binding a distinct gene were calculated. Samples exceeding twice the standard deviation of normal DNA were scored as genetically altered. Values > 1.9 were scored as gene amplification. Values between 1.9 and 1.31 were interpreted as increased gene dosage (borderline). Values between 1.3 and 0.8 were scored as normal gene dosage. Recently, thresholds of 1.2 and 0.8 were suggested for gains and losses with this kit.[17] We interpreted values between 0.79 and 0.4 as reduced gene dosage, caused by loss of one allele. Values below 0.4 were interpreted as loss of both alleles. GBM 6236 and the breast cancer sample 31842 with known gene amplification served as positive controls for *EGFR* (31 copies) and *ERBB2* (4 copies) amplification, respectively. Interpretation was sometimes difficult because probes that localized to different regions of a gene produced nonuniform results. If two or more probes produced signals below 0.8, we scored the gene dosage to be reduced. Few cases showed reduced gene dosage according to single probes. The results were

accepted if they were reproducible and if adjacent probes yielded normal gene dosage.

Fluorescence In Situ Hybridization

Slices 3–4 μm thick from paraffin material and cytospins, fixed in 3:1 methanol:acetic acid, were used for fluorescence in situ hybridization (FISH). Samples were incubated according to the manufacturer's recommendations in pretreatment solution (Abbott, Ludwigshafen, Germany) and then in protease or pepsin. The LSI EGFR SpectrumOrange/CEP 7 SpectrumGreen probes (Abbott) were used for overnight hybridization in a HYBrite denaturation/hybridization system (Abbott) according to the manufacturer's protocol. Slides were slightly counterstained with 4',6-diamidino-2-phenylindole (DAPI) and analyzed using a fluorescence microscope with appropriate filters (Leica, Wetzlar, Germany). For each FISH analysis, 60 tumor cells were analyzed. Green and red signals were counted for each cell. Amplification was noted if the ratio of target signals to CEP 7 probe signals was ⩾2 or if clusters (i.e., more than 15 or innumerable target signals) were seen.

Reverse Transcriptase PCR Analysis of EGFR, EGF, *and Transforming Growth Factor α Gene* TGFA

Real-time PCR was performed as reported previously.[5] EGFR primers 5'-ATGCCCG-CATTAGCTCTTAG-3' and 5'-GCAACTTCCCAAAATGTGCC-3' generated a product of 98 bp. Desmin primers 5'-ACTCCCAGC-CCCTGGTATAG-3' and 5'-AGGGTAAGGAGCCCA-GACAG-3' served as reference and generated a product of 180 bp. Conventional reverse transcriptase (RT)-PCR was performed for the EGFR ligands using EGF primers (5'-CCTGCCTAGTCTGCGTCTTT-3' and 5'-CACAATACCCAGAGCGAACA-3') and transforming growth factor α (*TGFA*) primers (5'-GGATTGACA-CAGAAGGAACCA-3' and 5'-GCCTTGACCCAT-TCAGAAAA-3') in a volume of 12.5 μl. Optimal PCR cycles for semiquantitative analysis were determined to be 36 cycles for *EGF* and *TGFA* (155 bp and 150 bp) and 32 cycles for the reference gene *RPS3* (205 bp). PCR fragments (5 μl) were separated on 2% agarose gels.

Western Blotting

Tissues and cell cultures were homogenized in ice-cold lysis buffer (1% Triton X-100, 100 mM NaCl, 50 mM Tris-HCl [pH 7.5], 5 mM EDTA) containing protease and phosphatase inhibitor cocktail. Homogenization was enhanced by sonification. Tumor lysates were heat denaturated and loaded onto 7.5% acrylamide gels for subsequent protein separation. MagicMark XP from Invitrogen was applied as a size standard. After transfer of proteins to nitrocellulose membranes (Invitrogen), the membranes were blocked in 3% nonfat dry milk with 0.05% Tween/Tris-buffered saline for 1 h and incubated overnight at 4°C with antibodies to cellular-erbB2 (diluted 1:600; A0485), EGFR (diluted 1:200; sc-03), phosphorylated EGFR (diluted 1:200; sc-12351), and phosphorylated tyrosine residues (diluted 1:10,000; sc-7020). All antibodies were purchased from Santa Cruz Biotechnology (Heidelberg, Germany), with the exception of c-erbB2 antibody (DakoCytomation, Hamburg, Germany). After washing, the membranes were incubated for 1 h with a secondary peroxidase-labeled antibody. Visualization was performed with enhanced chemiluminescence (ECL 1&2 Substrate or Advanced ECL 1&2 Substrate; Amersham Biosciences, Freiburg, Germany). Sensitivity of erbB2 detection was enhanced by biotin-conjugated second antibodies, followed by 1 h incubation with a 1:2,000 dilution of ExtrAvidin from Sigma (Munich, Germany). Rehybridization of membranes was performed with anti-β-actin antibody (diluted 1:6,000; AC-15) from Sigma.

Immunohistochemistry and Scoring

Detection of EGFR was performed with the Ventana Benchmark system (Ventana, Strasbourg, France). EGFR antibody (diluted 1:100; M3563) was obtained from DakoCytomation. Antigen retrieval was achieved by pretreatment of the tissue slices for 8 min with pronase. Visualization was performed with diaminobenzidine. Expression of erbB2 was analyzed by immunofluorescence using an erbB2 antibody (diluted 1:50; A0485 from DakoCytomation) and a second Cy3-conjugated antibody. Nuclei were counterstained with DAPI I from Abbott, and antigen retrieval was enhanced by heating. Negative controls without primary antibodies were carried out and did not produce signals. As positive controls, we used skin for EGFR expression and a breast cancer metastasis for erbB2 expression. Scoring was performed according to the percentage of positive cells: <5% was classified as negative (–), and 6%–100% was classified as positive: 6%–30% of positive cells were scored with +, 31%–60% with ++, and >60% with +++. A blinded repeated test produced similar results.

Cell Culture Assays

MPNST cell lines S462, ST88-14, NSF-1, and low-passage culture 31002 were maintained in Dulbecco's modified Eagle's medium (DMEM) plus Glutamax-I (1,000 mg/l glucose; Invitrogen) containing 10% fetal bovine serum (FBS) and 5 μg/ml gentamycin. During the drug assays, cells were maintained in DMEM containing 5% FBS. We seeded 3×10^3 cells (4×10^3 for ST88-14) in 300 μl medium into 24-well plates and allowed them to adhere overnight. Erlotinib and trastuzumab (kindly provided by Genentech, San Francisco, CA, USA) and imatinib (kindly provided by Novartis Pharma AG, Basel, Switzerland) were added in 100 μl medium to obtain the indicated concentrations. Negative controls contained vehicle only. We exchanged 300 μl medium containing respective drug concentrations on days 3 and 5. Cell proliferation was evaluated on days 4 and 7 posttreatment with the CellTiter 96 AQueous One Solution Cell Proliferation Assay (Promega, Mannheim, Germany). The experiments were performed in duplicate and repeated three times. The fractional product con-

cept was used to determine whether drug combinations yielded additive or synergistic effects. Erlotinib effects on EGFR phosphorylation were determined in cell culture dishes (diameter, 10 cm). Semiconfluent cells were serum starved for 24 h. Erlotinib was added to a final concentration of 5 μM and incubated for 1 h. Cells were then stimulated with EGF (100–50 ng/ml) for 10 min at 37°C, washed with phosphate-buffered saline, scraped, centrifuged, and resuspended in 70 μl lysis buffer.

Statistical Methods

SPSS version 12.0 (SPSS, Chicago, IL, USA) was used for statistical analysis. Survival rates were determined using the Kaplan-Meier method and the log rank test. Association of parameters was assessed with the Pearson correlation and Fisher exact test. A p-value of <0.05 was considered significant.

Results

Genetic Alterations of EGFR, ERBB2, *and Tumor Suppressor Genes*

Tyrosine-kinase–encoding domains (exon 18–24) of *EGFR* and *ERBB2* were screened for sequence alterations by single-strand conformational polymorphism in samples from 34 patients (37 MPNSTs, 4 corresponding pNFs, and MPNST cell lines S462 and ST88-14). In addition, *ERBB2* exon 17, encoding the transmembrane domain, was analyzed because point mutations have been described in this region in peripheral nerve sheath tumors of domesticated animals.[18] Somatic mutations were not found, but polymorphisms were detected in exons 20, 21, and 23 of *EGFR* and in exon 17 of *ERBB2* (Table 2). All *EGFR* variants were silent. The *ERBB2* variant in codon 655 results in an exchange from isoleucine to valine. Comparison with the National Center for Biotechnology Information's dbSNP database (www.ncbi.nlm.nih.gov/SNP) revealed no significant differences in polymorphism frequency in our series compared to that in the normal population (data not shown).

DNA from 31 patients was available for gene dosage analysis by multiplex ligation-dependent probe amplification (MLPA; Table 3). Initial analysis of *EGFR* dosage was performed by real-time PCR and produced results similar to those from MLPA. For nine samples, indicated in Table 3, only PCR data are available. Increased *EGFR* dosage was observed in 28% of MPNSTs. Most of these samples yielded borderline values between 1.3 and 1.9. However, three MPNSTs harbored *EGFR* gene dosages > 4.0. *EGFR* amplification in MPNST 21914 was repeatedly shown to be restricted to exon 1 (Fig. 1A). *ERBB2* gene dosage was reduced in 32% of MPNSTs. Reduction in gene dosage was also observed for *TP53* (39%) and for *PTEN* and *CDKN2A* (58% each). The *PTEN* pattern of MPNST 26584 was remarkable (and reproducible) because two probes recognizing exon 1 yielded values of 0.5, whereas probes binding to exons 2–9 generated values of 2.0.

Benign precursor pNFs were available from three patients and were compared to corresponding MPNSTs (Table 4). MPNST 21914 exhibited multiple genetic alterations, whereas the corresponding pNF had normal gene dosage within the analyzed genes (Fig. 1A). *EGFR* gene dosage was increased in MPNST 24324 by a factor of 6.9, whereas the corresponding pNF 28580 showed an increase by a factor of 2.2 relative to the normal dosage. MPNST 24626 had stronger alterations in, for example, *CDKN2A* than in two corresponding pNFs. pNF 24624 was pure neurofibroma, whereas pNF 28578 was scraped from a slice also containing MPNSTs. One patient contributed primary MPNST 21852 and corresponding relapse 22318 (resected 5 months later). The relapse had acquired a reduction of *ERBB2* and *CDKN2A*.

In order to verify MLPA data with an independent method we applied FISH in selected cases with increased *EGFR* values. FISH analysis revealed chromosome 7 polysomy in all samples. Moreover, MPNSTs 21914 and 24256 also harbored *EGFR* gene amplification in most cells (Table 5 and Fig. 1A). MPNST 21852 and the corresponding recurrent MPNST 22318 had borderline amplifications (1.6 and 2.0) that matched well with MLPA data (1.5 and 1.8).

Expression of EGFR, erbB2, and EGFR Ligands

EGFR and erbB2 expression was determined by immunohistochemistry in MPNSTs from 28 patients (Table 2; Fig. 1, B and C). EGFR was detected in 29% (8 of 28) and erbB2 in 82% (23 of 28) of MPNSTs. Stronger EGFR expression in MPNST 24324 than in adjacent pNF (Fig. 1B) corresponds well with underlying *EGFR* amplification in these tumors (Table 4).

Western blot detected EGFR in all five MPNSTs, four MPNST cell cultures, and seven of eight neurofibromas (Fig. 2A). Interestingly, different EGFR isoforms were detected in MPNSTs (170 kDa) and in neurofibromas (150 kDa), as depicted in Fig. 2, A and B. MPNST 21914 was exceptional because the major signal was detected at 50 kDa (Fig. 2C). To determine whether this small EGFR isoform was active, we examined phosphorylation of tyrosine residues. EGF-stimulated A431 carcinoma cells served as positive control. Phosphorylated EGFR was detected at 170 kDa in A431 lysate and at 50 kDa in MPNST 21914. ErbB2 was present in four of five MPNSTs and all MPNST cultures but in only one of eight neurofibromas (Fig. 2A). The signals were detected at the expected size of 185 kDa. For comparison, EGFR and erbB2 were also examined in nontumorous cells (dermal fibroblasts), which showed weak expression of both receptors.

EGFR ligand expression (*EGF*, *TGFA*) was performed with RT-PCR on five MPNSTs, two MPNST cell lines, and six neurofibromas (Fig. 2D). *EGF* was absent in neurofibromas and expressed in two of five MPNSTs and in both MPNST cell lines. Weak *TGFA* expression was detected in three of six neurofibromas. By contrast, MPNSTs showed stronger expression, with the exception of MPNST 26580 and cell line S462, which were negative.

Table 2. Genetic alterations and expression of epidermal growth factor receptor (EGFR) and receptor tyrosine-protein kinase (erbB2) in malignant peripheral nerve sheath tumors (MPNSTs) and MPNST cell lines

MPNST ID	NF1[a]	Grade[b]	*EGFR* amp[c,d]	EGFR IHC/WB[e]	*ERBB2* amp[c,d]	erbB2 IHC/WB[e]	*PTEN*[d]	*CDKN2A*[d]	*TP53*[d]
24256	Y	3	4.5 amp	+	R	+++	R	L	n
24326	Y	2	n[f]	–	NA	+++			
24626	Y	2	R	–	n	+++	R	L	n
24534	Y	3	n[f]	–	NA	++			
24668	Y	3	n[f]	–	–	+			
24670	Y	3	n	–	n	+	R	L	R
24748	Y	2	n	–	n	+++	L	R	R
24772	Y	2	1.36 amp	++	R	+++	L	L	n
24776	Y	1	n[f]	–	NA	–			
24472[g]	Y	3	n	+/WB++	R	–/WB++	n	n	R
24480	Y	2	n	+	n	–	R	n	n
24484	Y	3	n	NA	n	++	n	n	n
24476	Y	2	n	–	n	–	n	n	n
24784	Y	1	n	–/WB++	n	++/WB++	n	n	n
21914	Y	2	7.5 amp exon 1	–/WB+++ truncated	R	–	R	L	R
21852	Y	2	1.45 amp	WB+	n	WB+	R	n	R
24308	Y	3	n	NA	R	NA	R	R	n
24310	Y	2	n	NA	n	NA	L	R	n
24324	Y	1	6.9 amp	+++	R	+	n	L	R
24332	Y	2	n[f]	–	NA	++			
24354	Y	1	n[f]	–	NA	+			
24694	Y	2	n	–	n	+++	R	n	n
26592	Y	2	n[f]	–	NA	+++			
28650	Y	2	n	–	n	+++	n	n	n
28652	Y	1	n	–	n	+++	n	n	n
27724	Y	3	n[f]	–	NA	+++			
26580	N	3	n	NA	R	NA	n	L	R
26582	N	3	n	–	R	+++	R	n	R
26584	N	2	R	(+)	n	++	Amp/R	L	L
26586	N	2	n[f]	–	NA	+++			
26588	N	3	1.38 amp	–	n	NA	R	R	R
168	NF2	NA	n	NA	n	NA	n	R	n
524	N	NA	1.8 amp	NA	n	NA	R	R	n
5050	N	NA	R	NA	1.33 amp	NA	n	n	n
29250	Y	3	n	WB+	n	WB++	n	L	n
31472	Y	3	1.42 amp	+++	n	++	1.43 amp	L	n
31474	Y	3	n	+++	n	++	n	L	R
S462[g]	Y	—	1.47 amp	WB+++	R	WB++	n	n	R
ST88-14	Y	—	n	WB+++	R	WB+	R	n	R
31002	N	—	1.48 amp	WB++	n	WB++	R	n	n
NFS-1	Y	—	1.76 amp	WB+++	n	WB+++	R	L	n

Abbreviations: *PTEN*, phosphatase and tensin homolog deleted on chromosome 10; *CDKN2A*, cyclin-dependent kinase inhibitor 2A; *TP53*, tumor protein p53; NA, not assessed (lack of material). Cell lines are listed in the lower part of the table.

[a]Neurofibromatosis type 1 status of the patient: N, no; Y, yes; NF2, neurofibromatosis type 2.

[b]Tumor grade according to the modified Fédération Nationale des Centres de Lutte Contre le Cancer system.

[c]Amplification status (amp) according to multiplex ligation-dependent probe amplification is indicated by fold increase relative to the normal gene dose. ErbB2, receptor tyrosine-protein kinase.

[d]R, monoallelic loss; L, biallelic loss; n, normal gene dose.

[e]Immunohistochemistry (IHC)/Western blot quantification (WB): strong (+++), medium (++), weak (+).

[f]Samples analyzed for *EGFR* dosage by real-time PCR.

[g]Samples belonging to the same patient.

Table 3. Allelic variants of epidermal growth factor receptor (EGFR) and receptor tyrosine-protein kinase (erbB2) in malignant peripheral nerve sheath tumor patients

Gene	Codon	Triplet	Amino acid	Allele frequency (f)
EGFR exon 20	787	CAG>CAA	Silent	$A^{787} = 0.63$
				$G^{787} = 0.37$
EGFR exon 21	836	CGC>CGT	Silent	$C^{836} = 0.97$
				$T^{836} = 0.03$
EGFR exon 23	903	ACC>ACT	Silent	$C^{903} = 0.80$
				$T^{903} = 0.20$
ERBB2 exon 17	655	ATC>GTC	I >V	$Ile^{655} = 0.74$
				$Val^{655} = 0.26$

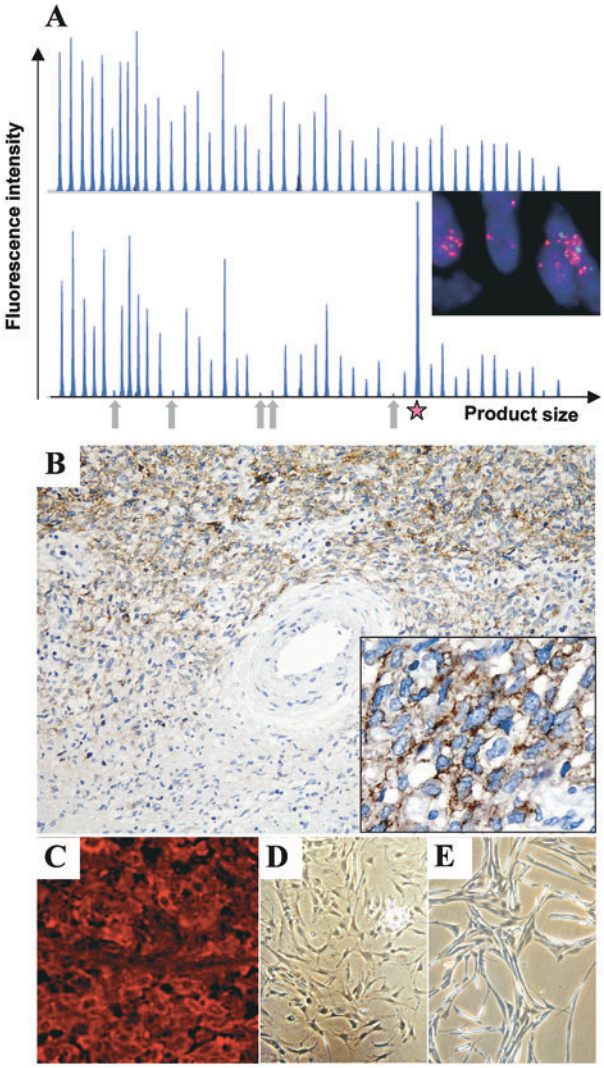

Fig. 1. Genetic alterations, receptor expression, and morphology of malignant peripheral nerve sheath tumors (MPNSTs) and MPNST cell cultures. (A) Electropherograms depicting gene dosage of MPNST 21914 (lower panel) and corresponding plexiform neurofibroma (pNF) 21912 (upper panel) generated with the SALSA P105 Oligodendroglioma-2 multiplex ligation-dependent probe amplification kit (Vs. 04). The arrows indicate signal reduction of the five *CDKN2A* probes in the MPNSTs. The star marks the increased signal of the *EGFR* exon 1 probe (inset). Fluorescence in situ hybridization analysis demonstrates cluster amplification of epidermal growth factor receptor gene *EGFR* (red signals; centromer: green signals). (B) Immunohistochemistry of EGFR on MPNST 24324. Note the strong EGFR expression in the cellular MPNSTs compared to the area with differentiation corresponding to pNF. Original magnification: ×200; right corner, ×400. (C) Receptor tyrosine-protein kinase erbB2 immunofluorescence of MPNST 24626. Original magnification: ×400. (D and E) Morphology of low-passage MPNST culture 31002 and MPNST cell line NSF-1, respectively.

Effect of Receptor Tyrosine Kinase Inhibitors on MPNST Cells

The effects of erlotinib and trastuzumab on MPNST cells were examined. Trastuzumab, tested in a concentration range of 10–100 μg/ml on S462 and ST88-14 cells, yielded a 20%–30% reduction of proliferation on S462 cells with concentrations of 10 μg/ml and 50 μg/ml (data not shown). A concentration of 100 μg/ml resulted in 20% inhibition, demonstrating that a dose-dependent effect was not achieved. ST88-14 cells were not affected by trastuzumab treatment.

Erlotinib concentrations of 1, 5, and 10 μM were tested on MPNST cell lines S462, ST88-14, NSF-1, and low-passage culture 31002 (Fig. 3A). Morphology of low-passage culture 31002 and cell line NSF-1 is shown in Fig. 1, D and E. Proliferation was measured on days 4 and 7 posttreatment. Effect of incubation times on cell growth was negligible (data not shown). The erlotinib concentration inhibiting cell growth by 50% (IC_{50}) on day 7 posttreatment was 7 μM for 31002, 5 μM for S462, and 4 μM for ST88-14. NSF-1 cells were not affected by erlotinib treatment. The fractional product concept was applied to determine the effect of drug combination. This method can be used for drugs that act

Table 4. Multiplex ligation-dependent probe amplification analysis on tumor pairs

Tumor ID	EGFR	*ERBB2*	*PTEN*	*CDKN2A*	*TP53*
21914 MPNST	7.5 amp	R	R	L	R
21912 pNF	n	n	n	n	n
24324 MPNST	6.9 amp (7.6)[a]	R	n	L	R
28580 pNF	NA (2.2)[a]	NA	NA	NA	NA
24626 MPNST	R	n	R	L	n
28578 pNF I	n	n	R	R	n
24624 pNF II	n	n	R	n	n
21852 MPNST	1.5 amp	n	R	n	R
22138 relapse	1.8 amp (2.4)[a]	R	R	R	R

Abbreviations: EGFR, epidermal growth factor receptor; erbB2, receptor tyrosine-protein kinase; *PTEN*, phosphatase and tensin homolog deleted on chromosome 10; *CDKN2A*, cyclin-dependent kinase inhibitor 2A; *TP53*, tumor protein p53; MPNST, malignant peripheral nerve sheath tumor; amp, amplification status; R, monoallelic loss; L, biallelic loss; pNF, plexiform neurofibroma; n, normal gene dose; NA, not assessed.

[a]*EGFR* dosage determined by real-time PCR.

Table 5. Fluorescence in situ hybridization analysis of malignant peripheral nerve sheath tumors with increased epidermal growth factor receptor (*EGFR*) dosage

Tumor ID	% Amp[a]	% Polysomy[b]	Ratio[c]
21914	90	40	Cluster[d]
21852	<10	60	1.6
22138	50	55	2.0
24772	<10	15	1.3
S462 cells	0	90	1.0
24256	80	30	Cluster[d]

[a]Gene amplification was accepted when target gene/centromer was ⩾2 and is given as percentage of cells with gene amplification.

[b]Polysomy was accepted when centromer signals were three or more per nucleus and is given as percentage of cells with polysomy.

[c]Ratio: *EGFR* signals/centromer signals.

[d]Cluster indicates ⩾15 signals per target and nucleus.

mutually nonexclusively. Fractions of unaffected, proliferating cells treated with single drugs were multiplied. The result is the calculated effect for additive-acting drugs. Experimental data were compared to the calculated value. If experimental and calculated data match, the effect is additive. Smaller experimental values indicate a synergistic effect, whereas larger values indicate an antagonistic mode of action.

Combinations of erlotinib and imatinib (5 μM each) approximated an additive effect on S462 and 31002 cells (Fig. 3B). The effect on ST88-14 appeared to be stronger than additive. While erlotinib and imatinib had similar effects on S462 and 31002 cells, imatinib was superior on ST88-14. To determine if growth inhibition of erlotinib is actually mediated by inhibition of EGFR signaling, the effect of 5 μM erlotinib on EGF-induced EGFR phosphorylation was determined. Reduction of EGFR phosphorylation was achieved in 31002 and S462 but not in ST88-14 cells (Fig. 3C). To clarify whether stimulation with 100 ng/μl EGF may override the effect of erlotinib, we tested 50 ng/μl EGF. Under these conditions, erlotinib inhibited EGFR phosphorylation (Fig. 3D).

Statistical Analysis

Molecular characteristics of the tumors as determined by MLPA, immunohistochemistry, and Western blotting were compared with each other and with clinical information of MPNST patients. Presence of metastasis was associated with reduced *CDKN2A* ($p = 0.054$, Fisher exact test; $n = 22$). Survival analysis was close to significance ($p = 0.09$, log rank). Notably, all patients with metastases ($n = 5$) had reduced *CDKN2A*. *EGFR* status and EGFR protein expression were significantly associated ($p = 0.026$, Fisher exact test; $n = 26$). When the four different staining and gene status levels were taken into account, the correlation was even more significant ($p = 0.016$, Pearson correlation). Tumor grade was linked to *PTEN* gene dosage ($p = 0.017$, Fisher exact test; $n = 24$). None of the grade 1 MPNSTs had affected *PTEN*, whereas 82% of grade 2 and 40% of grade 3 MPNSTs had reduced *PTEN*.

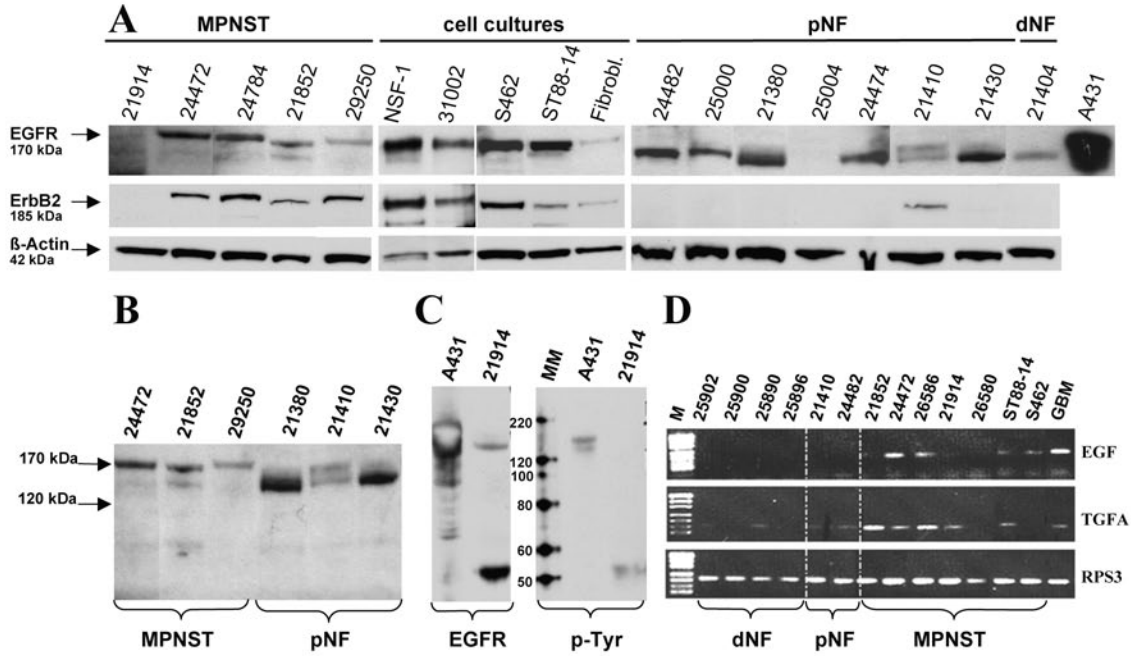

Fig. 2. Detection of epidermal growth factor receptor (EGFR), EGFR ligands, and receptor tyrosine-protein kinase (erbB2). (A) Western blot showing EGFR and erbB2 expression in malignant peripheral nerve sheath tumors (MPNSTs), MPNST cell lines, fibroblasts (Fibrobl.), and neurofibromas (NF). Lysate of EGF-stimulated A431 carcinoma cells served as EGFR positive control. Detection of β-actin demonstrates equal loading. (B) Different EGFR isoforms in MPNSTs and plexiform neurofibromas (pNFs) separated on the same gel. (C) Detection of phosphorylated proteins using the p-Tyr antibody specific for phosphotyrosine residues. Two sets of A431 and 21914 lysates were run on the same gel and blotted. After cutting the membrane one set was incubated with an EGFR antibody, the other set was incubated with p-Tyr. MM, MagicMark XP size standard. (D) Expression of EGFR ligands *EGF* and transforming growth factor α (*TGFA*) was determined by reverse transcriptase PCR in neurofibromas, MPNSTs, and MPNST cell lines ST88-14 and S462. *RPS3* served as housekeeping gene. Abbreviations: M, size standard PUC 19 DNA/MspI; GBM, glioblastoma cell line DBTRG-05 MG, serving as positive control; dNF, dermal neurofibromas.

Discussion

We detected gene dosage alterations in the oncogenes *EGFR* and *ERBB2* and in the tumor suppressor genes *PTEN*, *CDKN2A*, and *TP53*. Increased EGFR dosage was present in 28% of MPNSTs and resulted from chromosome 7 polysomy sometimes combined with *EGFR* amplification. Gain of chromosome 7 in MPNSTs has been reported previously.[7,19,20] Most cell lines (three of four) showed slightly elevated *EGFR* values. Enrichment of cells with EGFR amplifications under culture conditions is possible but appears unlikely since EGFR amplifications have been reported to disappear under culture conditions.[21]

The frequent reduction of *ERBB2* dosage may be explained by its colocalization with the *NF1* gene on the long arm of chromosome 17. Frequent loss of chromosome 17 in MPNSTs has been shown.[19] *TP53*, localizing to the short arm of chromosome 17, showed reduced gene dosage in 40% of MPNSTs (3% corresponding to biallelic inactivation) and might also be caused by chromosome 17 loss. However, 9 of 31 MPNSTs showed alterations in either *ERBB2* or *TP53*, indicating that their loss is not always combined. Reduced *CDKN2A* dosage in 57% of MPNSTs (37% with values corresponding to homozygous deletions) agrees with a previous study showing *CDKN2A* deletions in 75% of MPNSTs (45% with homozygous deletions).[7] Similar results were found by other groups.[4,22] Here, we provide evidence for an association of reduced *CDKN2A* with metastasis. However, these results need confirmation with larger patient numbers. Nevertheless, the association of *CDKN2A* alteration and disease progression, including metastasis, has been reported for other cancers.[23,24] We show for the first time reduced *PTEN* dosage, which was present in 57% of MPNSTs (10% with values corresponding to homozygous deletions). *PTEN* reduction corresponded mainly to monoallelic loss. It remains to be clarified whether the remaining allele is also inactivated. Up to now, only one study determined *PTEN* mutations in 12 MPNSTs but did not detect any.[25] However, epigenetic regulation of *PTEN* has been reported for different tumors[26–28] and could also take place in MPNSTs. In fact, our preliminary data point toward PTEN promoter methylation in the majority of MPNSTs but not in neurofibromas. A detailed analysis of PTEN alterations is currently being performed.

Further, *PTEN* haploinsufficiency may be sufficient to promote tumor progression.[29] PTEN controls the Akt/mTOR (mammalian target of rapamycin) pathway by antagonizing phosphoinositide 3-kinase. MPNST cell lines were found to be sensitive to the mTOR inhibitor rapamycin.[30] It is possible that PTEN loss contributes to the activation of this pathway. Therefore, it might be of

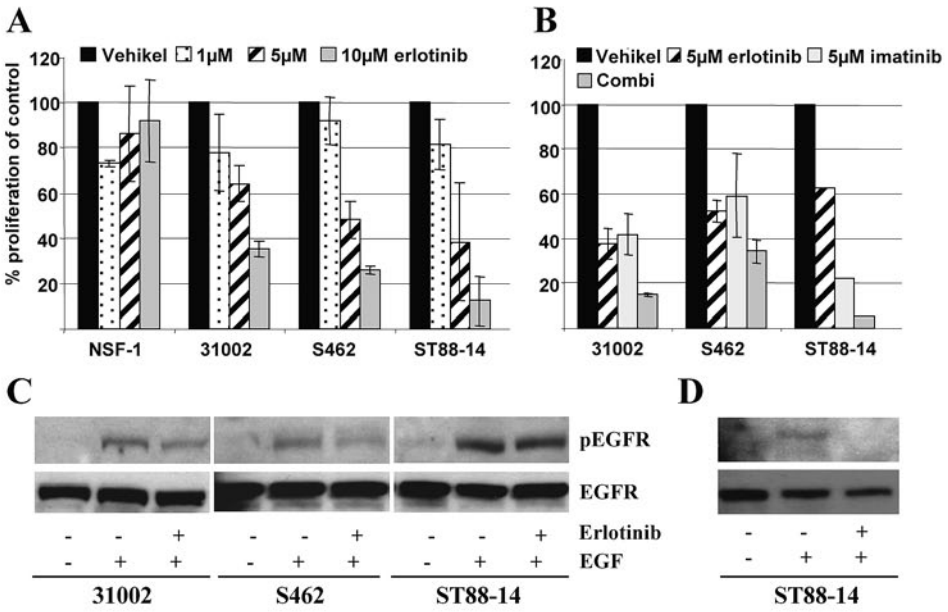

Fig. 3. Effect of erlotinib and imatinib on proliferation and epidermal growth factor receptor (EGFR) phosphorylation. (A) Effect of different erlotinib concentrations on cell proliferation in four malignant peripheral nerve sheath tumor lines after 7 days of incubation. (B) Single and combination (Combi) treatment with 5 μM of erlotinib and imatinib. Error bars represent the SEM of three independent experiments. ST88-14 in B was tested once in duplicate. (C) Effect of erlotinib on EGF-induced EGFR phosphorylation. The cells were cultivated 24 h without serum and then treated with vehicle, EGF (100 ng/ml), or erlotinib (5 μM) plus EGF. (D) Cells were stimulated with 50 ng/ml EGF. The phosphorylated form of EGFR (pEGFR) was detected by a phospho-specific EGFR antibody. Rehybridization of the membranes with an EGFR antibody shows equal loading.

interest to test whether MPNSTs with affected *PTEN* respond better to mTOR inhibitors than do those with unaffected *PTEN*.

EGFR and erbB2 were frequently expressed in MPNSTs, as shown by immunohistochemistry and Western blotting. ErbB2, detected in the vast majority of MPNSTs, was rarely expressed in neurofibromas, thereby pointing toward a progression-associated event. The proliferation-associated expression of erbB2 is also observed physiologically, with erbB2 being expressed in developing Schwann cells and downregulated in adulthood, but reexpressed in proliferating Schwann cells of traumatic neuromas or upon stimulation with growth factors.[31,32] Although reduction of *ERBB2* dosage was detected in 32% of MPNSTs, most of the affected cases still expressed erbB2. This result may appear contradictory, but haploinsufficiency does not necessarily lead to reduced expression. Given a scenario in which one allele of *ERBB2* is accidentally co-deleted with *NF1*, regulatory processes could account for erbB2 expression, which might be important for tumor cell proliferation. EGFR was detected in MPNSTs and neurofibromas, but the isoforms differed. In MPNSTs, we detected bands at 170 kDa, which correspond to glycosylated EGFR. Neurofibromas mainly showed bands at 150 kDa, possibly representing an unglycosylated isoform of EGFR.[33] Proper glycosylation is important for ligand binding, correct folding, and kinase activity.[33] Therefore, it is tempting to speculate that glycosylated EGFR in MPNSTs is more potent in transmitting mitogenic signals upon ligand binding than is the unglycosylated form in neurofibromas. EGFR may also be upregulated during disease progression, as shown in Fig. 1B. In general, EGFR expression was associated with increased *EGFR* dosage, thereby providing evidence for the underlying mechanism. Furthermore, increased transcript levels of EGF and TGFα were detected in MPNSTs compared to neurofibromas. Thus, stronger expression of EGF ligands might contribute to tumor progression.

Our in vitro assays demonstrated a dose-dependent effect of erlotinib but not trastuzumab on MPNST cell proliferation. Trastuzumab is approved for treatment of erbB2-overexpressing breast cancers with underlying *ERBB2* amplification. Although the exact mode of trastuzumab action is not fully understood, it is anticipated that trastuzumab is effective only in tumor cells with *ERBB2* amplification surpassing a certain erbB2 expression threshold.[34] A unique feature of erbB2 is its ability for spontaneous dimerization when overexpressed. Further, antibody-dependent cell-mediated cytotoxicity is thought to contribute to the effect mediated by trastuzumab in vivo.[35] Absence of *ERBB2* amplification in MPNST cell lines and lack of immune cells in our assay may explain failure of trastuzumab. Erlotinib, targeting the kinase domain of EGFR, inhibited most tested cell lines. NSF-1 cells were not affected, although they express EGFR. Independence from EGFR signaling may be explained by numerous other alterations. Modulating effects of tumor suppressor genes on therapy have been reported.[36] Recently, an inhibitory effect of erlotinib on MPNST cell lines S462 and STS26T was reported.[37] IC_{50} values in S462 cells were similar to ours,

and an antiangiogenic effect was observed in an STS26T xenograft model. Taken together, IC_{50} values of our cell culture assays were similar to plasma concentrations in patients[38] and suggest that erlotinib may be a candidate for therapeutic use in MPNST patients.

Combination therapies are likely to yield best results in highly malignant tumors with numerous genetic and epigenetic alterations. Therefore, we combined imatinib, previously shown to be effective on S462 cells,[5] with erlotinib. ST88-14 cells were more sensitive to combination treatment than were the other cells. A possible explanation is the *TP53* wild-type status of ST88-14, whereas S462 cells harbor mutant *TP53* (unpublished observation, Nikola Holtkamp). A modulating effect of p53 status on sensitivity to the EGFR inhibitor cetuximab was observed in two hepatocellular cancer cell lines. Despite strong EGFR expression in both cell lines, the one with mutant p53 responded less to cetuximab than the one with wild-type p53.[39] Thus, *TP53* alterations may be considered for individualized therapies of MPNSTs.

In summary, our results provide a molecular rationale for clinical application of EGFR inhibitors. Further, erbB2 was expressed by most MPNSTs. In contrast to other erbB family members (EGFR, erbB3, erbB4), erbB2 lacks a ligand-binding domain. ErbB2 must therefore form heterodimers with other family members, all of which were detected in MPNSTs,[15] to respond to growth factors. Application of pan-erbB inhibitors appears tempting to inhibit this cross talk (heterodimerization). Prior analysis of EGFR and erbB2 expression in tumors will probably help to choose patient subgroups most likely to benefit from treatment with specific inhibitors. Finally, a combination of drugs is likely to be most effective in combating MPNSTs.

Acknowledgments

We thank Petra Matylewski for excellent technical assistance, Horst Skarabis for his advice on statistical evaluation, and Michael Baier for helpful discussion. This work was supported by the U.S. Department of Defense Neurofibromatosis Research Program (NF050145).

References

1. Huson SM. Neurofibromatosis 1: a clinical and genetic overview. In Huson SM, Hughes RAC, eds. *The Neurofibromatoses*. London: Chapman and Hall Medical; 1994:160–203.
2. Menon AG, Anderson KM, Riccardi VM, et al. Chromosome 17p deletions and p53 gene mutations associated with the formation of malignant neurofibrosarcomas in Recklinghausen neurofibromatosis. *Proc Natl Acad Sci U S A*. 1990;87:5435–5439.
3. Legius E, Dierick H, Wu R, et al. TP53 mutations are frequent in malignant NF1 tumors. *Genes Chromosomes Cancer*. 1994;10:250–255.
4. Kourea HP, Orlow I, Scheithauer BW, Cordon-Cardo C, Woodruff JM. Deletions of the INK4A gene occur in malignant peripheral nerve sheath tumors but not in neurofibromas. *Am J Pathol*. 1999;155:1855–1860.
5. Holtkamp N, Okuducu AF, Mucha J, et al. Mutation and expression of PDGFRA and KIT in malignant peripheral nerve sheath tumors, and its implications for imatinib sensitivity. *Carcinogenesis*. 2006;27:664–671.
6. Holtkamp N, Mautner V, Friedrich R, et al. Differentially expressed genes in neurofibromatosis 1-associated neurofibromas and malignant peripheral nerve sheath tumors. *Acta Neuropathol Berl*. 2004;107:159–168.
7. Perry A, Kunz SN, Fuller CE, et al. Differential NF1, p16, and EGFR patterns by interphase cytogenetics (FISH) in malignant peripheral nerve sheath tumor (MPNST) and morphologically similar spindle cell neoplasms. *J Neuropathol Exp Neurol*. 2002;61:702–709.
8. Holtkamp N, Reuss DE, Atallah I, et al. Subclassification of nerve sheath tumors by gene expression profiling. *Brain Pathol*. 2004;14:258–264.
9. DeClue JE, Heffelfinger S, Benvenuto G, et al. Epidermal growth factor receptor expression in neurofibromatosis type 1-related tumors and NF1 animal models. *J Clin Invest*. 2000;105:1233–1241.
10. Ling BC, Wu J, Miller SJ, et al. Role for the epidermal growth factor receptor in neurofibromatosis-related peripheral nerve tumorigenesis. *Cancer Cell*. 2005;7:65–75.
11. Li H, Velasco-Miguel S, Vass WC, Parada LF, DeClue JE. Epidermal growth factor receptor signaling pathways are associated with tumorigenesis in the Nf1:p53 mouse tumor model. *Cancer Res*. 2002;62:4507–4513.
12. Kindler-Rohrborn A, Kolsch BU, Fischer C, Held S, Rajewsky MF. Ethylnitrosourea-induced development of malignant schwannomas in the rat: two distinct loci on chromosome of 10 involved in tumor susceptibility and oncogenesis. *Cancer Res*. 1999;59:1109–1114.
13. Nakamura T, Ushijima T, Ishizaka Y, et al. Neu proto-oncogene mutation is specific for the neurofibromas in a N-nitroso-N-ethylurea-induced hamster neurofibromatosis model but not for hamster melanomas and human Schwann cell tumors. *Cancer Res*. 1994;54:976–980.
14. Carroll SL, Stonecypher MS. Tumor suppressor mutations and growth factor signaling in the pathogenesis of NF1-associated peripheral nerve sheath tumors: II. The role of dysregulated growth factor signaling. *J Neuropathol Exp Neurol*. 2005;64:1–9.
15. Stonecypher MS, Byer SJ, Grizzle WE, Carroll SL. Activation of the neuregulin-1/ErbB signaling pathway promotes the proliferation of neoplastic Schwann cells in human malignant peripheral nerve sheath tumors. *Oncogene*. 2005;24:5589–5605.
16. Coindre JM, Trojani M, Contesso G, et al. Reproducibility of a histopathologic grading system for adult soft tissue sarcoma. *Cancer*. 1986;58:306–309.
17. Jeuken J, Cornelissen S, Boots-Sprenger S, Gijsen S, Wesseling P. Multiplex ligation-dependent probe amplification: a diagnostic tool for simultaneous identification of different genetic markers in glial tumors. *J Mol Diagn*. 2006;8:433–443.
18. Stoica G, Tasca SI, Kim HT. Point mutation of neu oncogene in animal peripheral nerve sheath tumors. *Vet Pathol*. 2001;38:679–688.
19. Bridge RS Jr, Bridge JA, Neff JR, Naumann S, Althof P, Bruch LA. Recurrent chromosomal imbalances and structurally abnormal breakpoints within complex karyotypes of malignant peripheral nerve sheath tumour and malignant triton tumour: a cytogenetic and molecular cytogenetic study. *J Clin Pathol*. 2004;57:1172–1178.

20. Plaat BE, Molenaar WM, Mastik MF, Hoekstra HJ, te Meerman GJ, van den Berg E. Computer-assisted cytogenetic analysis of 51 malignant peripheral-nerve-sheath tumors: sporadic vs. neurofibromatosis-type-1-associated malignant schwannomas. *Int J Cancer*. 1999;83:171–178.
21. Pandita A, Aldape KD, Zadeh G, Guha A, James CD. Contrasting in vivo and in vitro fates of glioblastoma cell subpopulations with amplified EGFR. *Genes Chromosomes Cancer*. 2004;39:29–36.
22. Perrone F, Tabano S, Colombo F, et al. p15INK4b, p14ARF, and p16INK4a inactivation in sporadic and neurofibromatosis type 1-related malignant peripheral nerve sheath tumors. *Clin Cancer Res*. 2003;9:4132–4138.
23. Suzuki H, Sugimura H, Hashimoto K. p16INK4A in oral squamous cell carcinomas—a correlation with biological behaviors: immunohistochemical and FISH analysis. *J Oral Maxillofac Surg*. 2006;64:1617–1623.
24. Rodolfo M, Daniotti M, Vallacchi V. Genetic progression of metastatic melanoma. *Cancer Lett*. 2004;214:133–147.
25. Mawrin C, Kirches E, Boltze C, Dietzmann K, Roessner A, Schneider-Stock R. Immunohistochemical and molecular analysis of p53, RB, and PTEN in malignant peripheral nerve sheath tumors. *Virchows Arch*. 2002;440:610–615.
26. Mirmohammadsadegh A, Marini A, Nambiar S, et al. Epigenetic silencing of the PTEN gene in melanoma. *Cancer Res*. 2006;66:6546–6552.
27. Whang YE, Wu X, Suzuki H, et al. Inactivation of the tumor suppressor PTEN/MMAC1 in advanced human prostate cancer through loss of expression. *Proc Natl Acad Sci U S A*. 1998;95:5246–5250.
28. Salvesen HB, MacDonald N, Ryan A, et al. PTEN methylation is associated with advanced stage and microsatellite instability in endometrial carcinoma. *Int J Cancer*. 2001;91:22–26.
29. Kwabi-Addo B, Giri D, Schmidt K, et al. Haploinsufficiency of the Pten tumor suppressor gene promotes prostate cancer progression. *Proc Natl Acad Sci U S A*. 2001;98:11563–11568.
30. Johannessen CM, Reczek EE, James MF, Brems H, Legius E, Cichowski K. The NF1 tumor suppressor critically regulates TSC2 and mTOR. *Proc Natl Acad Sci U S A*. 2005;102:8573–8578.
31. Cohen JA, Yachnis AT, Arai M, Davis JG, Scherer SS. Expression of the neu proto-oncogene by Schwann cells during peripheral nerve development and Wallerian degeneration. *J Neurosci Res*. 1992;31:622–634.
32. Schlegel J, Muenkel K, Trenkle T, Fauser G, Ruschoff J. Expression of the ERBB2/neu and neurofibromatosis type 1 gene products in reactive and neoplastic Schwann cell proliferation. *Int J Oncol*. 1998;13:1281–1284.
33. Fernandes H, Cohen S, Bishayee S. Glycosylation-induced conformational modification positively regulates receptor-receptor association: a study with an aberrant epidermal growth factor receptor (EGFRvIII/DeltaEGFR) expressed in cancer cells. *J Biol Chem*. 2001;276:5375–5383.
34. Burstein HJ. The distinctive nature of HER2-positive breast cancers. *N Engl J Med*. 2005;353:1652–1654.
35. Clynes RA, Towers TL, Presta LG, Ravetch JV. Inhibitory Fc receptors modulate in vivo cytoxicity against tumor targets. *Nat Med*. 2000;6:443–446.
36. Fujita T, Doihara H, Kawasaki K, et al. PTEN activity could be a predictive marker of trastuzumab efficacy in the treatment of ErbB2-overexpressing breast cancer. *Br J Cancer*. 2006;94:247–252.
37. Mahller YY, Vaikunth SS, Currier MA, et al. Oncolytic HSV and erlotinib inhibit tumor growth and angiogenesis in a novel malignant peripheral nerve sheath tumor xenograft model. *Mol Ther*. 2007;15:279–286.
38. Hidalgo M, Siu LL, Nemunaitis J, et al. Phase I and pharmacologic study of OSI-774, an epidermal growth factor receptor tyrosine kinase inhibitor, in patients with advanced solid malignancies. *J Clin Oncol*. 2001;19:3267–3279.
39. Huether A, Hopfner M, Baradari V, Schuppan D, Scherubl H. EGFR blockade by cetuximab alone or as combination therapy for growth control of hepatocellular cancer. *Biochem Pharmacol*. 2005;70:1568–1578.